

Adapting Electrophoretic Exclusion to a Microdevice

by

Stacy Marie Kenyon

A Dissertation Presented in Partial Fulfillment
of the Requirements for the Degree
Doctor of Philosophy

Approved November 2012 by the
Graduate Supervisory Committee:

Mark Hayes, Chair
Alexandra Ros
Daniel Buttry

ARIZONA STATE UNIVERSITY

December 2012

ABSTRACT

Complex samples, such as those from biological sources, contain valuable information indicative of the state of human health. These samples, though incredibly valuable, are difficult to analyze. Separation science is often used as the first step when studying these samples. Electrophoretic exclusion is a novel separations technique that differentiates species in bulk solution. Due to its ability to isolate species in bulk solution, it is uniquely suited to array-based separations for complex sample analysis. This work provides proof of principle experimental results and resolving capabilities of the novel technique.

Electrophoretic exclusion is demonstrated at a single interface on both benchtop and microscale device designs. The benchtop instrument recorded absorbance measurements in a 365 μL reservoir near a channel entrance. Results demonstrated the successful exclusion of a positively-charged dye, methyl violet, with various durations of applied potential (30 – 60 s). This was the first example of measuring absorbance at the exclusion location. A planar, hybrid glass/PDMS microscale device was also constructed. One set of experiments employed electrophoretic exclusion to isolate small dye molecules (rhodamine 123) in a 250 nL reservoir, while another set isolated particles (modified polystyrene microspheres). Separation of rhodamine 123 from carboxylate-modified polystyrene spheres was also shown. These microscale results demonstrated the first example of the direct observation of exclusion behavior. Furthermore, these results showed that electrophoretic exclusion can be applicable to a wide range of analytes.

The theoretical resolving capabilities of electrophoretic exclusion were also developed. Theory indicates that species with electrophoretic mobilities as similar as 10^{-9} cm²/Vs can be separated using electrophoretic exclusion. These results are comparable to those of capillary electrophoresis, but on a very different format. This format, capable of isolating species in bulk solution, coupled with the resolving capabilities, makes the technique ideal for use in a separations-based array.

To Adam, for all of your patience, support, and encouragement.

ACKNOWLEDGMENTS

I must first thank my advisor, Dr. Mark Hayes, for accepting me into your group when I was a loner in the department, for your confidence in me, and for your hours of guidance (& candy) that have helped me become the scientist I am today. Thank you to my committee members, Drs. Daniel Buttry and Alexandra Ros for your time commitment and discussions over the years. I must also thank my first grad school advisor, Dr. Dana Spence, for showing me that analytical chemistry is more than titrations.

On a more personal level, I must acknowledge my husband, Adam. Thank you for being my best friend, for helping me to escape work (particularly the late night GnD runs during the writing process), and for encouragement while I pursued my academic goal. I will forever be grateful for your positive attitude, your willingness to support me, and your sacrifices over the last few years - you're just the partner I need in life. Secondly, thank you to my parents, Dennis & Linda, for demonstrating the value of hard work, for teaching me to believe in myself, and for funding innumerable life experiences (years of dance lessons, undergrad, and studying abroad, just to name a few). Thank you to my siblings, Nichole & Chris, my nieces, Sara & Haley, and my nephew, Aidan, for cheering for me from across the country.

My graduate career would not have been the same if it weren't for the friends I made along the way. First, thanks to all the Hayes lab group members, current and former, that I have had the pleasure of working with. Thank you to Dr. Michelle Meighan for befriending me before I started at ASU, for your

writing help, and for gmail chats, text messages, and emails. Your friendship has definitely helped me throughout the last few years! Dr. Noah Weiss – thank you for patiently answering my incessant questions (even all the way from Munich) and for your friendship. Thank you to Dr. Josemar (Josie) Castillo for your expert presentation advice, food/workout talks, and your encouragement throughout the last year. Paul – I will always value our random discussions (cooking, workouts, iPhones) over our cubicle walls and all of your presentation help before my defense! Thanks to Keebaugh for getting our project started; I wish I had your motivation and work ethic. Ryan – I really appreciate your help and company in the cleanroom. Casey Fadgen, thanks for letting me invade *your* office for a summer and for always being willing to go to lunch with me. Thank you to my friends from the Spence Lab: Andrea, Chia-Jui, Jen, Nicole, & Teresa – you set high standards for any future group members!

I would also like to recognize the influential people from my Albion College years: Drs. Cliff Harris, Daniel Steffenson, & David Green – thank you for the hours of homework help and the encouragement to go to grad school. I must also acknowledge GPSA for JumpStart research funding and travel grants to attend conferences, the NIH for grant funding for our lab research, and the CSSER staff for help in the cleanroom.

TABLE OF CONTENTS

	Page
LIST OF FIGURES	xi
CHAPTER	
1 INTRODUCTION.....	1
Complex Samples	1
Complex Sample Analysis.....	2
Capillary Electrophoresis	5
Equilibrium Gradient Techniques	6
Electrophoretic Exclusion.....	8
Dissertation Objectives.....	12
Dissertation Summary	13
References	14
2 RECENT DEVELOPMENTS IN ELECTROPHORETIC SEPARATIONS ON MICROFLUIDIC DEVICES.....	17
Introduction	17
External Field Acting Directly on Target	19
Free-Flow Electrophoresis.....	19
Temperature Gradient Focusing	22
Separation of Anions and Cations.....	26
Other Designs.....	27
Physical Structure of the Microdevice.....	27
Physical Elements for Trapping	28

CHAPTER	Page
Physical Structure Used to Define Local Field.....	30
Solution Properties Influencing Local Field	33
Isoelectric Focusing.....	34
Isotachophoresis.....	36
Concluding Remarks.....	45
References	46
3 ELECTROPHORETIC EXCLUSION ON A BENCHTOP DEVICE	52
Introduction.....	52
Material and Methods.....	54
Reagent Preparation	54
Instrumentation	54
Planar Prototypes	57
Results and Discussion	58
Exclusion Criteria.....	58
Calculated Concentration Enhancement Model.....	59
Exclusion of Methyl Violet	61
Stir Bar Experiments	63
Limitations of Benchtop Design	65
Concluding Remarks	67
References.....	67

CHAPTER	Page
4 USING ELECTROPHORETIC EXCLUSION TO MANIPULATE SMALL MOLECULES AND PARTICLES ON A MICRODEVICE	70
Introduction	70
Materials and Methods	74
Design and Fabrication of Microdevice	74
PDMS	74
Electrodes	75
Materials	76
Experimental Setup	76
COMSOL Multiphysics Modeling	77
Results and Discussion	77
Principles of Exclusion	77
Proof of Principle Experiments	78
Separation of Rhodamine 123 and Polystyrene Beads	85
The Effects of Variable Channel and Electrode Geometry on Electrophoretic Exclusion	86
Future Design: Separation-Based Array Format	89
Concluding Remarks	90
References	91
5 DEVELOPMENT OF THE RESOLUTION THEORY FOR ELECTROPHORETIC EXCLUSION	95
Introduction	95

CHAPTER	Page
Theory	97
Defining the Interface	100
Structure of Flow and Electric Fields Near/Within the Interface	101
Steady State, Fully Developed Concentration Profile	102
Determining the Two Closest Resolvable Species	105
Results and Discussion	109
Capillary Diameter and Flow Rate	109
Smallest Separable Difference in Electrophoretic Mobilities	111
Peak Capacity	113
Concluding Remarks	115
References	116
 6 THE DEVELOPMENT OF A MICROFLUIDIC ARRAY FOR USE IN ELECTROPHORETIC EXCLUSION SEPARATIONS	 118
Introduction	118
Materials and Methods	122
Design and Fabrication of Array Device	122
Materials	123
Experimental Design	124
Results and Discussion	126
Device Design	126

CHAPTER	Page
Device Parameters	126
Selection of Analytes	127
Terminology Used in the Array Device	127
Basics of Electrophoretic Exclusion in an Array Device	128
Assessment of Initial Array Device	131
Electrode Design.....	131
Voltage Divider.....	132
Addition of Posts to the Central Reservoirs	136
Interpretation of Results	137
Concluding Remarks	140
References.....	140
7 CONCLUDING REMARKS.....	143
Electrophoretic Exclusion at a Single Interface	143
Resolution and the Potential for Array-Based Separations	143
REFERENCES	145
APPENDIX	
A PUBLISHED PORTIONS	162

LIST OF FIGURES

Figure		Page
1.1.	Schematic of the Capillary Electrophoresis Instrument	6
1.2.	Fluid and Electrophoretic Velocities in Equilibrium Gradient Techniques	8
1.3.	Principles of Electrophoretic Exclusion	10
2.1.	Schematic of the Flow and Mobility in a Micro Free-Flow Electrophoresis Device.....	20
2.2.	Image Demonstrating Free-Flow Zone Electrophoresis	21
2.3.	TGF with Joule Heating	25
2.4.	Comparison of Simulated and Experimental Result for the Concentration of Fluorescent Dye Molecules Near an Electrode....	33
2.5.	Example of Two Different Samples Contacting in a Microchannel	38
2.6.	ITP Schematic Showing a Nucleic Acid Purification from Blood Lysate.....	41
3.1.	Benchtop Device Design.....	56
3.2.	Planar Prototypes.....	58
3.3.	Curves Representing Electrophoretic Exclusion of Methyl Violet Dye	60
3.4.	Change in Absorbance	63
3.5.	Change in Absorbance in Presence of Stir Bar	65
4.1.	Microdevice Used for Electrophoretic Exclusion	74
4.2.	Exclusion of Beads and Dye at a Channel Entrance.....	79

Figure	Page
4.3. Average Intensity Curve for Rhodamine 123	81
4.4. Change in Intensity Values for Varying Electric Field Strengths....	83
4.5. Average Intensity Changes for Various Times of Applied Potential	84
4.6. Still Images Taken from Video Demonstrating the Separation of Rhodamine 123 from Carboxylated Spheres	86
4.7. COMSOL Figures Demonstrating Fluid Velocity and Electric Fields	89
5.1. Device Schematic and Interface Description	100
5.2. Development of the Concentration Profile at the Interface.....	103
5.3. Using Distance to Determine the Two Closest Resolvable Species	107
5.4. Resolution as a Function of Capillary Diameter and Flow Rate ...	110
6.1. Experimental Array Device	122
6.2. Schematic representations of PDMS and electrode patterns	123
6.3. Voltage Divider Connected to an Array Device	125
6.4. Schematic Explaining the Array Device Terminology	128
6.5. Representative Potential Sequence Used for Exclusion Experiments.....	130
6.6. Fluorescence Intensity Graph	134
6.7. Voltage Divider Experiment.....	135
6.8. Images of Central Reservoirs with Various Post Designs.....	137

Figure	Page
6.9. Observation of Rhodamine 123 and True Blue Chloride in Array Device	138
6.10. Observation of Rhodamine 6G and True Blue Chloride in the Array Device	139

Chapter 1

Introduction

1.1 Complex samples

The world around us could be considered as being composed of complex samples, rich in information, though often difficult to analyze and understand. To obtain the valuable information from these samples, molecules of interest must be quickly isolated, analyzed, and sometimes concentrated. One field used to study these samples is analytical chemistry. The ability to isolate and differentiate specific analytes of interest can be extremely useful when examining samples from the environment and from biological sources. Its applicability to healthcare, for example, could have far-reaching effects that can lead to better understanding of disease and health states in humans.

To illustrate, human plasma is an example of a biological matrix that is rich in information and often biochemically examined to identify various maladies, including liver disease, malnutrition, and infection. As valuable as the information gleaned from plasma is, it is notoriously difficult to analyze due to its complexity. It contains thousands of proteins, with hundreds having been distinctly identified [1]. Not only does the number of proteins make examination difficult, varying abundances contribute to its intricacy. The concentration abundances cover at least 10 orders of magnitude, with serum albumin being one of the most abundant (concentrations at mg/ml) and interleukin 6 being an example at the lower end of the scale (concentrations at pg/ml) [2]. Because these specific proteins from complex matrices lead to better understanding of health

states (in biological samples) and the world around us (in environmental samples), it is essential to have methods to identify and discover these important molecules.

1.2 Complex sample analysis

Samples that contain as many analytes and cover as large of a concentration range as those in human plasma are difficult to examine. To interrogate these samples, ligand-binding technology has been used since the 1950's, while immunoassays, in particular gained widespread popularity in the late 1960's [3]. Immunoassays are so attractive for analysis because they can bind to specific molecules, providing sensitivity and selectivity [3, 4]. Both of these features are of great value when isolating molecules of interest from complex matrices.

After the popularity of immunoassays, "microspot assays" were developed and reported in 1986 [3]. These assays not only maintained the selectivity and sensitivity of ligand assays, but are also able to address multiple analytes simultaneously. This is incredibly useful when studying biological samples and identifying several markers simultaneously. These microspot assays or microarrays are so useful due to their high-throughput capabilities, decreased sample sizes, and decreased analysis time. Micro immunoassays have been valuable in biological sample analysis and have been developed for cancer and proteomic research [3, 5-7].

Due to their capability to selectively isolate species of interest, immunoassays, and other arrays, have been successfully employed for the study of complex samples. This ability is the result of the direct binding interactions

between ligand and analyte. Though successful, this required binding step is the limiting step, if you could call it that, of the technology. By using a binding step, it is essential to know beforehand exactly what molecules are of interest in the sample so that specific binding agents can be used and/or fabricated. Another, albeit more subtle, drawback is that because it necessary to know what molecules are being targeted by a specific binding step, only those molecules are designed to be identified, while similar molecules can be overlooked all together.

Additionally, unidentified and unknown species will not be interrogated or discovered using this technology, since binding agents are only created for known analytes; if there is not a binding agent, species will not be selected. Although arrays have many advantages, including high throughput, selective, sensitive, and fast analyses, they have the potential to be even further improved by introducing an adjustable property: specifically, a recognition step that allows for adjustments and isolation of molecules without binding steps. Separations science can be used to accomplish this.

In separations science, species are isolated relative to each other in time or space based upon the properties of the analytes. These techniques, such as chromatography and capillary electrophoresis (CE), use forces to manipulate molecules and particles, as opposed to probing for specific epitopes of biomolecules as in arrays. In chromatography, species are differentiated based upon how they interact with the stationary phase while flowing through the column, whereas CE separates species based upon their electrophoretic mobilities. Because forces influence the separations process, manipulations can be made to

accommodate different experiments, such as changing stationary phases or flow rates in chromatography or changing buffer pH and electric field strength in CE. Furthermore, unlike arrays, separation science designs can also isolate species without knowing their specific properties, and in some cases, without knowing they exist. For example, if a sample is injected onto a CE column, exact electrophoretic mobilities are not needed to perform a successful separation; as long as species have different enough mobilities, they will be isolated in the column [8]. Also, in addition to known analytes, unexpected species can also be identified, such as impurities, or in some cases, other molecules of interest. The ability to discover analytes is due to fact that specific binding agents are not used for isolation of identified molecules, but instead forces influence the separation, exploiting the properties of the species in a sample. This, along with the dynamic properties of separation science, make it especially appealing for studying individual analytes from multifaceted matrices.

Accordingly, separation schemes have been used to study plasma and other complex biological samples. Chromatography [9], gel electrophoresis [1], capillary electrophoresis (CE) [10], and isoelectric focusing (IEF) [11, 12] have all been extensively used for species differentiation. Even with all of the valuable array and separations techniques, it is thought that many of the lower abundance proteins have yet to be identified in human plasma [13]. This is due to the difficulty associated with isolation of species from complex matrices.

Combining the benefits of arrays with the benefits of separations, could allow for better isolation and identification of molecules. This is because all of

the positive features of arrays (high throughput, fast, sensitive, and selective analyses) with the advantages of separations science (using forces to manipulate species), could allow for dynamic and fast analyses. One separations technique that is particularly applicable to arrays is electrophoretic exclusion.

Electrophoretic exclusion is a separations design related to CE and equilibrium gradient techniques, which will be discussed in this chapter.

1.3 Capillary electrophoresis

Many of the well-established separation schemes that have been used for complex sample analysis are based upon exploiting electric fields. Although gel electrophoresis is the most popular, CE, an electrophoretic separations technique that became commonplace in the 1990's, has been used for many types of applications, including biological samples [14-16]. Traditional CE separates species in a long thin channel, or capillary, based on differing electrophoretic mobilities. The CE instrument is constructed from two buffer vials, a capillary, a power supply, and a detector (Fig. 1.1). The velocity (v) at which species move through the capillary is the product of the electrophoretic mobility and applied electric field (E):

$$v = \mu_{ep} E \quad (1)$$

When potential is applied to the system, species move along the channel according to the ratio between their charge and frictional forces [8]:

$$\mu_{ep} = q/6\eta\pi r \quad (2)$$

where μ_{ep} is electrophoretic mobility, q is ionic charge, η is solution viscosity and r is ionic radius.

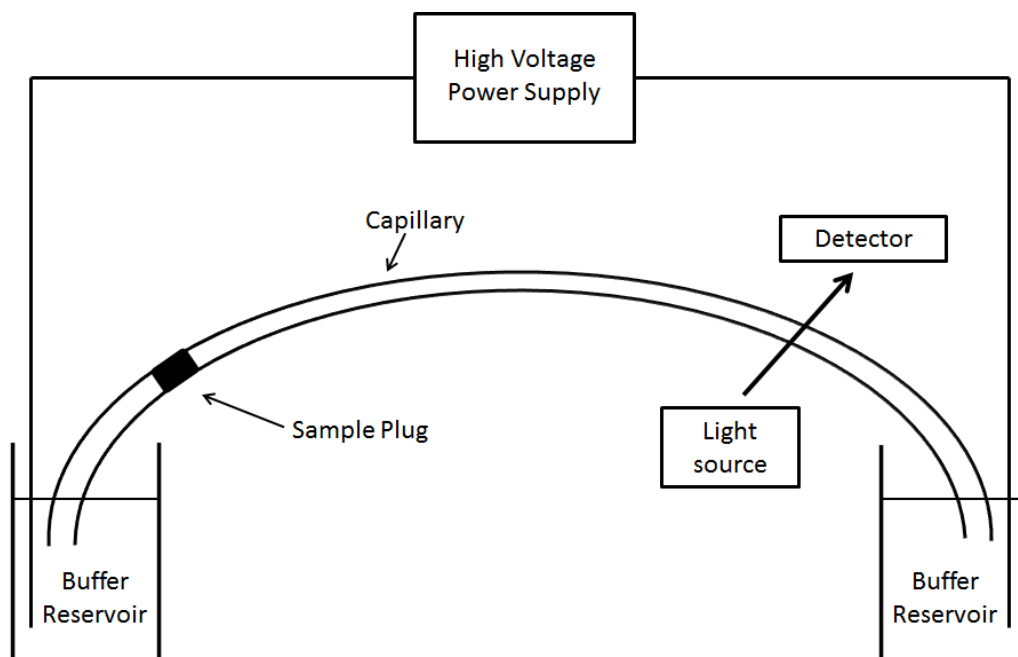


Figure 1.1. Schematic of the capillary electrophoresis instrument.

At physiological pH, most species in the capillary move toward the cathode due to electroosmotic flow (EOF). At pH values above 3, the inside of the capillary wall is negatively charged as a result of the deprotonation of the silanol groups on the interior of the capillary wall. The negatively-charged walls attract a layer of positively-charged ions in solution. This layer, called the diffuse layer, moves under the influence of the electric field and causes the general motion of buffer towards the cathode, with positively charged species eluting first, followed by neutral species, and finally by negatively charged species [14-16].

1.4 Equilibrium gradient techniques

CE, though a useful and versatile technique, suffers from poor concentration detection limits. To overcome this, researchers have developed

sample concentration methods, including moving reaction boundary [17], sample stacking [18, 19], and counterflow electrophoresis [20], for enhancing samples in CE analysis.

Equilibrium gradient techniques, on the other hand, are capable of overcoming low sample concentration in separations (along with potentially improving resolution) [21, 22]. In these procedures, species migrate through a capillary or channel until counteracting forces balance each other. At this location, the focusing point, species collect, and those with unique properties collect at different positions along the channel, due to some type of velocity gradient. Here, at the focusing point, the counteracting forces concentrate species and additionally limit the effects of diffusion. These methods are considered steady-state methods [23] and focusing forces counteract dispersive forces during the course of separation, allowing for simultaneous concentration and differentiation.

A traditional equilibrium gradient technique, IEF, separates species in the presence of a pH gradient and electric field, using a combination of the charge state and electric field to induce a velocity gradient [24]. More recently, equilibrium gradient techniques have begun using hydrodynamic flow to counteract electrophoretic migration (with electric fields varying along the length of the channel to create differential transport) (Fig. 1.2). These counterflow electric field gradient focusing techniques include temperature gradient focusing (TGF) [25-27], conductivity gradient focusing [28, 29], dynamic field gradient focusing [30-32], gradient elution moving boundary electrophoresis (GEMBE)

[33, 34], and gradient elution isotachopheresis (GEITP) [35, 36]. In all of these devices, separation occurs in-channel. Even in GEMBE & GEITP experiments, separations are initiated outside of a channel, but the hydrodynamic flow is then slowly decreased, and allows differing species to enter the channel, where detection occurs.

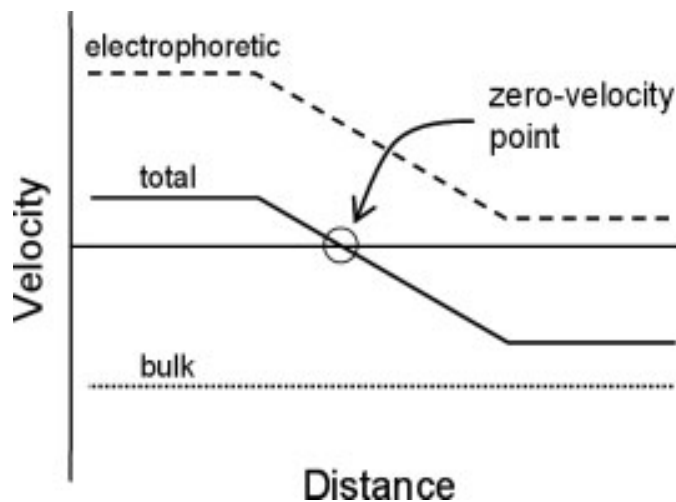


Figure 1.2. Fluid and electrophoretic velocities in equilibrium gradient techniques [37].

1.5 Electrophoretic exclusion

Electrophoretic exclusion, originally developed to address sample concentration concerns in CE [38], is a separations scheme that, like CE and some of the equilibrium gradient techniques, separates species based upon their charge and radius, described by their electrophoretic mobilities. In addition to utilizing electric fields for separation, electrophoretic exclusion takes advantage of a hydrodynamic flow through a channel that opposes the movement of the charged species being differentiated. The way that electric fields are applied in the device

causes separation in bulk solution, instead of in the channel as seen in CE, IEF, GEMBE, and GEITP. The advantage of being able to differentiate species in bulk solution is that it allows for the possibility of several individual compartments for species to be isolated. The compartments can be in parallel and/or series and permit sample components to travel in many different paths through the device, as opposed to only being allowed to travel one way through a channel. This variation, differentiation in bulk solution instead of in a channel, and the advantages of separation science mentioned previously, make electrophoretic exclusion ideal for complex sample analysis, specifically in an array format where many species can be isolated simultaneously.

It is also important to note electrophoretic exclusion can be used in conjunction with existing arrays and detection elements. Because species are separated in bulk solution, based upon their native properties, without a binding step, it can be combined with various techniques for detection, such as mass spectrometry, electrochemistry, spectroscopy, etc. This adds an additional layer of diversity to the technique.

In this method, differentiation occurs when the electrophoretic velocity of the species out of the channel is greater than or equal to the countering hydrodynamic flow. Successful exclusion requires three variables: hydrodynamic flow, an electric field, and species with an electrophoretic mobility in the buffer conditions. Assuming a constant hydrodynamic flow velocity and buffer conditions, electric fields can easily be manipulated to allow for selective distinction of species with different electrophoretic mobilities. When selecting an

electric field strength, it must be large enough for one species to be excluded, but allow the other to flow freely through the device with the fluid flow (Fig. 1.3). Before potential is applied to the system (top), all species are allowed to flow through the system with the hydrodynamic flow. When an appropriate potential is applied to the second channel, the species with the larger electrophoretic mobility that can oppose the hydrodynamic flow (represented with black circles) is prevented from entering the second channel and is excluded in the bulk solution reservoir (middle). If the electric field is removed, the collected species is again permitted to travel through the second channel (bottom).

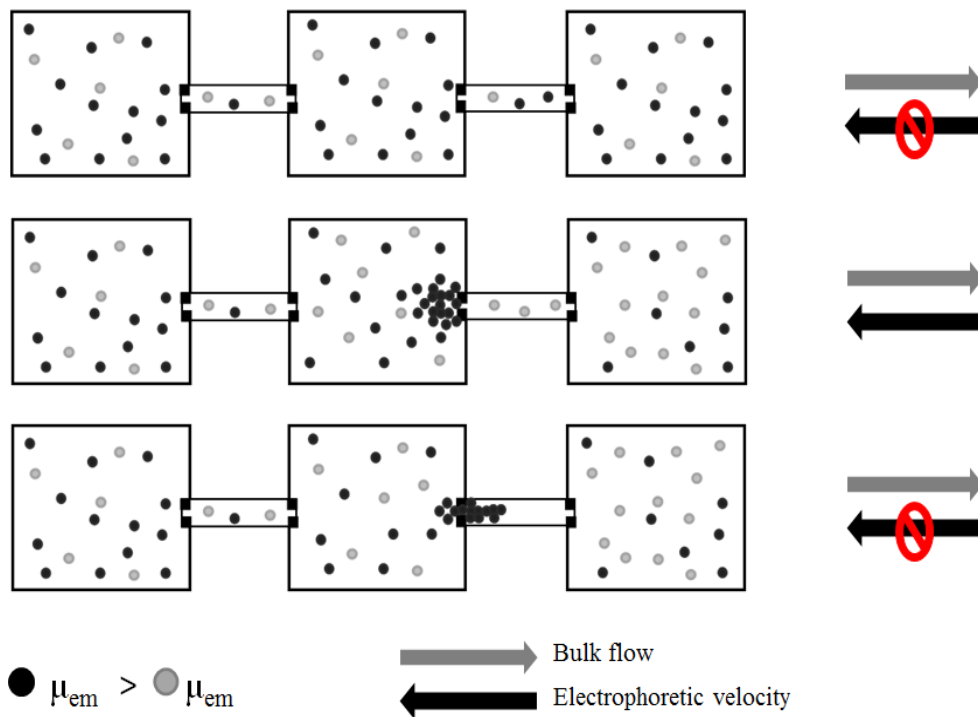


Figure 1.3. Principles of electrophoretic exclusion. In the presence of an appropriate electric field, species are excluded in bulk solution, near the entrance of a channel.

As previously mentioned, electrophoretic exclusion is a unique separations scheme because differentiation occurs in bulk solution. This is due to the nature of the electric field gradient. Unlike in CE and the equilibrium gradient techniques, the gradient is not in the channel, but instead is formed as a sharp gradient at the channel entrance (due to the electrode design). This sharp gradient allows for species with specific mobilities to be collected just outside of the channel entrance instead of inside the capillary. Current studies in the Hayes Lab indicate that this unusual microgradient leads to better separation resolution.

Resolution (R) is used to determine the efficiency of a separation scheme. Although methods for determining resolution may differ between experimental designs, it can generally be thought of as the ratio of the distance between the eluted peaks (ΔX) and the standard deviation (σ) of the peaks [21]:

$$R = \frac{\Delta X}{4\sigma} \quad (3)$$

The larger the value of R , the better the separation, but an R value of 1 is considered a good separation, with $R = 1.5$ being baseline resolution. Resolution theory for chromatography [39, 40] and CE [41] has been well-established and other equilibrium gradient techniques, such as equilibrium gradient focusing [29, 42], IEF [21], and GEMBE [43] have been explored. The resolving capabilities of electrophoretic exclusion have been preliminarily explored and results indicate that it is competitive with CE. These preliminary resolution numbers also indicate that electrophoretic exclusion can be used in an array format for complex separations, where analytes with similar properties will need to be differentiated.

Though electrophoretic exclusion has been studied extensively over the last few years as a method for complex sample analysis, it was initially used in the work performed by Polson et al., demonstrating the ability to preconcentrate 200 nm polystyrene microspheres [38]. Later studies modeled the exclusion behavior [44] and investigated the electrode/solution interface [45]. The versatility of the scheme was also demonstrated on a benchtop design by showing the exclusion and concentration of small dye molecules and proteins, indicating that electrophoretic exclusion can be applied to varying sample types [46, 47]. Microdevice experiments showed the first direct visualization of exclusion and showed the separation of small particles and dye molecules [48].

1.6 Dissertation objectives

This dissertation is dedicated to describing an electrophoretic separations technique that is envisioned as a tool for complex sample analysis. Electrophoretic exclusion, the novel separations method presented here, was initially performed on a bench-top device, with concentration enhancements of up to 1200 times in 60 s when differentiating proteins in a flow-injection device [47]. However, the bulk of the work presented in this document discusses the use of electrophoretic exclusion on a microdevice, demonstrating differentiation of small dyes and molecules. A discussion of its applicability for an array and resolution theory is also addressed, focusing on the importance of the electrode-solution interface.

1.7 Dissertation summary

To first introduce the field of electrophoretic separations on microdevices, a review of novel techniques is included as Chapter 2. This chapter covers practices that innovatively exploit the microfluidic format and increase separation efficiency by using continuous sampling and/or concentration enhancement on-chip. Schemes included in this chapter are those that have external fields acting directly on analytes, those that have behaviors defined by the physical structure of the microdevice, and those that have the separation defined by local solution properties. Articles that are reviewed in this chapter are from January 2008 to July 2010.

Chapters 3 – 5 present experiments using electrophoretic exclusion. Chapter 3 presents proof-of-principle data with a small dye molecule. Results were obtained on a benchtop design with exclusion and detection occurring in a central reservoir. A discussion for adapting the technique to a microdevice is also included. Chapter 4 demonstrates the ability to adapt electrophoretic exclusion to a microdevice and presents data differentiating polystyrene spheres and fluorescent dye molecules, as well as the separation of fluorescent dye from polystyrene beads. Chapter 5 develops the theory of resolution of electrophoretic exclusion at an interface and includes a brief analysis of experimental results from benchtop and microdevice designs. Chapter 6 details the development of a prototype array device and includes thorough trouble-shooting steps.

Chapter 7 will summarize the goals and results of the electrophoretic exclusion technique that were presented in Chapters 3 – 6. Conclusions and future directions will also be discussed.

1.8 References

- [1] Pieper, R., Gatlin, C. L., Makusky, A. J., Russo, P. S., Schatz, C. R., Miller, S. S., Su, Q., McGrath, A. M., Estock, M. A., Parmar, P. P., Zhao, M., Huang, S. T., Zhou, J., Wang, F., Esquer-Blasco, R., Anderson, N. L., Taylor, J., Steiner, S., *Proteomics* 2003, 3, 1345-1364.
- [2] Anderson, N. L., Anderson, N. G., *Mol Cell Proteomics* 2002, 1, 845-867.
- [3] Ekins, R. P., *Clin. Chem.* 1998, 44, 2015-2030.
- [4] Hartmann, M., Roeraade, J., Stoll, D., Templin, M., Joos, T., *Anal. Bioanal. Chem.* 2009, 393, 1407-1416.
- [5] MacBeath, G., *Nat. Genet.* 2002, 32, 526-532.
- [6] Soper, S. A., Brown, K., Ellington, A., Frazier, B., Garcia-Manero, G., Gau, V., Gutman, S. I., Hayes, D. F., Korte, B., Landers, J. L., Larson, D., Ligler, F., Majumdar, A., Mascini, M., Nolte, D., Rosenzweig, Z., Wang, J., Wilson, D., *Biosens. Bioelectron.* 2006, 21, 1932-1942.
- [7] Wu, J., Fu, Z. F., Yan, F., Ju, H. X., *Trac-Trend Anal Chem* 2007, 26, 679-688.
- [8] Giddings, J. C., *Unified Separation Science*, Wiley-Interscience Publication, New York 1991.
- [9] Shen, Y. F., Kim, J., Strittmatter, E. F., Jacobs, J. M., Camp, D. G., Fang, R. H., Tolie, N., Moore, R. J., Smith, R. D., *Proteomics* 2005, 5, 4034-4045.
- [10] Bushey, M. M., Jorgenson, J. W., *J. Chromatogr.* 1989, 480, 301-310.
- [11] Capriotti, A. L., Cavaliere, C., Foglia, P., Samperi, R., Lagana, A., *J. Chromatogr. A.* 2011, 1218, 8760-8776.
- [12] Hjerten, S., Liao, J. L., Yao, K., *J. Chromatogr.* 1987, 387, 127-138.
- [13] Jacobs, J. M., Adkins, J. N., Qian, W. J., Liu, T., Shen, Y. F., Camp, D. G., Smith, R. D., *J. Proteome Res* 2005, 4, 1073-1085.
- [14] Jorgenson, J. W., Lukacs, K. D., *Anal. Chem.* 1981, 53, 1298-1302.

- [15] Jorgenson, J. W., Lukacs, K. D., *Clin. Chem.* 1981, 27, 1551-1553.
- [16] Jorgenson, J. W., Lukacs, K. D., *Science* 1983, 222, 266-272.
- [17] Cao, C. X., *J. Chromatogr. A.* 1997, 771, 374-378.
- [18] Beard, N. R., Zhang, C. X., deMello, A. J., *Electrophoresis* 2003, 24, 732-739.
- [19] Mikkers, F. E. P., Everaerts, F. M., Verheggen, T., *J. Chromatogr.* 1979, 169, 11-20.
- [20] Culbertson, C. T., Jorgenson, J. W., *Anal. Chem.* 1994, 66, 955-962.
- [21] Giddings, J. C., Dahlgren, K., *Sep. Sci.* 1971, 6, 345-&.
- [22] O'Farrell, P. H., *Science* 1985, 227, 1586-1589.
- [23] Giddings, J. C., *Sep. Sci. Technol.* 1979, 14, 871-882.
- [24] Hjerten, S., Zhu, M. D., *J. Chromatogr.* 1985, 346, 265-270.
- [25] Danger, G., Ross, D., *Electrophoresis* 2008, 29, 3107-3114.
- [26] Huber, D. E., Santiago, J. G., *Proc. R. Soc. A* 2008, 464, 595-612.
- [27] Ross, D., Locascio, L. E., *Anal. Chem.* 2002, 74, 2556-2564.
- [28] Greenlee, R. D., Ivory, C. F., *Biotechnol. Prog.* 1998, 14, 300-309.
- [29] Kelly, R. T., Woolley, A. T., *J. Sep. Sci.* 2005, 28, 1985-1993.
- [30] Ansell, R. J., Tunon, P. G., Wang, Y. T., Myers, P., Ivory, C. F., Keen, J. N., Findlay, J. B. C., *Analyst* 2009, 134, 226-229.
- [31] Huang, Z., Ivory, C. F., *Anal. Chem.* 1999, 71, 1628-1632.
- [32] Shim, J., Dutta, P., Ivory, C. F., *Electrophoresis* 2007, 28, 572-586.
- [33] Ross, D., Kralj, J. G., *Anal. Chem.* 2008, 80, 9467-9474.
- [34] Strychalski, E. A., Henry, A. C., Ross, D., *Anal. Chem.* 2009, 81, 10201-10207.
- [35] Davis, N. I., Mamunooru, M., Vyas, C. A., Shackman, J. G., *Anal. Chem.* 2009, 81, 5452-5459.

- [36] Mamunooru, M., Jenkins, R. J., Davis, N. I., Shackman, J. G., *J. Chromatogr. A* 2008, *1202*, 203-211.
- [37] Shackman, J. G., Ross, D., *Electrophoresis* 2007, *28*, 556-571.
- [38] Polson, N. A., Savin, D. P., Hayes, M. A., *J. Microcolumn Sep.* 2000, *12*, 98-106.
- [39] Giddings, J. C., *J. Chromatogr.* 1960, *3*, 520-523.
- [40] Giddings, J. C., *Anal. Chem.* 1963, *35*, 2215-&.
- [41] Foret, F., Deml, M., Bocek, P., *J. Chromatogr.* 1988, *452*, 601-613.
- [42] Tolley, H. D., Wang, Q. G., LeFebre, D. A., Lee, M. L., *Anal. Chem.* 2002, *74*, 4456-4463.
- [43] Ross, D., *Electrophoresis* 2010, *31*, 3650-3657.
- [44] Pacheco, J. R., Chen, K. P., Hayes, M. A., *Electrophoresis* 2007, *28*, 1027-1035.
- [45] Keebaugh, M. W., Mahanti, P., Hayes, M. A., *Electrophoresis* 2012, *33*, 1924-1930.
- [46] Meighan, M. M., Keebaugh, M. W., Quihuis, A. M., Kenyon, S. M., Hayes, M. A., *Electrophoresis* 2009, *30*, 3786-3792.
- [47] Meighan, M. M., Vasquez, J., Dziubcynski, L., Hews, S., Hayes, M. A., *Anal. Chem.* 2011, *83*, 368-373.
- [48] Kenyon, S. M., Weiss, N. G., Hayes, M. A., *Electrophoresis* 2012, *33*, 1227-1235.

Chapter 2

Recent Developments in Electrophoretic Separations on Microfluidic Devices

2.1 Introduction

Separations science is often a necessary first step in performing a chemical analysis. Separations has received significant attention as older, more established techniques such as chromatography are leveraged, or entirely new techniques are developed. Separation techniques that exploit the electrostatic and electrodynamic properties of analytes have become increasingly popular. Many of these focus on unique properties of the analytes that have not been fully examined for separations. Several of the new methods are related to electrophoresis and some of the standard bearers include isoelectric focusing (IEF) [1-3] and free-flow electrophoresis (FFE) [4, 5]. Various processes, such as FFE, are well-known on the preparative-scale, while others, such as IEF, have been well-characterized for analytical-scale separations. There have been many innovative areas of development on the smaller-scale, including: taking advantage of hydrodynamic counterflow [6, 7], different channel designs [8], and applying electric fields perpendicular to the flow of the sample [9-13].

Several groups continue to develop variations on standard electrophoretic separation techniques, including Astorga-Wells [14], Gebauer [15, 16], Hayes [17, 18], and Ivory [19, 20], but the current paper will center on elements that are essentially new or are significant advances in strategies that uniquely exploit microfluidic formats. The advantages of microfluidic devices include lower sample consumption, portability, and shorter analysis times. These qualities are

desirable for studying complex samples, especially in the current age where onsite and quick analyses are being sought. One of the advantages of microfluidic devices is the small sample size; however, this creates detection limit issues, as analytes of interest may actually not be present at concentration or mass levels high enough to detect. This review will discuss techniques that develop ways to overcome this limitation, either through continuous sampling or concentration enhancement on-chip before separation, or a combination of both.

Several topics are excluded for clarity and focus. These include chromatographic techniques, as well as channels that contain particle packing, membranes, and gels. Because this chapter aims to describe the separation methods themselves, fabrication methods and new chip and electrode materials will not be addressed. Other areas of interest with clear connectivity to the current work will also be omitted, such as carbon nanotubes, electrophoresis in nanochannels, electrophoretic separations used for immunoassays, and dielectrophoretic separations. The topics that are addressed are categorized into three topics: 1) external field directly acting on analytes, 2) behaviors defined by the physical structure of the microdevice, and 3) separations defined by local solution properties. Although the papers have been divided into categories to aid in organization, not all categories are mutually exclusive and many techniques could be placed in more than one designation. Lastly, the time frame that will be discussed is between January 2008 and July 2010.

2.2 External field acting directly on target

In this section, processes that involve the direct interaction of the electric field on the analyte for focusing and differentiation are discussed. Some of the techniques described here include free-flow electrophoresis and its variations, temperature gradient focusing, and methods that simultaneously separate anions and cations.

2.2.1 Free-flow electrophoresis

Free-flow electrophoresis is a continuous separation technique that utilizes two components: hydrodynamic flow and an applied electric field [4], where the electric field is applied perpendicularly to the flow. The sample is introduced into the flow via an inlet at one end, and is separated perpendicular to the flow based on the species' electrophoretic mobilities. At the opposite end, the separated species exit through individual outlets. This technique has more recently been applied to microscale devices [21].

The Bowser group from the University of Minnesota has made several contributions to FFE since 2008 [10-12, 22]. In one study, Fonslow *et al.* used a microchip with varying depths to study the effects of a buffer concentration gradient on separations [10] and in another study, to separate mitochondria [11]. In the first paper, a concentration gradient in cyclodextrin was created and the effect on amino acid separation was examined, as well as an efficient determination of the ideal separation conditions [10]. Figure 1 shows the FFE system used by Kostal *et al.* In the paper, mitochondria were separated using less sample and in less time than traditional FFE systems [11]. In both examples, the

channel was on a microchip; however, the channel length was 5 cm and the width was 3 cm.

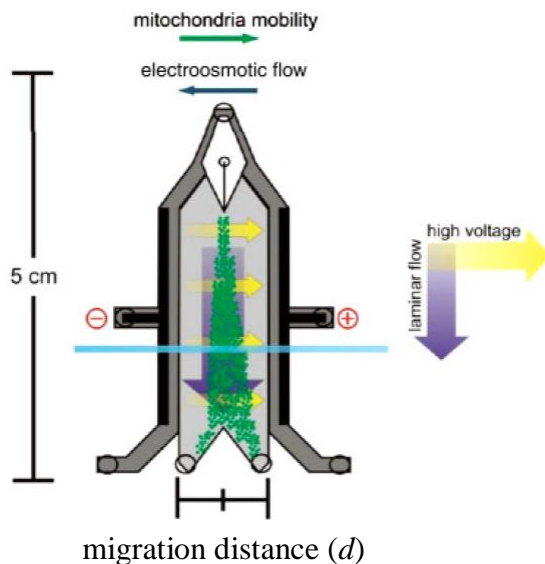


Figure 2.1. Schematic of the flow and mobility in a micro free-flow electrophoresis device. The dark arrow represents laminar flow while the lighter arrow represents the direction of the voltage [11].

Kohlheyer *et al.* described a new method for preventing electrolysis in a microfluidic free-flow device [23]. Quinhydrone (QH), a complex of hydroquinone (H_2Q) and *p*-benzoquinone (Q), was added to the system as strategy to electrochemically quench hydrolysis. Instead of the typical generation of oxygen and hydrogen when water is oxidized and reduced at their respective electrodes, H_2Q was oxidized and Q was reduced, which prevented the formation of bubbles. Aside from the addition of QH, the chip design was also slightly modified. Rather than a single inlet channel, there were five inlet channels, two of which were used for the injecting HQ solution, another for sample introduction,

and the other two for sample focusing as shown in Figure 2.2. Fluorescein, rhodamine B, and rhodamine 6G were successfully separated; however, this technique was only effective with low current densities, limited by the depletion of HQ.

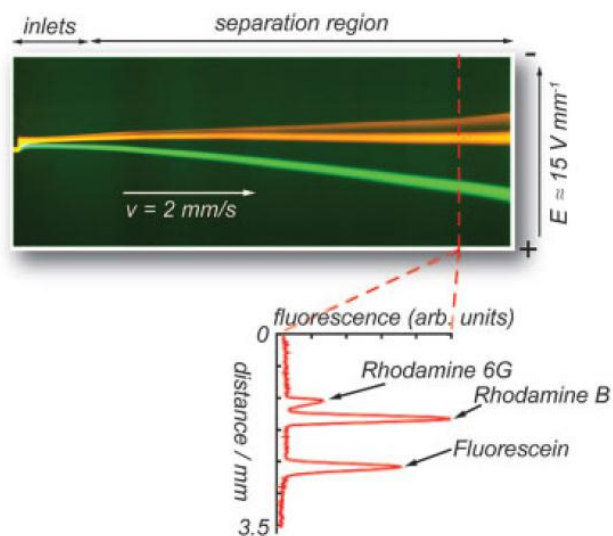


Figure 2.2. Image demonstrating free-flow zone electrophoresis. Three fluorescent dyes diverge in the free-flow zone electrophoresis microdevice (top), and an intensity profile of the separated dyes (bottom) [23].

A variation of FFE was demonstrated in 2009 by the Janasek group from Germany [9]. In their apparatus, a microfluidic glass chip with nine outlet channels was designed and used for the separation of proteins. Instead of a single inlet, there were a total of 67 inlet channels used for buffer and sample introduction. The 67 channels were formed by branching from two main channels that were connected to syringe pumps. The separation channel had posts incorporated to prevent channel collapse and to effectively increase the path length. The main separation channel had 222 shallow side conduits connected on each side. These areas were used to join the main channel to a large buffer

reservoir on each side, where the electrodes were placed, as well as prevented bubble formation in the main separation chamber by acting like membranes. Myoglobin and trypsin inhibitor proteins were labeled with fluorescein isothiocyanate (FITC) and temperature gradient focusing (TGF) was used to demonstrate separation. The species were focused to different outlets based upon their different electrophoretic mobilities and two concentrated peaks were visible.

Zalewski *et al.* performed the first example of synchronized, continuous-flow zone electrophoresis on a microfluidic device [13]. This technique is also related to FFE, except that hydrodynamic flow, as well as separation, is electrokinetically-driven. The borosilicate glass chip contained three inlets and three outlets connected to the separation channel. The sample was introduced into the chamber from the center inlet and was focused by buffer streams from the inlets on either side. The position of the sample stream was adjusted by manipulating the buffer streams and electric potential was applied perpendicularly. The combination of a varying position of sample stream and the axial electric field created a wavelike sample stream path. The path was then manipulated to separate species with different apparent electrophoretic mobilities. Theoretical and experimental data were presented and indicate that this method was successful. Rhodamine B and fluorescein were separated, as well as a three component mixture of fluorescein, rhodamine B, and rhodamine 6G.

2.2.2 Temperature gradient focusing

TGF is part of a novel group of separation techniques that differentiates and concentrates species in a channel based on their electrophoretic velocities

varying with temperature [24]. In these counterflow techniques a bulk flow opposes, or counters, the electrophoretic velocity of the species. When the bulk flow is equal to and opposite of the electrophoretic velocity, the species are retarded and focused. Species move from both directions in the channel to reach this focusing point. Because the electrophoretic velocity of a species is the product of the electrophoretic mobility and the electric field, an electric field gradient must be created in the channel to allow for the movement and eventual retardation of the species. In TGF, the electric field gradient is created by employing buffers whose conductivities vary with temperature. Typically, one end of the channel is heated, while the other is cooled to create a temperature gradient, which results in an electric field gradient.

Studies in this area since 2008 have covered theoretical, simulated, and experimental aspects, as well as large-scale and micro-scale devices. The Ross group at NIST has reported on several applications of TGF. One paper emphasized the effects of high ion concentration on separation and focusing [25] and another described using scanning TGF for the separation of chiral amino acids [26]. These devices, however, all utilized capillaries that were several centimeters in length. Also from NIST were applications of TGF that used the technique to prevent species from entering a channel, instead of solely for sample concentration [27, 28]. In these examples, biological samples that can damage devices by adsorption and those with high concentration sample matrices were being used. By preventing species from entering the channel, reusable devices and less sample interference was achieved. However, these devices also were

larger scale, as separations took place in capillaries that were several centimeters in length.

Although TGF commonly utilizes external physical heating or cooling of the capillary, there have also been reports of using joule heating to induce a temperature gradient [6, 7]. In these papers, the separation channel had a change in width at one location. Tang *et al.* numerically demonstrated this phenomenon in a PDMS microfluidic device [6]. When the channel narrowed, the heat density increased in the presence of applied potential, which caused an increase in the temperature in the narrow part of the channel. The group simulated this effect and indicated that concentration slowly increases at this interface (Fig. 2.3). Results indicated that after 190 s of applied potential, concentration increased by 350-fold (original concentration of 0.280 M). Results were compared to work performed by Ross *et al.* [24] and were in good agreement.

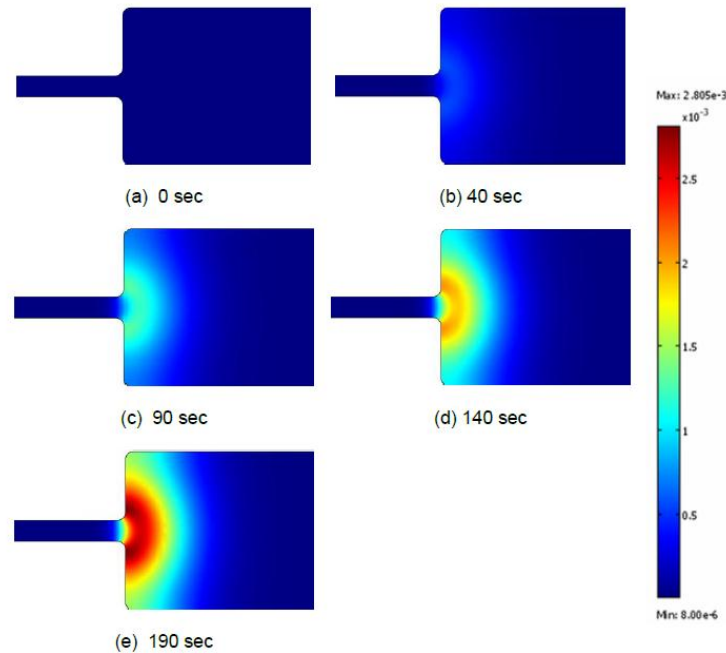


Figure 2.3. TGF with joule heating. Simulation of sample concentrations at the junction between wide and narrow microchannels is demonstrated at various times for a TGF experiment that uses joule heating to induce a temperature gradient [6].

Ge *et al.* also presented experimental and numerical studies of joule heating-induced TGF in microchannels [7]. Several factors were investigated using fluorescein-Na, including channel width ratio, applied potential, and buffer concentration on TGF in PDMS/glass and PDMS/PDMS devices. It was found that increasing the applied potential, buffer concentration, and channel width ratio all lead to greater concentration enhancement. Overall, it was found that the PDMS/PDMS device required lower potential and shorter time to accomplish the same concentration enhancement as the PDMS/glass device, due to the lower thermal conductivity of the PDMS/PDMS device. In addition to the experimental data, numerical data using COMSOL Multiphysics were presented and were supported by the experimental data.

2.2.3 Separation of anions and cations

Reschke *et al.* from West Virginia University described devices that were used for the separation of ions [29, 30]. In the first paper, a glass microfluidic device where flow is controlled by electrophoresis was used for anion and cation separation and detection [29]. The results showed both theoretically and experimentally that ions could be “electrophoretically extracted” from the hydrodynamic flow stream at the intersection between two channels. A sample was pumped through the main channel and a potential was then applied at the intersecting channel. When the charged species came under the influence of the electric field, they were extracted from the main channel to the intersection channel based on their electrophoretic mobilities. Cations moved towards one side of the intersecting channel, while anions moved toward the opposite side. The behavior of fluorescein was analyzed and had nearly complete extraction.

In a subsequent paper by the Reschke *et al.* [30], the glass microfluidic device for simultaneous cation and anion detection was modified. The device retained the single, hydrodynamically-pumped sample stream, but separation and detection occurred in two separate channels, one for anions and one for cations. When the sample stream passed the intersection where the injection channel meets the separation channels, the anions traveled towards the anode, while the cations traveled toward the cathode in different channels with separate outlets. A sample containing rhodamine 123 (cation), FLCA (anion), and FL (anion) was separated in the individual channels, and the analytes were only detected in the appropriate channels, indicating that the ions were successfully “extracted.”

Additional experiments with a positively-charged peptide (TMRIA) and negatively-charged proteins (bovine serum albumin, casein, and avidin) showed similar results. Separation efficiencies were all greater than 300 and at least 87% of the ions were extracted.

2.2.4 Other Designs

In work by Kawanata *et al.*, a new design was investigated that employs electroosmotic pumping for particle separation and collection [31]. The method, termed pinched flow fractionation, uses a microdevice with two inlets and five outlets. With the method, flow rates can be controlled and adjusted by varying the voltages of the inlets and outlets of the channels. Using the multi-channel scheme, 0.50 - 3.0 μm diameter particles were separated.

Baker *et al.* presented a paper on the development of a glass microfluidic chip that incorporated continuous electrophoretic separation of an amino acid mixture followed by collection of the species [32]. The chip was designed with a separation channel, connected to seven small columns used for collection of the separated samples. At the end of the separation channel, there were two sheath flow channels and two shaping channels used to focus the separated species into the collection columns. It was demonstrated that the amino acids could be separated and detected after optimization of the device design with COMSOL Multiphysics.

2.3 Physical structure of the microdevice

Here, we will summarize techniques that rely on the actual structure of the device for concentration enhancement and separation. In some cases, a physical

element was used to prevent samples from entering the channel, while in other instances, electrode placement and/or channel shape influenced the concentration enhancement.

2.3.1 Physical elements for trapping

As stated in the introduction of this chapter, this review focuses on recently developed electrophoretic techniques on the microfluidic format that both concentrate and separate in free solution (in the absence of gels, particle packing, etc.). Recently, device designs have been developed that utilize physical features in the device to aid in concentration enhancement before separation. These chip modifications include valves, nanofissures, and ion-selective membranes.

An example of a nanofissure used for preconcentration is described by Yu *et al.* [33]. The PET-toner microfluidic device consisted of two mirror image V-shaped channel designs that were printed on transparency film with a laser printer (PET-toner chip). Between the mirror images was a 100 μm gap. Additional PET films were then laminated over the toner chip. The nanofissures were formed at the gap between the two mirror images. When potential was applied across the mirror image V-shaped channels, protein was concentrated in the gap. At the pH used in these experiments, the channels and nanofissures were negatively charged, causing them to be selective for cations. Because the proteins were negatively charged, they were excluded from entering and were concentrated. An enhancement of 10^3 - 10^5 -fold was achieved for a FITC-labeled protein in 8 minutes. Additional experiments using rhodamine B (positively-charged) and fluorescein (negatively-charged) demonstrated that there was no concentration

increase of the positively-charged species because it was allowed to travel through the nanofissures. Fluorescein, however, was not allowed to enter the nanofissures, so it was concentrated near the entrance of the structures. Further experiments with FITC-DSA and rhodamine B demonstrated that the device could be used for sample purification. The positively-charged rhodamine B was allowed to pass through the nanofissures while the negatively-charged FITC-DSA was concentrated in front of the fissures.

Kuo *et al.* fabricated a PDMS chip for electrophoretic DNA separations that contained a PDMS valve to concentrate the DNA before electrophoresis [34]. The chip had a sample reservoir, buffer reservoir, buffer waste reservoir, a DNA preconcentration area (nanoscale channel), a valve, and a separation channel. The valve was connected to an area linked to a pneumatic pump. For preconcentration, DNA was first introduced into the reservoir and then potential was applied between the sample reservoir (ground) and the buffer waste (anode). During this step, the DNA migrated toward the anode, but the valve remained closed, so the DNA became concentrated in front of the closed valve. After the DNA was concentrated, the normally closed valve was opened via pneumatic suction and the concentrated DNA flowed to the separation channel. The valve was then closed, potential was applied between the buffer reservoir (ground) and the buffer waste (anode), and separation of DNA occurred according to size in the separation channel. Laser-induced fluorescence (LIF) detection was used, and a 3750-fold enhancement of all DNA fragments (initial concentration of 5 $\mu\text{g}/\text{mL}$) was achieved in under 2 min. of preconcentration time. Separation of 11 DNA

fragments took approximately 2.8 minutes in a 40 mm separation channel. Preconcentration times for separations ranged from 20 – 100 s. Signal enhancement was observed for all preconcentrated fragments and an inverse relationship between concentration time and separation time was observed.

Lastly, a proteomic sample electrophoretic preconcentrator using PDMS and a surface patterned ion-selective membrane was developed by Lee *et al.* [35]. A thin-printed Nafion membrane was integrated between a PDMS chip and glass substrate to create a simple means for preconcentration. The ability of the chip to concentrate species was dependent on the voltage difference across the sample channel, with higher voltages resulting in larger preconcentrations. The chip was able to concentrate β -phycoerythrin almost 1000 times in 5 min.

2.3.2 Physical structure used to define local fields

Borofloat glass microfluidic chips were used to separate and trap particles of interest in two different types of channels [8]. One study used straight channels with a uniform diameter to better understand the behavior of the particles, followed by the use of elements with converging and diverging dimensions. The technique presented is referred to as flow-induced electrokinetic trapping (FIET), and particles were trapped with pressure-induced flow, electroosmotic flow (EOF), and their electrophoretic motion. In both channel designs, the cathode was at the inlet and EOF transport was towards the inlet, while pressure-induced flow was in the opposing direction. Experimental data was gathered with polystyrene microspheres that were similar in size but had varying zeta-potentials. All particles had a negative zeta-potential, so their

electrophoretic migration was opposite to EOF. Particles with a given zeta-potential were trapped, while those with a higher zeta-potential were carried through the device by EOF. In the channels with converging and diverging elements, most trapping occurred in the diverging areas. The main advantage of this technique is that no physical barriers were needed for particle trapping.

The Henry group at Colorado State University implemented an expanded detection area, or a bubble cell, during electrophoretic separations with contact conductivity detection [36]. The bubble cell allowed for increased separation field strengths, which lead to shorter separation times. Initial experiments included testing the separation efficiency with fluorescein, followed by experiments with inorganic anions. Results indicated separation efficiency remains statistically the same with or without the bubble cell three times the diameter of the capillary. Bubble cell size was also investigated using sulfamate, perchlorate, and iodate. Results indicated that as the size increased above fourfold, separation efficiency decreased proportionally with the bubble size. Amongst other experiments, threefold bubble cells were used with dilute background electrolyte concentrations, allowing for field-amplified stacking. Detection limits for dithionate (9 ± 1 nM), perchlorate (22 ± 5 nM), and sulfamate (44 ± 10 nM) were lower than the non-stacked methods.

Discontinuous bipolar electrodes (BPEs) were used for both concentration and separation in a glass/PDMS microfluidic device [37]. In this technique, anions were both concentrated and separated when their electrophoretic velocities were equal to and opposite of the EOF. Once immobilized, the focused species

were then moved through the channel. Fluorescence was used to determine the concentration enhancement of BODIPY disulfonate. The electric field was monitored in each experiment to ensure it remained constant and to determine where and how much concentration takes place. Current was monitored through the BPEs, noting that when current increased, concentration enhancement began. Concentration increased approximately 70 times in 180 s. Once the anion was concentrated, it was directed within the channel by switching the electrodes where potential was applied.

A technique used for sample concentration in a straight closed-end microchannel is presented by the Li group from the University of Waterloo in Canada [38, 39]. The device was fabricated with a straight channel connected by two reservoirs and three electrodes. Two electrodes were placed at the ends of the reservoirs, while the remaining electrode was located at the exit of the first reservoir/entrance of the channel. Electroosmotic flow and fluid velocity variation at the closed end of the channel all contributed to fluid movement. Daghighi *et al.* presented a theoretical model and experimental data on separation and concentration in the microchannel [38]. Initially, potential was applied to the device so that species were collected and concentrated near one end of the channel. After concentration, a different potential scheme was applied causing collected species to migrate down the channel and separate based on their electrophoretic mobilities. After theoretical studies were conducted, two types of DNA molecules were concentrated and separated. The combined processes of concentration and separation took just over 200 s, with a concentration increase of

over 90 times in 115 s. Using the same channel design, Jiang *et al.* also described the concentration and separation of a fluorescent dye experimentally and theoretically (Fig. 2.4) [39]. Similar results were obtained as concentration enhancements of 90 times were achieved in 110 s.

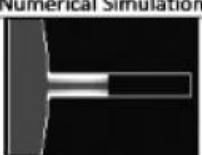
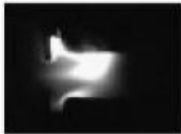






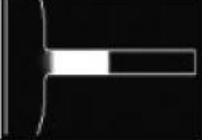

Time	Numerical Simulation	Experimental Results
t=15(s)		
t=30(s)		
t=60(s)		
t=100(s)		
t=110(s)		

Figure 2.4. Comparison of simulated and experimental results for the concentration of fluorescent dye molecules near an electrode. Simulated (left) and experimental (right) results both indicate that fluorescence intensity increases with times of applied potential [39].

2.4 Solution properties influencing local field

Designs that allow for sample separation when an electric field acts directly on the analyte of interest and methods that allow for sample concentration and separation based on some physical features of the device were described in

the above sections. In this section, isoelectric focusing and isotachopheresis and its variations will be described. These two formats exploit solution properties to influence the electric fields.

2.4.1 Isoelectric focusing

IEF is an electrophoretic technique that is used to separate and concentrate molecules, most notably proteins and peptides [3]. Proteins and peptides are examples of amphoteric molecules, or those that are either positively or negatively charged depending on the pH of the solution. During operation, a pH gradient is created in the separation channel, and when potential is applied, the amphoteric molecules move under the influence of the electric field until they reach their isoelectric points (*pI*s), or the pH at which they have a net neutral charge. At this point, species are focused. This technique has been adapted to capillaries (cIEF) [40] and microdevices [1]. Capillary IEF designs from the last two years utilized capillaries in the tens of centimeters range [41, 42], falling outside the scope of this review.

Although there are several applications of IEF in microdevices in the last two years, these designs still use channels whose lengths are in the centimeter range [43-48]. Shimura *et al.* presented a microfluidic chip for IEF that incorporated a valve for loading each solution in individual channels, followed by selective injection, to eventually be incorporated with sample preparation before IEF separations [48]. Four tetramethylrhodamine-labeled peptide *pI* markers were used to test the chip and focusing took from 2-4 min., depending on the marker. A comparison between a glass and a PDMS chip design for separation of

allergenic whey protein was outlined by Poitevin *et al.* out of Paris [47]. Two coatings, HPC and PDMA-AGE, were tested on both chips and it was determined that glass chips coated with HPC resulted in the best IEF separations. Ou *et al.* presented a paper on a hybrid microfluidic device for IEF, using ultraviolet whole channel image detection (UV-WCID) [46]. This design was intended to eliminate the step of placing in a metal optical slit when using whole channel detection. It was determined that the device successfully separated *pI* markers and protein samples of myoglobin and hemoglobin and the fabrication process was more simple and less costly than the chips typically used for whole channel detection. Chou *et al.* performed IEF simulations using the space-time conservation element and solution element (CESE) and Courant-Friedrichs-Lewy number insensitive conservation element and solution element (CNI-CESE) for two different types of channels: one with a varying cross-width (contraction-expansion channel) and one with a constant width [43]. It was found that performing the simplified 1-D model was much faster than the previous 2-D simulations [49].

Cong *et al.* presented a modified IEF technique that changes the electric field strength during the separation process [44]. In the short communication, proteins from *Escherichia coli* were focused on a glass IEF microchip using stepwise increases in electric field strength. Once proteins were separated, the electric field was decreased so that future increases in field strength could be incorporated later for more separations. This step technique resulted in better separations than standard IEF. Dauriac *et al.* also presented a modified IEF design [45]. The group developed a PDMS microfluidic device for separations

containing PDMS micropillars. The micropillars were created as part of the original casting of PDMS and the pillar size and arrangement were studied. The separation of a mixture of seven proteins with pI 's ranging from 4.7 – 10.6 took less than 10 min. Although the pillars were part of the original PDMS casting, they behaved as a dilute gel, so results were compared to IEF minigel electrophoresis. The minigel separations took 20 min., but resulted in less band broadening than the micropillar separations.

2.4.2 Isotachophoresis

A common separation technique used for stacking is isotachophoresis (ITP) [50]. In this technique, there are three different zones: a leading zone with higher mobility ions (LE), a sample zone, and a terminating zone of lower mobility ions (TE). When a voltage is applied, an electric field gradient is created, and the field strength in each zone is inversely related to the ion mobility, which results in separated zones of ions of decreasing mobility. Each zone is defined by a sharp steady state boundary, and these zones are sustained by the differing field strengths. Although ITP is a separation method, it is mostly used as a preconcentration technique for other electrophoretic methods. When ITP is used for preconcentration, it is referred to as transient ITP, or tITP. For a successful ITP enhancement, the ITP step must be completed (i.e., all of the analytes must be stacked) before the other separations technique is employed.

Nagata *et al.* investigated a modified form of tITP, or heterogeneous buffer combination, on a microchip [51]. In the method, the DNA sample is mixed with the TE, which contains taurine anions. Because the mobility of the

taurine ions is lower than that of the acetate ions in the LE, tITP occurs. In addition, hydroxyethylcellulose (HEC) is utilized in the LE buffer. HEC is commonly used as a sieving matrix, but for this technique it is used to limit the diffusion of the sample plug. The separation length was 10 mm, which is three times shorter than the average microchip separation length and DNA ladders, where 10-100 bp were separated. The 10-bp ladders were separated within 60 s while the 100-bp ladders were separated within 50 s and resolution was comparable to the chips with longer channels.

In the work by Goet *et al.*, they developed a microfluidic contractor based on ITP [52]. It operates similarly to micromixers in that it brings samples into contact in order to assist chemical reactions, receptor-ligand interactions, or similar processes. However, micromixers typically use complex channel designs. This novel method utilizes two connected cross-style designs, and several types of experiments were performed. After characterizing the ITP zone transportation in a simple cross-channel chip, ITP zone synchronization was demonstrated using the more complex chip. Using the same sample at different injection sites, it was shown that the zones were able to merge using the method. Next, the group employed two different samples (bromophenol blue and fluorescein-Na). It was found that even if the fluorescein-Na enters the main chamber first, the bromophenol blue can overtake it (Fig. 2.5). Lastly, to demonstrate the utility of such a device, the dyes were replaced with two complementary DNA oligonucleotide strands. To image the hybridization, one strand was tagged with a fluorophore, while the other was tagged with its corresponding quencher. Again,

the zones appeared to overlap, and in this case, interact, resulting in the hybridization of DNA. Through these series of unique experiments, the group has demonstrated a simple means to bring samples into contact using an ITP microcontractor.

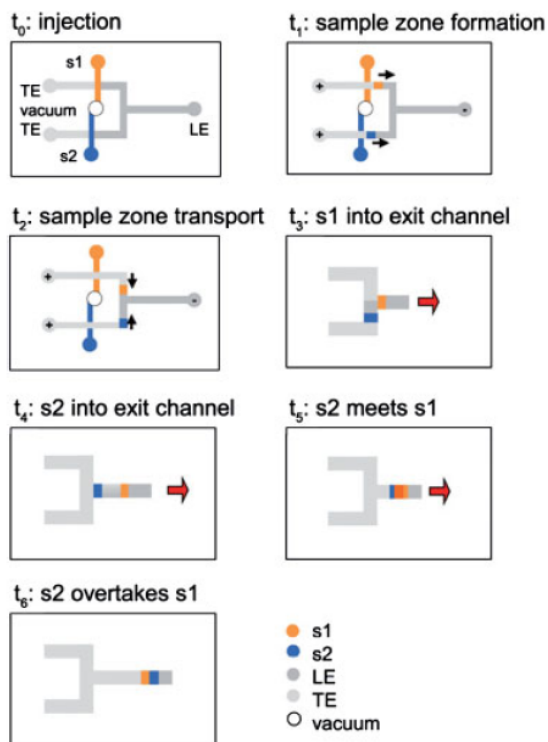


Figure 2.5. Example of two different samples contacting in a microchannel. Fluorescein-Na and bromophenol blue enter the chamber from separate sample ports, then come together in one separation channel [52].

The group of Hirokawa from Japan contributed several new electrophoretic microchip papers, all investigating a method termed electrokinetic supercharging (EKS) [53,54]. EKS is a preconcentration method that combines electrokinetic injection with tITP. In a 2008 contribution, Hirokawa *et al.* investigated a novel injection approach using floating electrodes, termed floating electrokinetic supercharging (FEKS) [53]. Standard Shimadzu electrophoresis

microchips were employed; however, rather than pinched injection, two ports were utilized to facilitate a rapid switch from ITP to microchip gel electrophoresis (MGE). Models of the system were developed and examined using a mixture of 50-bp step ladder DNA. It was found that his strategy improved LODs ten-fold as compared to conventional pinched-injection. Furthermore, resolution was improved over EKS-MGE from 0.77 to 1.62 for 50-100-bp DNA fragments and 0.89 to 1.32 for 200-250-bp DNA fragments.

The FEKS technique was further studied by Xu *et al.* [54]. In this contribution, the microchip for FEKS was modified so that the EKS concentration occurred in a curved channel with five U-shaped turns. This curved design allowed for longer ITP prior to MGE. Some modeling was performed, followed by experiments using DNA fragments. Overall, by extending the ITP steps by incorporating a curved channel, LOD was improved to 9.7, 5.0, and 5.5 ng/mL for 100, 300, and 500-bp DNA fragments, respectively. These LODs are a significant improvement over pinched injection EKS and cross-chip EKS.

Various aspects of microchip ITP are under investigation by the Treves Brown research group [55-58]. A novel means of sample injection is introduced for microchip ITP devices [55]. Whereas many sample injections are traditionally cross or double-T configurations, their work presents a modified four channel injection. The injection scheme has a wide bore sample loop and narrower side arm channels for separation and injection. The device enables variable volumes to be delivered, including smaller volumes (for highly concentrated samples) or larger volumes (for dilute samples). Another ITP microchip modification

introduced by the Treves Brown group includes a low-cost, robust polystyrene chip that includes both integrated drive and detection electrodes [57]. The microchip design contains polystyrene as well as 40% carbon fiber loaded polystyrene electrodes. These electrodes are utilized to drive the separations and for conductivity detection.

Other ITP microchip research by the group includes detecting magnesium as well as chlorate, chloride, and perchlorate anions in inorganic explosive residues [56, 57]. For the magnesium studies, various complexing agents were employed in the LE, which impacted the mobilities of the cations. It was determined that malonic acid was most effective as a complexing agent in microchip ITP for magnesium [56]. In order to analyze chloride, chlorate, and perchlorate, various electrolytes were investigated. These ions are difficult to analyze with ITP because of their very high electrophoretic mobilities (often making them suitable LEs). In order to overcome these challenges, a nitrate-based LE was employed with indium (III) and α -cyclodextrin as complexing agents. Inorganic explosive residues were analyzed with the method, and the results obtained were confirmed with ion chromatography [57].

The Santiago group has published numerous interesting papers investigating electrophoretic methods on a microchip from 2008-2010 [59-77], including several that contribute to the theoretical basis of the technique [59, 64, 67, 69-72, 75, 76, 78] and some novel approaches for indirect detection [77, 66]. A select group of these works were chosen for discussion here. In a 2009 contribution, his group demonstrated an ITP method capable of purifying nucleic

acids from whole blood [60]. The LE and TE are chosen based upon their compatibility with the contents of blood lysate. Figure 2.6 shows how the nucleic acids are focused while the proteins and other blood lysate contents move slower than the ITP interface. The nucleic acids were collected and interrogated with PCR to ensure the fractions were purified DNA. The efficiency of the method is comparable to other microchip purification methods, obtaining 100% efficiency for λ -DNA, and between 30 and 70% for whole blood.

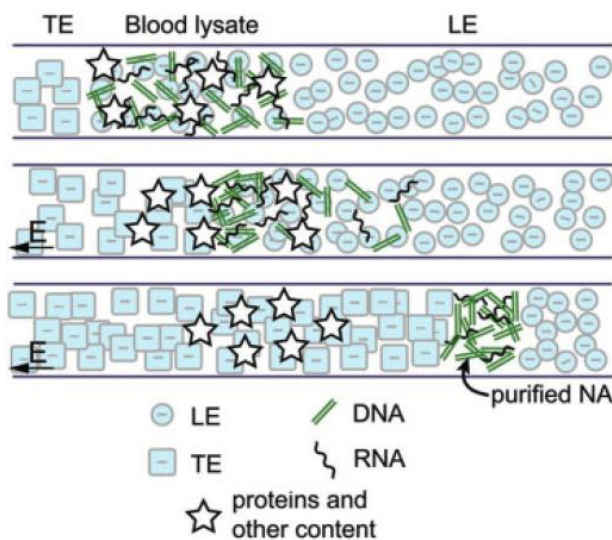


Figure 2.6. ITP schematic showing a nucleic acid purification from blood lysate. The DNA is represented by rods, while the proteins and other content is signified by the stars. When an electric field is applied, the nucleic acids focus between the LE (circles) and TE (squares), while the proteins move slower than the ITP interface [60].

In another contribution, the group investigated simultaneous preconcentration and separation of analyte zones in ITP without the use of spacers or further separation steps [68]. Their studies show that carbonate ions formed from dissolved atmospheric CO_2 and carbamate ions formed from the CO_2 and its

reactions with primary and secondary amines in the buffer create zones during ITP separation. The carbonate ions were found to interfere with the ITP, resulting in a broadening of the TE-LE interface. Although such zones can have adverse effects on ITP preconcentration efficiency, the group demonstrated how these zones can improve on-chip CE. For example, by utilizing these zones, both preconcentration and separation can occur simultaneously without the need for further buffer exchange steps. The benefits of these zones were demonstrated on 25-bp DNA ladders and DNA ladders with green fluorescent protein and allophycocyanin.

Masar *et al.* presented a commercial PMMA column-coupling device design that couples ITP for sample concentration and CZE with contact conductivity detection [79]. The chip contained two separation channels and was used for the separation of cations commonly found in drinking water: ammonium, calcium, magnesium, potassium, and sodium. It was determined that the chip was able to sensitively and reproducibly separate the cations.

Wang *et al.* combined ITP with microcapillary electrophoresis (MCE) for the concentration and separation of bovine serum albumin (BSA) and its immunocomplex with mAb [80]. A PMMA microchip with a single cross design was utilized in the work. Six different LEs and six different TEs were studied for their ability to enhance the ITP stacking. By employing tris- H_3PO_4 as a LE and tris- γ -aminobutyric acid, a 2000-fold enhancement of the BSA and mAb was obtained.

A microchip ITP method capable of analyzing highly saline PCR samples was investigated in a contribution by Wang *et al.* [81]. The method utilized the chloride ions in the PCR buffer to act as the LE and HEPES for the TE in a cross-style microchannel. Digested DNA samples and DL-2000 DNA markers were shown to have a 20-fold concentration enhancement. Overall, the technique increased the sensitivity of the PCR samples with no loss in resolution.

Qi *et al.* designed a microchip that combined ITP preconcentration with gel electrophoretic separation (ITP-GE) [82]. The chip contained a negative pressure sampler comprised of a three-way electromagnetic valve and a single high voltage power supply. The ITP step occurred in free solution, and the sample stacks between the LE and TE in less than 1 s at the interface between the gel and solution. The samples are then separated by gel CE. The apparatus was examined using DNA fragments. This ITP-GE method, compared to microchip GE alone, was found to enhance sensitivity by 185 times.

The theoretical basis of different electrophoretic systems are examined by Chou *et al.* [83] using a space-time conservation element assimilated with an adaptive mesh redistribution scheme (AMR-CESE). By assigning initial conditions, such as parameters of analytes, applied voltage, and grid size, the end time can be ascertained, as well as the concentration, pH, profile, and conductivity distribution within the channel. Three different electrophoretic techniques were investigated: ITP, IEF in an immobilized pH gradient, and IEF of a sample within 10 background ampholytes. This novel AMR-CESE technique was found to

resolve points of discontinuity in the concentration distribution and compared to uniform mesh methods, fewer grid points were required for a given resolution.

Danger and Ross have developed a novel isotachophoretic approach termed gradient elution isotachopheresis (GEITP) [84]. In this method, a counterflow is applied that opposes the channel entrance and is slowly varied to selectively elute the LE, analytes, and TE into the capillary. Using the GEITP method, the group performed chiral separations with fluorescently-labeled amino acid mixtures. Capillary lengths of 3 cm were employed, and various parameters including electrolyte pH, pressure scan rate, and chiral selector concentration were manipulated to achieve high-resolution separations. Studies from the Shackman group at Temple University have also investigated this technique [85, 86].

A technique similar to GEITP was introduced by Ross and Kralj called gradient elution moving boundary electrophoresis (GEMBE) [87]. The method utilizes a buffer reservoir with sixteen 3-mm capillaries, each with individual sample reservoirs, and conductivity detection. This combines electrophoresis with a gradient counterflow to elute species into the capillary. To demonstrate the technique, the activity of protein kinase A and the inhibition of that activity by H-89 dihydrochloride were monitored. The GEMBE technique was further studied by Ross and Romantseva both theoretically and through experiments to optimize various parameters, including channel length, electric field, and counterflow acceleration [88]. Using various organic acids, detection limits of the method were found to be in the low micromolar range. Even though the basic method

was 10-20 times slower than CE, fast separations (less than 1 s) can be attained, and higher field strengths could be applied with modest voltages due to the short capillary lengths.

2.5 Concluding remarks

This literature review has focused on elements that are essentially new or are significant advances in strategies that uniquely exploit microfluidic formats during the time span of January 2008 to summer 2010. These papers contributed new and valuable capabilities to the field by addressing issues such as long analysis times and poor detection limits. These designs kept devices simple, allow for an array of sample types, and could be incorporated with several other aspects of analysis on a chip.

In examining the literature over this relatively short period of time, there were a large number of papers published in the area of ITP. This was largely driven by the Santiago group and was based on its sample preconcentration properties, as well as its feasibility to be incorporated on-chip. Closely related, but with a creative twist, GEMBE and GEITP used counterflow to preconcentrate while separating species of interest, much like the ingenious TGF technique. TGF, while rather brilliant in its inception, does have the disadvantage of being tied to specific buffer systems. In contrast, IEF a long-standing and well-established technique, can also focus while separating; however, IEF has limited applicability with protein samples, due to their low solubility at their pI .

Another broad category of techniques, those we classify as relying on the direct interaction of the electric field with the analyte, has been used to

successfully separate diverse samples. These techniques are obviously practical, as they can be used for many different types of mixtures. One popular method in this area—based on numbers of contributions—is on-chip FFE, given its advantage of not requiring elution after separation. Its ultimate limitation (if it could be called that) is that analytes must be spatially separated after the separative/diffusive processes, resulting in possible design and size constraints.

Many designs described here use physical elements, such as valves, nanofissures, and variable channel geometries to either trap samples or to shape electric fields. Although these devices are effective at capturing species, they must be completely reworked to accommodate small changes. However, these methods are to be applicable to a wide range of samples and represent a truly unique microfluidic approach to separations.

A very select group of electrophoretic techniques that uniquely exploited the microfluidic format or addressed a significant obstacle of the paradigm have been presented here. These methods have the potential to affect a wide variety of research fields that require complex sample analysis. Overall, this research looks to address the challenges of applying basic attributes for separations sciences to create portable, fast, and low analyte-consumption devices for better biochemical analysis.

2.6 References

- [1] Hofmann, O., Che, D. P., Cruickshank, K. A., Muller, U. R., *Anal. Chem.* 1999, *71*, 678-686.
- [2] Righetti, P. G., Drysdale, J. W., *Ann. NY Acad. Sci.* 1973, *209*, 163-186.
- [3] Vesterbe, O., Svensson, H., *Acta Chem. Scand.* 1966, *20*, 820-&.

- [4] Hannig, K. Z., *Anal. Chem.* 1961, *181*, 244-254.
- [5] Hoffstetterkuhn, S., Kuhn, R., Wagner, H., *Electrophoresis* 1990, *11*, 304-309.
- [6] Tang, G. Y., Yang, C., *Electrophoresis* 2008, *29*, 1006-1012.
- [7] Ge, Z. W., Yang, C., Tang, G. Y., *Int. J. Heat Mass Transfer* 2010, *53*, 2722-2731.
- [8] Jellema, L. C., Mey, T., Koster, S., Verpoorte, E., *Lab Chip* 2009, *9*, 1914-1925.
- [9] Becker, M., Marggraf, U., Janasek, D. J., *Chromatogr. A* 2009, *1216*, 8265-8269.
- [10] Fonslow, B. R., Bowser, M. T., *Anal. Chem.* 2008, *80*, 3182-3189.
- [11] Kostal, V., Fonslow, B. R., Arriaga, E. A., Bowser, M. T., *Anal. Chem.* 2009, *81*, 9267-9273.
- [12] Turgeon, R. T., Bowser, M. T., *Electrophoresis* 2009, *30*, 1342-1348.
- [13] Zalewski, D. R., Kohlheyer, D., Schlautmann, S., Gardeniers, H., *Anal. Chem.* 2008, *80*, 6228-6234.
- [14] Vollmer, S., Astorga-Wells, J., Alvelius, G., Bergman, T., Jornvall, H., *Anal. Biochem.* 2008, *374*, 154-162.
- [15] Gebauer, P., Mala, Z., Bocek, P., *Electrophoresis* 2010, *31*, 886-892.
- [16] Mala, Z., Gebauer, P., Bocek, P., *Electrophoresis* 2009, *30*, 866-874.
- [17] Meighan, M. M., Keebaugh, M. W., Quihuis, A. M., Kenyon, S. M., Hayes, M. A., *Electrophoresis* 2009, *30*, 3786-3792.
- [18] Weiss, N. G., Zwick, N. L., Hayes, M. A., *J. Chromatogr. A* 2010, *1217*, 179-182.
- [19] Ansell, R. J., Tunon, P. G., Wang, Y. T., Myers, P., Ivory, C. F., Keen, J. N., Findlay, J. B. C., *Analyst* 2009, *134*, 226-229.
- [20] Burke, J. M., Smith, C. D., Ivory, C. F., *Electrophoresis* 2010, *31*, 902-909.
- [21] Raymond, D. E., Manz, A., Widmer, H. M., *Anal. Chem.* 1994, *66*, 2858-2865.

- [22] Turgeon, R. T., Fonslow, B. R., Jing, M., Bowser, M. T., *Anal. Chem.* 2010, 82, 3636-3641.
- [23] Kohlheyer, D., Eijkel, J. C. T., Schlautmann, S., van den Berg, A., Schasfoort, R. B. M., *Anal. Chem.* 2008, 80, 4111-4118.
- [24] Ross, D., Gaitan, M., Locascio, L. E., *Anal. Chem.* 2001, 73, 4117-4123.
- [25] Lin, H., Shackman, J. G., Ross, D., *Lab Chip* 2008, 8, 969-978.
- [26] Danger, G., Ross, D., *Electrophoresis* 2008, 29, 3107-3114.
- [27] Munson, M. S., Meacham, J. M., Locascio, L. E., Ross, D., *Anal. Chem.* 2008, 80, 172-178.
- [28] Munson, M. S., Meacham, J. M., Ross, D., Locascio, L. E., *Electrophoresis* 2008, 29, 3456-3465.
- [29] Reschke, B. R., Luo, H., Schiffbauer, J., Edwards, B. F., Timperman, A. T., *Lab Chip* 2009, 9, 2203-2211.
- [30] Reschke, B. R., Schiffbauer, J., Edwards, B. F., Timperman, A. T., *Analyst* 2010, 135, 1351-1359.
- [31] Kawamata, T., Yamada, M., Yasuda, M., Seki, M., *Electrophoresis* 2008, 29, 1423-1430.
- [32] Baker, C. A., Roper, M. G., *J. Chromatogr. A* 2010, 1217, 4743-4748.
- [33] Yu, H., Lu, Y., Zhou, Y. G., Wang, F. B., He, F. Y., Xia, X. H., *Lab Chip* 2008, 8, 1496-1501.
- [34] Kuo, C. H., Wang, J. H., Lee, G. B., *Electrophoresis* 2009, 30, 3228-3235.
- [35] Lee, J. H., Song, Y. A., Han, J. Y., *Lab Chip* 2008, 8, 596-601.
- [36] Noblitt, S. D., Henry, C. S., *Anal. Chem.* 2008, 80, 7624-7630.
- [37] Perdue, R. K., Laws, D. R., Hlushkou, D., Tallarek, U., Crooks, R. M., *Anal. Chem.* 2009, 81, 10149-10155.
- [38] Daghighi, Y., Li, D. Q., *Electrophoresis* 2010, 31, 868-878.
- [39] Jiang, H., Daghighi, Y., Chon, C. H., Li, D. Q., *J. Colloid Interface Sci.* 2010, 347, 324-331.
- [40] Hjerten, S., Zhu, M. D., *J. Chromatogr.* 1985, 346, 265-270.

- [41] Horka, M., Ruzicka, F., Hola, V., Slais, K., *Electrophoresis* 2009, 30, 2134-2141.
- [42] Poitevin, M., Peltre, G., Descroix, S., *Electrophoresis* 2008, 29, 1687-1693.
- [43] Chou, Y., Yang, R. J., *Electrophoresis* 2009, 30, 819-830.
- [44] Cong, Y. Z., Liang, Y., Zhang, L. H., Zhang, W. B., Zhang, Y. K., *J. Sep. Sci.* 2009, 32, 462-465.
- [45] Dauriac, V., Descroix, S., Chen, Y., Peltre, G., Senechal, H., *Electrophoresis* 2008, 29, 2945-2952.
- [46] Ou, J. J., Glawdel, T., Ren, C. L., Pawliszyn, J., *Lab Chip* 2009, 9, 1926-1932.
- [47] Poitevin, M., Shakalisava, Y., Miserere, S., Peltre, G., Viovy, J. L., Descroix, S., *Electrophoresis* 2009, 30, 4256-4263.
- [48] Shimura, K., Takahashi, K., Koyama, Y., Sato, K., Kitamori, T., *Anal. Chem.* 2008, 80, 3818-3823.
- [49] Shim, J., Dutta, P., Ivory, C. F., *Electrophoresis* 2007, 28, 572-586.
- [50] Everaerts, F. M., Verheggen, T., Mikkers, F. E. P., *J. Chromatogr.* 1979, 169, 21-38.
- [51] Nagata, H., Ishikawa, M., Yoshida, Y., Tanaka, Y., Hirano, K., *Electrophoresis* 2008, 29, 3744-3751.
- [52] Goet, G., Baier, T., Hardt, S., *Lab Chip* 2009, 9, 3586-3593.
- [53] Hirokawa, T., Takayama, Y., Arai, A., Xu, Z. Q., *Electrophoresis* 2008, 29, 1829-1835.
- [54] Xu, Z. Q., Murata, K., Arai, A., Hirokawa, T., *Biomicrofluidics* 2010, 4.
- [55] Baldock, S. J., Fielden, P. R., Goddard, N. J., Kretschmer, H. R., Prest, J. E., Brown, B. J., T. *Microelectron. Eng.* 2008, 85, 1440-1442.
- [56] Prest, J. E., Baldock, S. J., Fielden, P. R., Goddard, N. J., Brown, B. J. T., *Anal Bioanal Chem* 2009, 394, 1299-1305.
- [57] Prest, J. E., Beardah, M. S., Baldock, S. J., Doyle, S. P., Fielden, P. R., Goddard, N. J., Brown, B. J. T., *J. Chromatogr. A* 2008, 1195, 157-163.

- [58] Prest, J. E., Fielden, P. R., Goddard, N. J., Brown, B. J. T., *Meas. Sci. Technol.* 2008, *19*.
- [59] Mani, A., Zangle, T. A., Santiago, J. G., *Langmuir* 2009, *25*, 3898-3908.
- [60] Persat, A., Marshall, L. A., Santiago, J. G., *Anal. Chem.* 2009, *81*, 9507-9511.
- [61] Persat, A., Santiago, J. G., *New J. Phys.* 2009, *11*.
- [62] Persat, A., Suss, M. E., Santiago, J. G., *Lab Chip* 2009, *9*, 2454-2469.
- [63] Schoch, R. B., Ronaghi, M., Santiago, J. G., *Lab Chip* 2009, *9*, 2145-2152.
- [64] Zangle, T. A., Mani, A., Santiago, J. G., *Langmuir* 2009, *25*, 3909-3916.
- [65] Zangle, T. A., Mani, A., Santiago, J. G., *Chem. Soc. Rev.* 2010, *39*, 1014-1035.
- [66] Khurana, T. K., Santiago, J. G., *Anal. Chem.* 2008, *80*, 279-286.
- [67] Khurana, T. K., Santiago, J. G., *Anal. Chem.* 2008, *80*, 6300-6307.
- [68] Khurana, T. K., Santiago, J. G., *Lab Chip* 2009, *9*, 1377-1384.
- [69] Lin, H., Storey, B. D., Santiago, J. G., *J. Fluid Mech.* 2008, *608*, 43-70.
- [70] Bahga, S. S., Bercovici, M., Santiago, J. G., *Electrophoresis* 2010, *31*, 910-919.
- [71] Baldessari, F., Santiago, J. G., *J. Colloid Interface Sci.* 2009, *325*, 526-538.
- [72] Baldessari, F., Santiago, J. G., *J. Colloid Interface Sci.* 2009, *325*, 539-546.
- [73] Bercovici, M., Kaigala, G. V., Backhouse, C. J., Santiago, J. G., *Anal. Chem.* 2010, *82*, 1858-1866.
- [74] Bercovici, M., Kaigala, G. V., Santiago, J. G., *Anal. Chem.* 2010, *82*, 2134-2138.
- [75] Bercovici, M., Lele, S. K., Santiago, J. G., *J. Chromatogr. A* 2009, *1216*, 1008-1018.
- [76] Bercovici, M., Lele, S. K., Santiago, J. G., *J. Chromatogr. A* 2010, *1217*, 588-599.

- [77] Chambers, R. D., Santiago, J. G., *Anal. Chem.* 2009, *81*, 3022-3028.
- [78] Huber, D. E., Santiago, J. G., *Proc. R. Soc. A* 2008, *464*, 595-612.
- [79] Masar, M., Sydes, D., Luc, M., Kaniansky, D., Kuss, H. M., *J. Chromatogr. A* 2009, *1216*, 6252-6255.
- [80] Wang, J., Zhang, Y., Mohamadi, M. R., Kaji, N., Tokeshi, M., Baba, Y., *Electrophoresis* 2009, *30*, 3250-3256.
- [81] Wang, L. H., Liu, D. Y., Chen, H., Zhou, X. M., *Electrophoresis* 2008, *29*, 4976-4983.
- [82] Qi, L. Y., Yin, X. F., Liu, J. H., *J. Chromatogr. A* 2009, *1216*, 4510-4516.
- [83] Chou, Y., Yang, R. J., *J. Chromatogr. A* 2010, *1217*, 394-404.
- [84] Danger, G., Ross, D., *Electrophoresis* 2008, *29*, 4036-4044.
- [85] Mamunooru, M., Jenkins, R. J., Davis, N. I., Shackman, J. G., *J. Chromatogr. A* 2008, *1202*, 203-211.
- [86] Vyas, C. A., Mamunooru, M., Shackman, J. G., *Chromatographia* 2009, *70*, 151-156.
- [87] Ross, D., Kralj, J. G., *Anal. Chem.* 2008, *80*, 9467-9474.
- [88] Ross, D., Romantseva, E. F., *Anal. Chem.* 2009, *81*, 7326-7335.

Chapter 3

Electrophoretic Exclusion on a Benchtop Device

3.1 Introduction

The role of separations science techniques, such as chromatography [1-4] and capillary electrophoresis [5, 6], for complex sample analysis has been established (Chapter 1). To further exploit the capabilities of separations when studying complex matrices, equilibrium gradient techniques, first described by Giddings and Dahlgren in 1971, are often employed to simultaneously differentiate and concentrate species [7]. For successful separation and concentration, analytes move to a focusing point in a channel, where they are also concentrated. The focusing point is a result of opposing forces and is specific to the analytes' properties. Therefore, species with dissimilar properties stop at different points in the channel. Isoelectric focusing, described previously (Chapters 1 & 2), is an example of a traditional equilibrium gradient separation scheme. Many contributions of capillary isoelectric focusing are reviewed [8].

More recently, researchers have begun adding hydrodynamic counterflow to equilibrium gradient techniques. This addition innovatively increases concentration factors. Counterflow was first applied to CE systems in the mid-1990's [9], and is now more widely used in equilibrium gradient techniques research. These counterflow equilibrium gradient techniques include electric field gradient focusing [10-13], dynamic field gradient focusing [14], temperature gradient focusing [15-18], conductivity gradient focusing [19], gradient elution moving boundary electrophoresis (GEMBE) [20-23], and gradient elution

isotachopheresis (GEITP) [24-26]. Briefly, in the counterflow equilibrium gradient techniques mentioned above, species are separated in a channel when their electrophoretic velocities are exactly equal to and opposite of the hydrodynamic flow through the channel. Molecules therefore become stationary at unique points in the column. A more thorough description is presented in Chapter 1.

Electrophoretic exclusion takes advantage of a hydrodynamic counterflow. As mentioned previously, this separations technique differentiates species based upon their electrophoretic mobilities by applying an opposing fluid flow into a channel to counteract the velocity of the species exiting the channel in the presence of an electric field. Electrophoretic exclusion differs from the other counterflow techniques by separating species in bulk solution, as opposed to in a channel. Work performed by Hori *et al.* used a similar theory on the macroscale [27]. A 1.5 mm diameter tube was used to connect two chambers where samples were held, and much larger sample volumes were used (tens of milliliters). Additionally, experiments performed by Polson *et al.* excluded fluorescent particles (200 nm in diameter) from the entrance of a 20 μm i.d. capillary when potential was applied to the system [28]. More recently, studies have demonstrated the successful exclusion of small dye molecules and proteins at the entrance of a capillary using a flow-injection method [29, 30].

The work summarized here is an investigation of the electrophoretic exclusion method at the entrance of one capillary in a central reservoir. The significant differences between what is being proposed here and the flow-

injection system above is that the apparatus has been modified to include the central reservoir and larger bore capillaries. Larger inner diameter capillaries were used as a method for increasing the flow rate so that more fluid could be transferred through the system, potentially allowing for a reduced time for concentration increase as more of the analyte would be transferred to the reservoir in less time. The central reservoir was added so that exclusion could occur in a constrained volume, with flow both entering and leaving the chamber. The advantage of exclusion in a constrained volume is that it allows for the possibility of having several reservoirs in a single device where multiple analytes could be separated simultaneously simply by applying different potentials. Here, the reservoir design was able to successfully trap methyl violet dye when potential was applied to the system for various times.

3.2 Materials and methods

3.2.1 Reagent preparation

DL aspartic acid (FW: 133) and Methyl Violet (FW: 393), purchased from Sigma-Aldrich (St. Louis, MO) and hydrochloric acid (HCl), purchased from Mallinckrodt (Hazelwood, MO) were used as received. Aspartic acid buffer was prepared to 5 mM using 18 M Ω water and adjusted to pH 2.85 using 1 M HCl. A stock solution of methyl violet was prepared at a concentration of 1 mM in 5 mM aspartic acid buffer. Methyl violet was diluted to 20 μ M for individual trials.

3.2.2 Instrumentation

The electrophoretic exclusion device was made in-house (Fig. 3.1). Two polyimide-coated fused silica capillaries (5 cm in length, 180 μ m i.d., 350 μ m

o.d.) were expoxied to opposite sides of a 350 μ L reservoir that was made by modifying a 1.5 mL plastic cuvette (Fig. 3.1A). An electrode was fabricated on one side of the reservoir by sputter-coating one of the capillaries with 30 nm of titanium and 50 nm of platinum after removing \sim 3 mm of the polyimide coating. This sputtered portion was then physically connected to a piece of platinum wire (\sim 0.5 cm in length) with silver conductive epoxy (Fig. 3.1B). The ends of the capillaries not connected to the reservoir were attached to 2 mL glass vials to complete the device (Fig. 3.1C).

The gate system was mounted on a rotatable board that allowed for the control of the flow rate by adjusting the height difference between the menisci, resulting in pressure-driven flow (Fig. 1C, bottom). The glass vials were open to air, while the central reservoir was sealed using wax. All experiments used a height difference of 0.5 cm between the menisci with a calculated flow rate of 25 nL/s. Samples were introduced to the system by using a syringe to add dye to one of the glass vials. Compressed nitrogen was then passed through the system to more quickly force the sample through the entire system.

The exclusion system was built using a CZE1000R high voltage power supply (Spellman High Voltage Electronics Corporation, Hauppauge, NY), a USB4000 detector, a Mikropak halogen light source (both Ocean Optics, Dunedin, FL), and a plastic holder for the reservoir (made in-house). Fiber optic cables were secured on the outside of the central reservoir with the plastic reservoir holder and absorbance was measure at 585 nm and 670 nm for all trials

(Fig. 3.1C). Data was recorded using SpectraSuite software (Ocean Optics, Dunedin, FL).

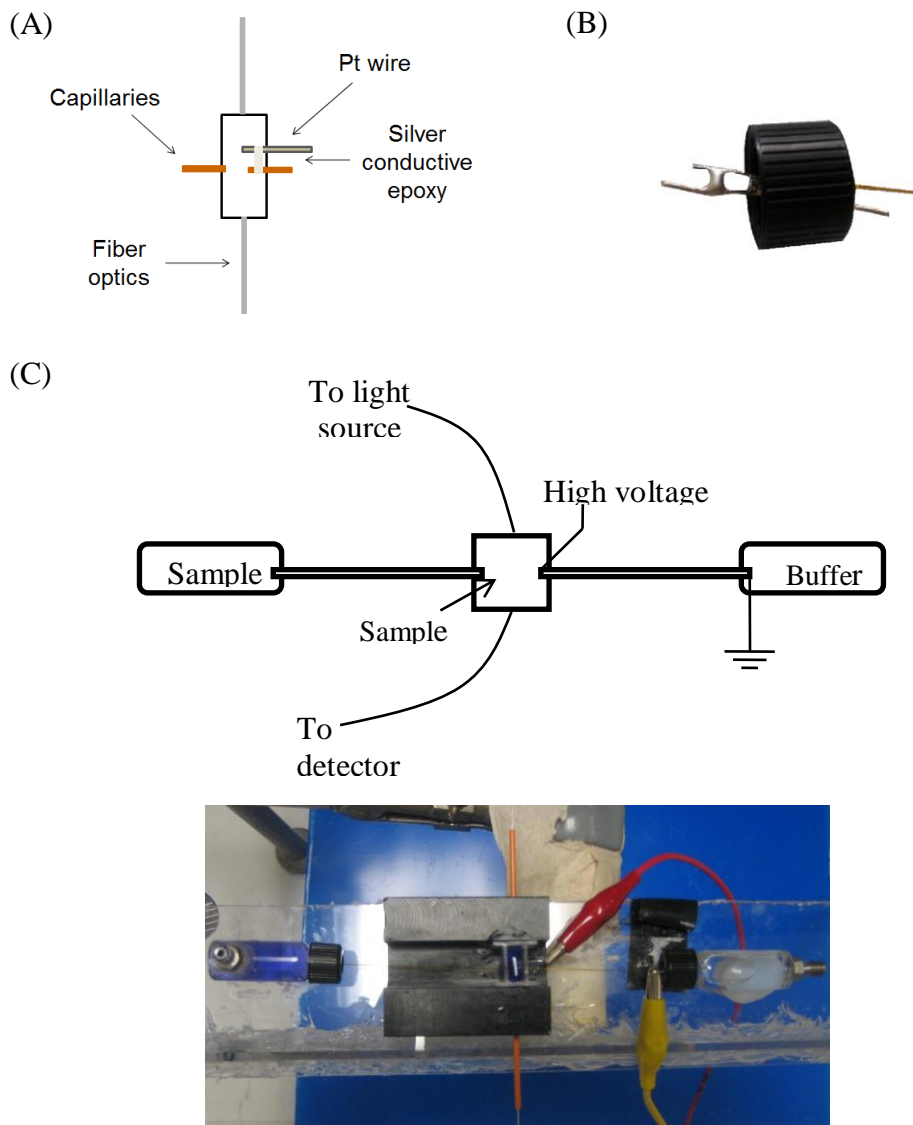


Figure 3.1. Benchtop device design. (A) Schematic of central reservoir. (B) Photograph of the electrode, showing the capillary tip and sputter-coated capillary tip. (C) Schematic (top) and top view photograph (bottom) of electrophoretic exclusion device (wax on central reservoir is excluded to better show reservoir).

3.2.3 Planar prototypes

Two planar electrophoretic exclusion prototypes were constructed in-house (Fig. 3.2). Prototype 1 was assembled with PDMS and capillaries (Fig. 3.2A). A 10:1 weight percent ratio of elastomer to curing agent was poured onto an unpatterned silicon wafer. Five short capillaries were then laid in the PDMS, followed by another five capillary bundle, so that there was a space of approximately 5 mm between the ends of the bundles. A short piece of platinum wire (~ 2 cm) was bent at a 90 degree angle and laid in the PDMS next to each end of the capillary bundles. The PDMS, capillaries, and wires were baked in a 70°C oven for 1 hour. The entire device was then peeled from the silicon wafer. Holes were cut using a razor blade at each end of the capillary bundles (air bubbles had formed where the air had escaped during the baking process) to create entrance, central, and exit reservoirs. A thin layer of cured PDMS was attached with silicone glue to the bottom of the entire device and over the top of each of the reservoirs. Syringes with attached needles were then pushed through the sides of the exit and entrance reservoirs.

Prototype 2 was constructed from a standard glass microscope slide, three 4 mL plastic cuvettes, and 10 short (~2 cm) capillaries (Fig. 3.2B). Two of the cuvettes were used as entrance and exit reservoirs. The ends were removed using a hacksaw and a small groove (~ 3 mm wide and 1 mm high) was sanded from one end on each of these cuvettes so that capillaries were allowed to penetrate into the cuvette once attached to the microscope slide. The third cuvette was used as a central reservoir and was modified by removing the upper 4 cm of the cuvette and

flipped upside down on the microscope slide. Grooves were also sanded in each side of the central reservoir to allow for capillaries. The device was completed by laying out the entrance reservoir, followed by a 5 capillary bundle, the central reservoir, another 5 capillary bundle, and the exit reservoir to the microscope slide. Silicone epoxy was used to secure the reservoirs and to prevent fluid leaks.

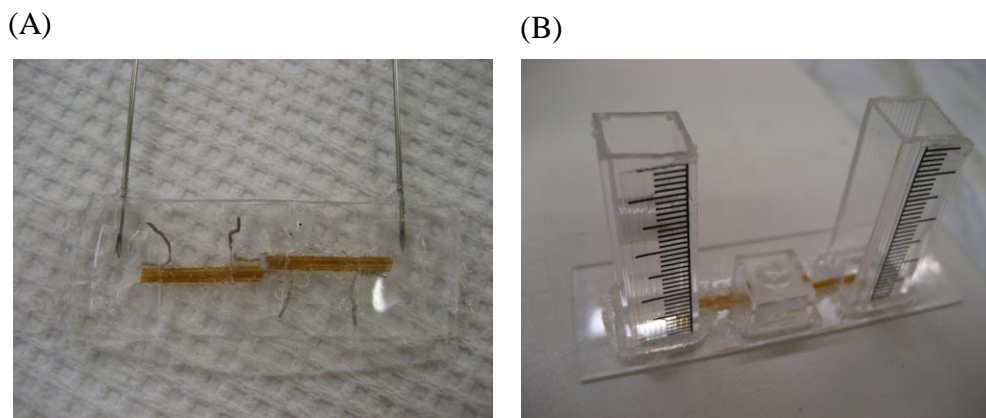


Figure 3.2. Planar prototypes. (A) PDMS/capillary hybrid device. (B) Device fabricated using cuvettes.

3.3 Results and discussion

3.3.1 Exclusion criteria

Electrophoretic exclusion uses counterflow and the electrophoretic velocity of species to prevent molecules from entering a channel. Briefly, a species is excluded or captured when its electrophoretic velocity is greater than or equal to the opposing hydrodynamic flow. In this benchtop design, exclusion of methyl violet dye in the central reservoir occurred when an electric field of an appropriate magnitude was applied at the second capillary entrance (Fig. 3.1). Based upon this description, the three parameters necessary for exclusion are

applied electric field, hydrodynamic flow, and the electrophoretic mobility of the species of interest. Methyl violet was used in 5 mM aspartic acid buffer for all experiments, so the electrophoretic mobility ($\mu_{ep} = 1.7 \times 10^{-4} \text{ cm}^2/\text{Vs}$) was assumed to remain constant in all trials. Additionally, the hydrodynamic flow rate was held constant throughout all experiments, so varying the applied electric field allowed for the control of exclusion from the capillary.

3.3.2 Calculated concentration enhancement model

A simple model of the concentration change in the reservoir was constructed (Fig. 3.3A). In the absence of an electric field, the only force acting on the system is the hydrodynamic flow, which is induced by creating a height difference between the menisci in the sample vials and the central reservoir. Under these conditions, the amount of methyl violet entering the central reservoir is equal to the amount leaving the central reservoir. The amount of methyl violet in the central reservoir was determined by calculating the flux of methyl violet into and out of the central reservoir at a specific time, using the equation:

$$J = cxA, \tag{1}$$

where J is the mass flux, c is equal to concentration, x is equal to linear flow velocity, and A is the cross sectional area of the channel. Because the flux into and out of the central reservoir is equal before potential is applied, the concentration is expected to remain constant.

Once a large enough electric field is applied to the system, the amount of methyl violet entering the reservoir remains constant; however, there is no methyl violet leaving the central reservoir (though buffer is still allowed to leave and is

unaffected by the electric field). This is expected to cause a concentration increase in the central reservoir, as predicted in the model. Immediately after potential is applied, the concentration of methyl violet begins to increase. Once the potential is removed the concentration of methyl violet in the reservoir asymptotically returns to baseline, suggesting that the excluded dye is allowed to again flow through the system.

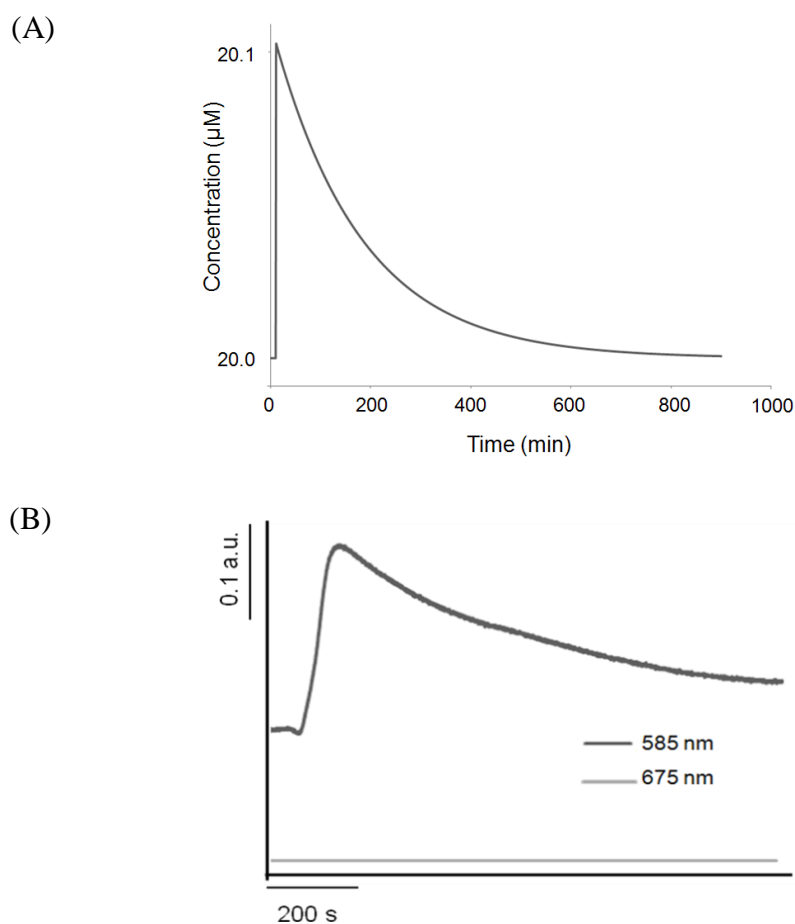


Figure 3.3. Curves representing electrophoretic exclusion of methyl violet dye. (A) Model of concentration increase and decrease calculated using the flux into and out of the central reservoir when potential is applied to the system for 60 s. (B) Absorbance curve showing the change in absorbance when potential was applied to the system for 60 s.

3.3.3 Exclusion of methyl violet

Initial experiments included the exclusion of cationic methyl violet from the entrance of the second capillary. A representative example of an absorbance curve for 60 s of applied potential is shown (Fig. 3.3B). Similar to the model (Fig. 3.3A), before potential is applied to the system, the absorbance, (concentration in the model), remains constant in the central reservoir. Once potential is applied, the methyl violet collects near the tip of the capillary and results in an increase of absorbance. This increase in absorbance can be interpreted as the methyl violet being captured in the central reservoir, as expected, and predicted, by the concentration model. When the potential is removed, the absorbance decreases in the same manner that the concentration decreases in the model. As a control, in addition to recording absorbance at 585 nm (λ_{max} for methyl violet), the absorbance at 675 nm was also measured. Methyl violet does not absorb at 675 nm, so these wavelengths were monitored simultaneously to ensure that the absorbance increase was due to exclusion of methyl violet and not physical disturbances to the system. Based upon the unchanging absorbance observed at 675 nm, it is concluded that the absorbance change at 585 nm is the result of methyl violet being excluded, and therefore, causing a concentration increase, in the central reservoir.

In addition to a control wavelength being simultaneously monitored, other control experiments were performed to ensure that the pattern of absorbance increase in the presence of an electric field and decrease in the absence of an electric field were a result of methyl violet being excluded due to the

counteracting forces of electrophoretic velocity and hydrodynamic flow (not shown). In the first control experiment, hydrodynamic flow was absent from the system, but the cationic dye and the electric field were still present. The rotatable board was adjusted so that there was no height difference between the menisci. In the second control experiment, the normal hydrodynamic flow rate was present, as well as the applied field; however, there was no methyl violet, or other cationic species, in solution. For the final control experiment, methyl violet and hydrodynamic flow were present, but there was no potential applied to the system. In all three controls, no absorbance increases were observed. This supports that the exclusion of methyl violet was due to the opposing forces in the system.

Initial experiments measured the absorbance when potential was applied to the system for 30 s and 60 s (Fig. 3.4). The curves were of the same characteristic shape as earlier data (Fig. 3.3B). The ratio between the max absorbance and initial absorbance was calculated between the top of the curve (immediately before potential was removed from the system) and the initial absorbance (before potential was applied). The error bars represent the standard deviation of the measurement. For 30 s of applied potential, the absorbance change was 5.88 ± 1.68 , while for 60 s, the ratio was 45.7 ± 13.4 . Due to the observed larger increase in absorbance with the longer time of applied potential, it is suggested that more dye is excluded when potential is applied for a longer period of time.

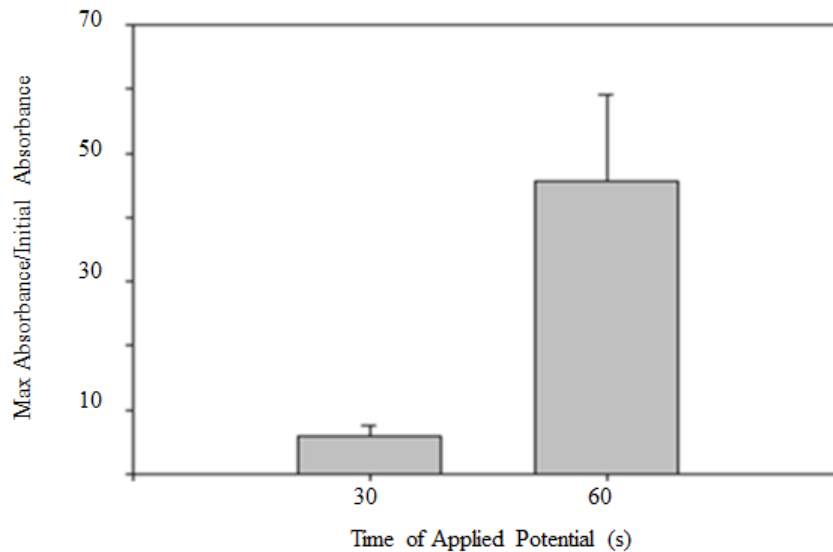


Figure 3.4. Change in absorbance. Error bars represent standard deviation ($n = 3$). Differences in absorbance observed in the absence of a stir bar.

3.3.4 Stir bar experiments

When compared to the model (Fig. 3.3A), the shapes of the experimental absorbance curves (Fig. 3.3B) are similar. However, according to the model, once the potential is removed, it takes approximately 1000 min for the concentration of the reservoir to return to baseline. Experimentally, it was observed to take only 1000 s for the absorbance to nearly reach baseline, tens of times faster than predicted. The likely explanation for this difference in time is that when the model was constructed, it took into account the entire volume of the reservoir. In actuality, the methyl violet was likely being concentrated in a bolus near the tip of the capillary and was not being evenly distributed in the entire volume of the solution. Therefore, when potential was removed, the material collected near the capillary tip was able to quickly (in comparison to evacuating

the entire reservoir) flow down the second capillary, and out of the path of light, resulting in an initially faster-than-anticipated decrease in absorbance.

For the second set of experiments, a stir bar was added to the system to aid in distributing the bolus throughout the entire solution during the exclusion process (Fig. 3.5). For all stir bar experiments, the solution was stirred only when potential was applied. Under these conditions, it was predicted that the entire bolus would be evenly distributed in solution, so that the absorbance curve would look more similar to the time-scale of the model. A curve from these experiments (not shown) showed that the time-scale was still more similar to the original data set than the model. This was probably due to the inefficient stirring method, so the bolus was not being broken up thoroughly and dispersed in the entire central reservoir volume. Because it was not broken up completely, it was still vacating the reservoir more quickly than if it had been distributed throughout solution.

A graph representing the change in absorbance for the stir bar experiments was constructed as described above. Potential was applied to the system for 30, 45, and 60 s and the data was recorded (Fig. 3.5). As can be seen from the graph, there is a general linear trend. As the amount of time potential was applied to the system increased, the change in absorbance increased. However, it is also evident that the error bars overlap, and therefore, there is no significant difference between the ratios. Even though there is overlap in error bars, the increase in signal supports the prediction that methyl violet is being successfully trapped when all three parameters for exclusion are present. Additionally, there is evidence that the bolus was being at least somewhat distributed in solution due to

the decreased change in absorbance values recorded for the stir bar experiments (Fig. 3.5) compared to the experiments without the stir bar (Fig. 3.4).

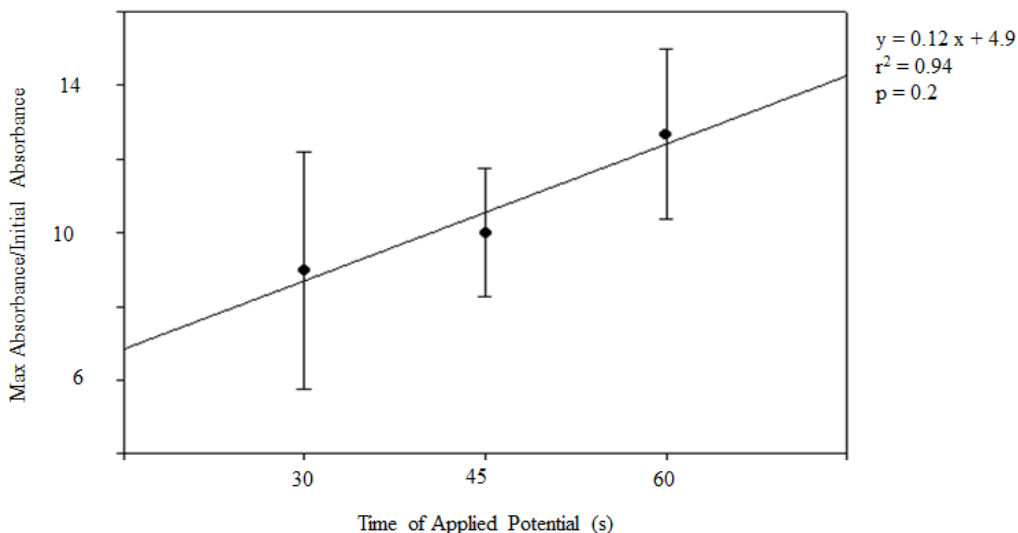


Figure 3.5. Change in absorbance in presence of stir bar. Error bars represent standard deviation ($n = 3$).

3.3.5 Limitations of benchtop design

Although the data support the hypothesis that methyl violet can be trapped outside the tip of a capillary in bulk solution, the percent increase in concentration was very low. For example, as shown in the model (assuming distribution throughout the entire reservoir), only a 0.5% increase in the concentration of methyl violet when potential is applied for 60 s is possible. Experimentally, due to the formation of a bolus, concentration enhancements were approximately 100% in 60 s. In comparison to several of the equilibrium gradient techniques, this is a small increase. An electric field gradient technique using a polymeric device demonstrated an enhancement of fluorescent green protein as large as

10,000-fold in 40 minutes [31]. However, the early work in electric field gradient methods only produced a 2-3 times enhancement of hemoglobin over the course of several hours. Although the concentration enhancement demonstrated in the initial experiments for electrophoretic exclusion is small in comparison to some of the more recent counter-flow gradient techniques, there is the potential to greatly increase the concentration factors. For example, using the flow injection electrophoretic exclusion method, a 1200 times increase of myoglobin was observed in 60 s. Other factors, including the size-scale of the current benchtop design, can be considered. The central reservoir, where detection occurs, is 365 μL in volume, and although there is a relatively high flow rate (in comparison to the flow injection design), the flush time of the reservoir is approximately 4 hours. To see a significant concentration increase would take hours. Transitioning to a smaller device, particularly on the microfluidic scale, would result in larger concentration enhancement, due to smaller detection volumes.

To address these size issues, two planar prototypes were fabricated (Fig. 3.2). Although not on the microscale, both of these devices had smaller central reservoirs than the benchtop design, and due to their size and planar design, detection could take place on a fluorescence microscope, allowing for lower detection limits. Additionally, five capillaries in parallel were incorporated to increase the flow rate through the system. This increases the amount of fluid traveling through the capillaries, into the central reservoir, and therefore, the amount of material that could be excluded, all without having to increase the electric field strength. Prototype 1 had the smallest central reservoir, but

alignment between capillary bundles and leaking were not overcome and the device was not practical. The central reservoir in Prototype 2 was smaller than that of the benchtop design; however, the volume was still large (200 μ L), assembly was time-consuming, and it was difficult to include the platinum wires in the design. The inability to create a realistic and useable planar device on the macroscale re-enforced the desire to design a microdevice for electrophoretic exclusion.

3.4 Concluding remarks

This work describes a novel separations technique that can be used for the exclusion of small dye molecules in bulk solution. The method utilizes the electrophoretic velocity of species opposed by the hydrodynamic flow to concentrate species near the entrance of a capillary. Proof-of-principle experiments have successfully demonstrated the exclusion of cationic methyl violet dye when potential was applied to the system, and indicates that with increased times of applied potential, more dye is excluded. Planar devices were then created to attempt to increase detection limits and concentration enhancement; however, future work lies in designing a microdevice that is suitable for electrophoretic exclusion.

3.5 References

- [1] Schmidt, T. C., Zwank, L., Elsner, M., Berg, M., Meckenstock, R. U., Haderlein, S. B., *Anal. Bioanal. Chem.* 2004, 378, 283-300.
- [2] Lee, W. C., Lee, K. H., *Anal. Biochem.* 2004, 324, 1-10.
- [3] Maurer, H. H., *Journal of Chromatography B* 1998, 713, 3-25.
- [4] Segura, J., Ventura, R., Jurado, C., *J. Chromatogr. B* 1998, 713, 61-90.

- [5] Jorgenson, J. W., Lukacs, K. D., *Anal. Chem.* 1981, 53, 1298-1302.
- [6] Bushey, M. M., Jorgenson, J. W., *J. Chromatogr.* 1989, 480, 301-310.
- [7] Giddings, J. C., Dahlgren, K., *Sep. Sci.* 1971, 6, 345-356.
- [8] Rodriguez-Diaz, R., Wehr, T., Zhu, M. D., *Electrophoresis* 1997, 18, 2134-2144.
- [9] Culbertson, C. T., Jorgenson, J. W., *Anal. Chem.* 1994, 66, 955-962.
- [10] Kelly, R. T., Li, Y., Woolley, A. T., *Anal. Chem.* 2006, 78, 2565-2570.
- [11] Lin, S.-L., Li, Y., Tolley, H. D., Humble, P. H., Lee, M. L., *J. Chromatogr. A* 2006, 1125, 254-262.
- [12] Petsev, D. N., Lopez, G. P., Ivory, C. F., Sibbett, S. S., *Lab Chip* 2005, 5, 587-597.
- [13] Sun, X. F., Li, D., Woolley, A. T., Farnsworth, P. B., Tolley, H. D., Warnick, K. F., Lee, M. L., *J. Chromatogr. A* 2009, 1216, 6532-6538.
- [14] Koegler, W. S., Ivory, C. F., *J. Chromatogr. A* 1996, 726, 229-236.
- [15] Danger, G., Ross, D., *Electrophoresis* 2008, 29, 3107-3114.
- [16] Ge, Z. W., Yang, C., Tang, G. Y., *Int. J. Heat Mass Transfer* 2010, 53, 2722-2731.
- [17] Lin, H., Shackman, J. G., Ross, D., *Lab Chip* 2008, 8, 969-978.
- [18] Tang, G. Y., Yang, C., *Electrophoresis* 2008, 29, 1006-1012.
- [19] Greenlee, R. D., Ivory, C. F., *Biotechnol. Prog.* 1998, 14, 300-309.
- [20] Ross, D., Kralj, J. G., *Anal. Chem.* 2008, 80, 9467-9474.
- [21] Ross, D., Romantseva, E. F., *Anal. Chem.* 2009, 81, 7326-7335.
- [22] Ross, D., Shackman, J. G., Kralj, J. G., Atencia, J., *Lab Chip* 2010, 10, 3139-3148.
- [23] Strychalski, E. A., Henry, A. C., Ross, D., *Anal. Chem.* 2011, 83, 6316-6322.
- [24] Danger, G., Ross, D., *Electrophoresis* 2008, 29, 4036-4044.

- [25] Davis, N. I., Mamunooru, M., Vyas, C. A., Shackman, J. G., *Anal. Chem.* 2009, *81*, 5452-5459.
- [26] Vyas, C. A., Mamunooru, M., Shackman, J. G., *Chromatographia* 2009, *70*, 151-156.
- [27] Hori, A., Matsumoto, T., Nimura, Y., Ikedo, M., Okada, H., Tsuda, T., *Anal. Chem.* 1993, *65*, 2882-2886.
- [28] Polson, N. A., Savin, D. P., Hayes, M. A., *J. Microcolumn Sep.* 2000, *12*, 98-106.
- [29] Meighan, M. M., Keebaugh, M. W., Quihuis, A. M., Kenyon, S. M., Hayes, M. A., *Electrophoresis* 2009, *30*, 3786-3792.
- [30] Meighan, M. M., Vasquez, J., Dziubcynski, L., Hews, S., Hayes, M. A., *Anal. Chem.* 2011, *83*, 368-373.
- [31] Humble, P. H., Kelly, R. T., Woolley, A. T., Tolley, H. D., Lee, M. L., *Anal. Chem.* 2004, *76*, 5641-5648.

Chapter 4

Using Electrophoretic Exclusion to Manipulate Small Molecules and Particles on a Microdevice

4.1 Introduction

Although capillary electrophoresis (CE) was established some thirty years ago [1, 2], it continues to advance both in its original capillary system and within microfluidic formats [3]. There are a number of advantages associated with CE for small volume analysis, but a challenge for both traditional and microchip CE, is concentration detection limits. Most of the advantages for CE are neutralized above 100 μm characteristic dimension for the channel, limiting the size of the sample, even though this is an advantage in some applications. Given this fact, sample enrichment has been the focus of many of the advances. Recent developments in this field vary from the “standard” microchip electrophoretic separation schemes (support materials such as gels, membranes, packing, frits, etc.) to new creative strategies that exploit electrokinetic properties, including continuous sampling formats, and complete separations on-chip, all of which have been recently reviewed in Chapter 2 and elsewhere [3-6]. While closely related to many of these strategies, electrophoretic exclusion sets the actual separation outside the channel entrance and was first introduced as “electrophoretic focusing” in 2000 [7]. It was originally developed within the enrichment vein, but it has evolved because of the geometric freedom of microfluidic devices. The technique is now envisioned as the bridge to creating highly efficient parallel or serial (or some mixture of the two) separations.

The exclusion principles examined in this thesis are closely related to all electrophoretic techniques where balancing forces or flow fields are invoked. In terms of development, the original exclusion work precedes many of the works noted below, but clearly, these are related in terms of comparing and contrasting the approach described here. Chapter 2 outlines several related enrichment techniques that have been developed for microchip formats including structural elements such as nanofissures [8], intersecting channels [9, 10], and valves [11]. Other methods include sample stacking techniques, such as field-amplified sample stacking [12-14], isotachopheresis (ITP) [15-20], and isoelectric focusing [21-25]. These techniques have improved separations on-chip and recent contributions have been reviewed [4, 26].

More closely related works include the application of a counterflow while performing an electrophoretic separation. Some of the initial applications of this technique were performed by the Tsuda laboratory [27] and the Jorgenson group [28]. In addition to those mentioned in previous chapters [6, 29-56], electrophoretic separations that take advantage of counterflow to increase separation efficiency include flow-induced electrokinetic trapping [57, 58] and the use of an electro-fluid-dynamic device [59, 60].

As published, GEMBE and GEITP—the techniques most similar to electrophoretic exclusion—are operated as linear separation schemes that differentiate species in a confined space, typically a channel. These designs allow for only a univariate data set—one separation at a time. The separation process begins in a reservoir, outside the channel, by stacking or providing temporally-

selective entry into the channel. The separation continues by introducing analytes sequentially into a, more or less, traditional capillary or channel. Once samples are introduced to a column, the species are no longer isolated from each other and the advantage of the initial bulk solution differentiation is lost, namely, the ability to operate in parallel [6, 47, 48, 50-56, 61].

Like gradient techniques, electrophoretic exclusion utilizes a hydrodynamic counterflow when performing separations [7, 62-64]. Briefly, this technique is able to differentiate species of interest in bulk solution when the hydrodynamic flow into a channel is opposed by the electrophoretic velocity of a species out of the channel. The interface itself can be considered a non-linear system. Even though there is contracting flow, the interface has a relatively constant flow field, whereas the electric field can reasonably be considered a discontinuity on the length scale of these experiments. As such, it can be integrated with other more traditional separation and detection schemes on a single microdevice. With its capacity to separate species in solution, it can be used in a highly parallel manner and therefore has the potential to achieve a separation-based array for complex sample analysis. There are further benefits to being able to differentiate species of interest in bulk solution, as opposed to inside of a channel. For instance, channel length is independent of separation efficiency and shorter channels produce much smaller footprints suited to a microdevice. More separation schemes can be included on one chip, and resolving elements of varying degree of orthogonality could also be integrated together, allowing for complex multistage separation.

To date, only one example of a true separation-based array exists [65-67]. The company formed to commercialize the technology, Protein Forest, has demonstrated the ability to successfully separate biological samples using parallel isoelectric focusing. Typically, the separated samples are then introduced to a mass spectrometer for further analysis. Although integrative, the technique is limited to resolving species by isoelectric points, where the analytes of interest (proteins and peptides) can, and do, suffer from low solubility. The Ivory group has also examined various electrokinetic techniques and provided a structured comparison [68].

Initial electrophoretic exclusion studies demonstrated the ability to concentrate polystyrene microspheres from the entrance of a 20 μm i.d. capillary [7], and was followed by theoretical modeling of the system [64]. More recently, work on a benchtop device included the separation and concentration of both small dye molecules [62] and proteins [63] near the entrance of a 75 μm i.d. capillary. Concentration enhancements of up to 1200 times in 60 s were observed when studying proteins. The current work focuses on adapting the electrophoretic exclusion technique to a microscale device by manipulating and separating dyes and polystyrene microspheres using a PDMS/glass hybrid design with fluorescence detection. This ties together the previous molecular and particle manipulations while demonstrating the technique on a microchip format. This study provides a foundation for exploration of widely varying geometries and unique capabilities including highly parallel and serial separation schemes.

4.2 Materials and methods

4.2.1 Design and fabrication of microdevice

A photograph of the device design (top-view), as well as a schematic of a single separation channel is shown (Fig. 4.1). Hybrid glass/PDMS devices were used for all experiments and each device contained nine separation channels.

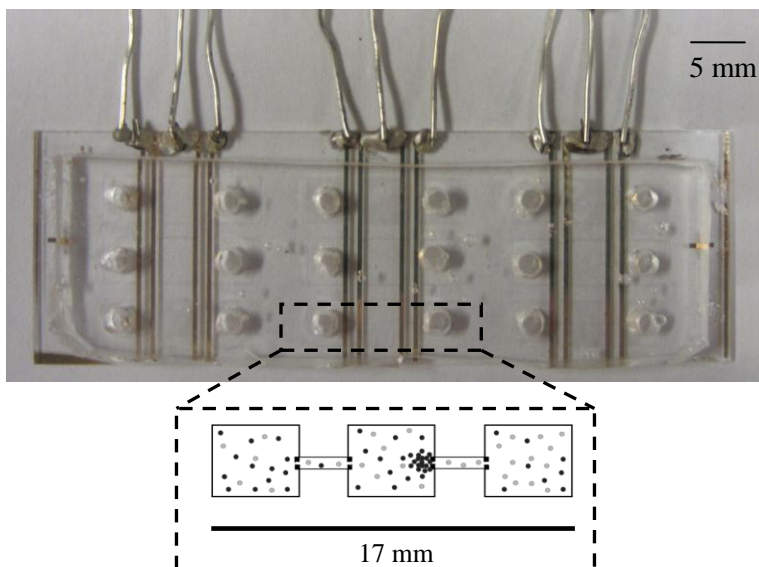


Figure 4.1. Microdevice used for electrophoretic exclusion. Photograph of the complete hybrid glass/PDMS chip with nine separation channels and a schematic of a single channel.

4.2.1.1 PDMS

One complete separation channel was 17 mm in length. Each separation channel contained a central reservoir connected to two end reservoirs by a short channel. Each reservoir was 5 mm x 5 mm; channels were 1 mm by 100 μm with a uniform depth throughout of 10 μm . Masks were designed in Illustrator (Adobe, San Jose, CA) and were printed on transparency at a resolution of 65,000

dpi (Fine Line Imaging, Colorado Springs, CO). Positive photoresist AZ 4620 was spun on a silicon wafer and then exposed with using an EVG®620 Automated UV-NIL, μ -CP System (EV Group, Austria) with the transparency mask. The PDMS microchannels were fabricated using the soft lithography technique. A 10:1 mass ratio of polymer to curing agent (Sylgard 184, Dow Corning, Midland, MI) was prepared and poured over the wafer for a thickness of approximately 5 mm and cured for 75 min. at 70 °C. The cured PDMS was removed from the wafer and holes (diameter: 3 mm) were punched in the end reservoirs of each separation channel using a quill.

4.2.1.2 Electrodes

Cr/Au electrodes were plated on microscope slides. A mask was designed in Adobe Illustrator and then printed on transparency at a resolution of 8000 dpi (Fine Line Imaging). Electrodes were 500 μ m wide and the length of the microscope slide. Positive photoresist AZ 4330 was spun on microscope slides and then the slides were exposed with the EVG®620 Automated UV-NIL, μ -CP System at 50 mJ/cm² using the mask. Two layers of metal were deposited on the glass slides using thermal evaporation with resistive heating (Edwards Auto 306, Edwards High Vacuum International, UK). A 5 nm layer of Cr was deposited onto the slides, followed by 50 nm of Au. Electric leads were attached to the electrodes with silver conductive epoxy to establish an electrical connection to the external power supply. It was designed so that each reservoir maintained a constant potential.

4.2.2 Materials

Aspartic acid (Sigma-Aldrich, St. Louis, MO), hydrochloric acid, rhodamine 123 (Invitrogen, Carlsbad, CA, USA), DMSO, and polystyrene microspheres (Invitrogen) were all used as received. Aspartic acid buffer was prepared to 5 mM concentration at a pH of 2.95 using 18 M Ω Milli-Q water. A 2 mM rhodamine 123 stock solution was prepared in DMSO and then diluted to 5 μ M in aspartic acid buffer on the day of experiments. Polystyrene microspheres were diluted in aspartic acid buffer (1:400) and sonicated for 10 minutes before use on the day of experiments. All polystyrene microspheres were functionalized with either a carboxyl (ex/em: 580/685 nm) or sulfate (ex/em: 505/515 nm) group and were 1 μ m in diameter.

4.2.3 Experimental Setup

The PDMS layer was bonded to the glass slide with the Cr/Au electrodes using oxygen plasma operated at 50 W for 60 s. Separation channels were filled with rhodamine 123 and/or polystyrene microspheres by pipetting the solution into one of the end reservoirs. Channels were filled by capillary action and bulk flow was induced by the height difference between the menisci of the end reservoirs. A total of 10 μ L of solution was pipetted into each channel. Flow rates for all experiments were approximately 10 nL/min. Potential (0 - 40 V, 0 - 3 min) was applied using a Bertram power supply (Series 225) so that differentiation occurred near the entrance to the second channel.

Experiments were monitored with an inverted microscope with darkfield and fluorescence capabilities (IX70, Olympus, Center Valley, PA, USA) using a

100 W high-pressure Hg lamp as the light source. Light from the lamp was passed through a band-pass filter and a 4X objective to the device. Emitted light was collected through a long-pass dichromatic mirror and a band-pass filter into the camera port on the microscope. Digital images were collected using a QICAM CCD camera from Q imaging, Inc. (Surrey, British Columbia, Canada) that was connected to a personal computer running Streampix III (NorPix, Montreal, Quebec, Canada). ImageJ (NIH, Bethesda, Maryland) was used for intensity measurement analysis. Intensity measurements were performed in the channels.

4.2.4 COMSOL Multiphysics Modeling

Flow and electric fields in the device were modeled using COMSOL Multiphysics (Palo Alto, California). One complete separation channel was drawn to-scale using the drawing tools in COMSOL. PDMS borders were designated as insulating material, while the interior of the channels and reservoirs were labeled as conducting materials. A potential drop of 30 V was added across the channel where the material of interest would be excluded.

4.3 Results and discussion

4.3.1 Principles of exclusion

As noted numerous times, electrophoretic exclusion can be achieved when the electrophoretic velocity of a species is greater than or equal to the counteracting hydrodynamic flow. When this occurs at an entrance to a channel, certain species can be prevented from entering the channel and are thus separated from the rest of the solution. Three parameters are required for electrophoretic

exclusion: hydrodynamic flow, a non-zero electrophoretic mobility of the species, and the applied electric field. For a given set of experiments, the electrophoretic mobility remains constant (based on the specific properties of analyte and buffer), so hydrodynamic flow and electric field strength can be varied to influence exclusion.

4.3.2 Proof of principle experiments

Proof of principle experiments demonstrating the functionality of the device were performed with negatively charged polystyrene microspheres (Fig. 2A) and positively charged rhodamine 123 (Fig. 2B), in aspartic acid buffer (pH 2.95). These studies are the first examples of direct observation of electrophoretic exclusion at a channel entrance, as opposed to inferring the behavior from a flow-injection-analysis format [62, 63]. In both experiments, bulk flow was from left to right, and when potential was applied, the electrophoretic velocity of the dye and the particles was opposing the hydrodynamic flow.

Successful exclusion was demonstrated with microspheres and dye. Before the application of the potential, beads and buffer flowed freely through the system (Fig. 4.2A, left). After the application of the electric field (300 V/cm) for 3 minutes, microspheres collected at the channel entrance (Fig.4.2A, right). This behavior is consistent with the electrophoretic velocity of the microspheres, induced by the applied electric field, countering the hydrodynamic flow and causing the beads to be excluded from the channel and thus locally collected. Similar patterns were observed while examining the exclusion behavior of rhodamine 123. Before the application of the electric field (-300 V/cm), the dye

and buffer were allowed to flow freely through the system (Fig. 4.2B, left image). Once the electric field (-300 V/cm) was applied for 30 s, there was an intensity increase near the channel entrance, consistent with an increased local concentration of fluorescent dye (Fig. 4.2B, right). This data suggests the exclusion of the dye from the channel, which resulted from the counteracting forces of hydrodynamic flow and electrophoretic velocity at the zone where the electric field is present, found at the channel entrance. In both cases, when the electric field was removed, the excluded species were again allowed to enter the channel (not shown).

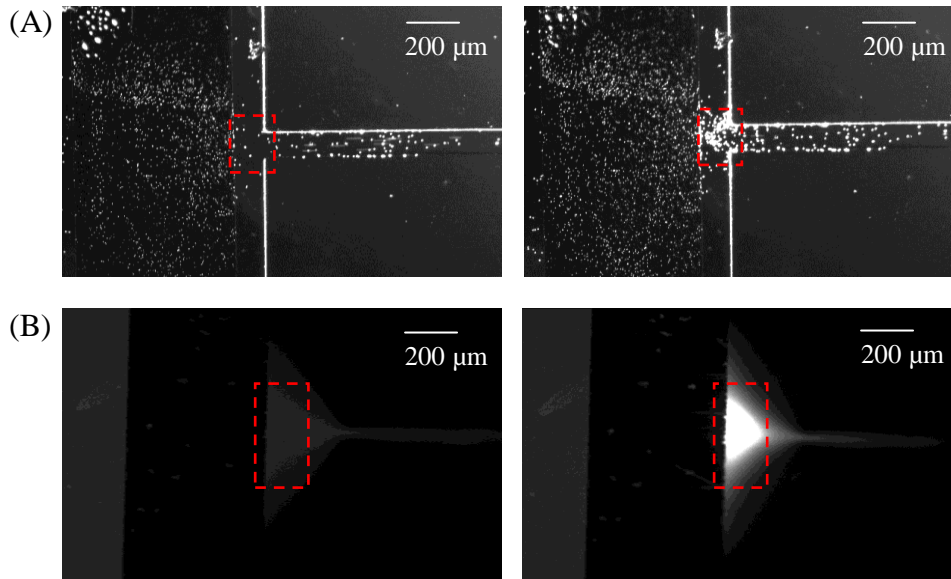


Figure 4.2. Exclusion of beads and dye at a channel entrance. Hydrodynamic flow is from left to right. (A) Exclusion of beads at a channel entrance (right, 300 V/cm). (B) Exclusion of rhodamine 123 at an entrance (right, -300 V/cm).

The intensity from small sections of the images was quantitated as a method to assist in describing the exclusion behavior. Intensity values were

assessed using ImageJ and all measurements were taken in the channel. This region was chosen for ease of viewing (the electrodes blocked the view within the reservoir area) and to avoid the highly asymmetric and nonlinear zone at the entrance. There is no radial symmetry at the entrance, as with traditional capillary entrances. Further, because the electrode only occupies the bottom of the reservoir, the resulting electric and flow fields differ dramatically in shape and location compared to a simple capillary entrance, and, as a consequence, the temporal data from the entrance was difficult to interpret. An average intensity curve for 30 s of applied electric field (-300 V/cm) is shown (Fig. 4.3). Initially, before potential was applied, the intensity remained steady, as dye at a constant concentration was flowing through the channel. Once potential was applied ($t = 5$ s), the intensity decreased as the dye was evacuated from the channel. In the presence of the electric field, dye remained excluded from the channel, within the local reservoir. After the potential was removed ($t = 35$ s), an increase in intensity was observed in the channel, suggesting the excluded dye had collected near the entrance and it was again allowed to flow through the system once the electric field was removed from the channel. This pattern of intensity changes was observed for all experiments where there was visual evidence of exclusion at the entrance area.

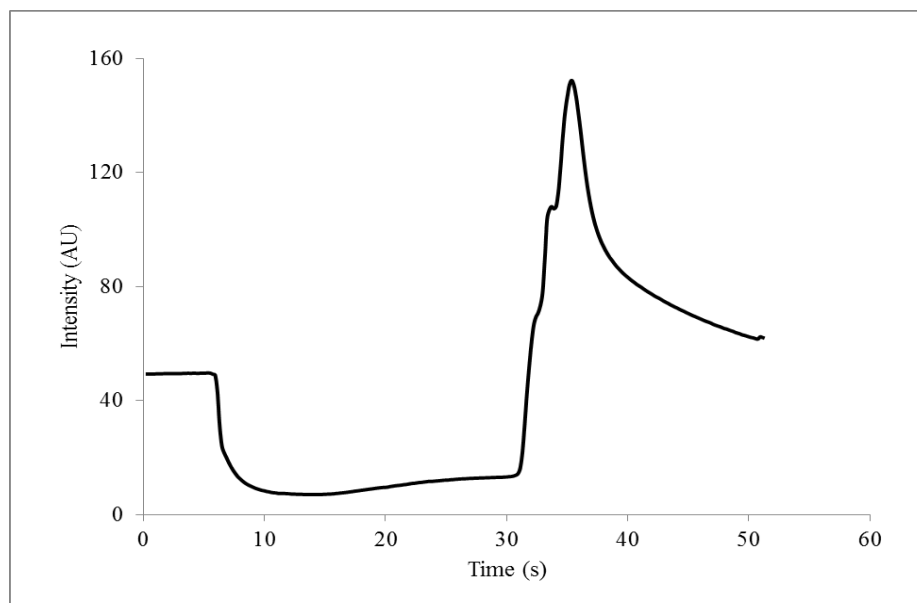


Figure 4.3. Average intensity curve for rhodamine 123. Measurements were taken in-channel for 30 s of applied potential (-300 V/cm, $n = 4$).

Experiments that varied the time of applied potential, as well as the electric field strength were performed to characterize the system when studying rhodamine 123. Control experiments that eliminated the electric field, hydrodynamic flow, or charged species were performed to demonstrate the necessity of all three parameters (data not shown). In the absence of one of the critical parameters, no evidence of exclusion, as determined by an increase in fluorescence intensity near the channel entrance, occurred or was below the detection limit of the methodology.

The magnitude of the electric field was varied to determine if there was an ideal strength for successful exclusion (Fig. 4.4). The change in intensity, calculated as the difference in intensity between the peak intensity (after removing the electric field) and the initial intensity (before application of the

electric field), was used as a method for comparing measurements between experiments. Electric field strengths greater than -300 V/cm appeared to result in no significantly greater intensity changes. Potentially, no additional amount of dye was being excluded or the additional amount of dye was not significantly greater than the amount excluded for the -300 V/cm electric field. Most likely, though, at higher field strengths, the excluded dye was pushed farther into the reservoir, where it was effectively dispersed by diffusion.

Any electric field less than -200 V/cm resulted in either little or no evidence of exclusion (0 V/cm) or incomplete exclusion (-50 and -100 V/cm). This was further supported by observation of the raw data (inset). At electric fields below -200 V/cm, the curves were absent, characterized by the decrease in intensity during the application of potential, followed by the increase in intensity once the potential is removed. Presumably, this is consistent with the dye was not being excluded because the hydrodynamic counterflow was greater than the electrophoretic velocity of the rhodamine 123.

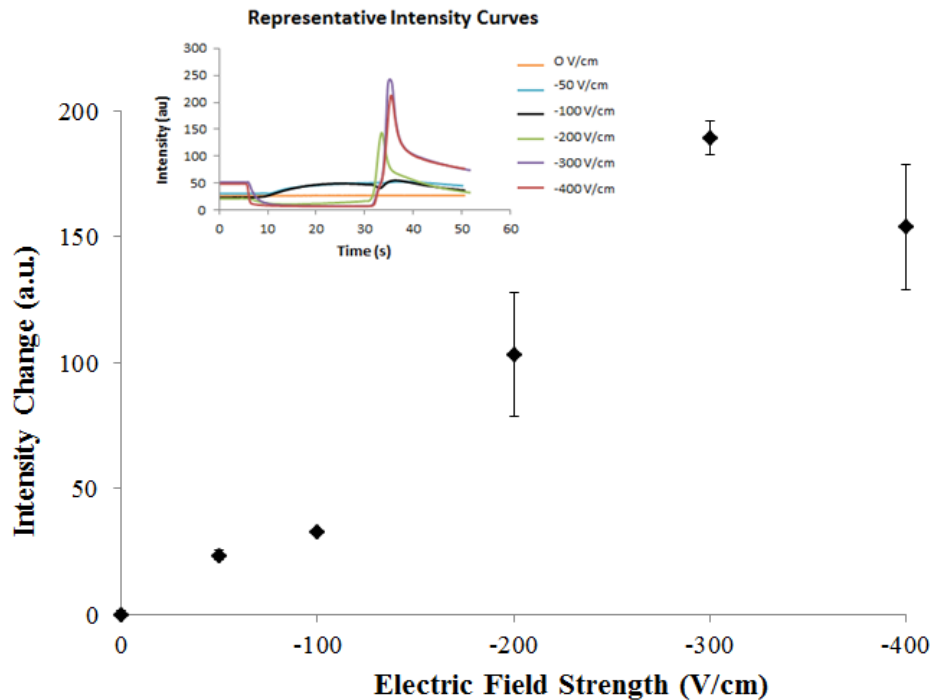


Figure 4.4. Change in intensity values for varying electric field strengths. Potential was applied for 30 s and error bars represent standard deviation ($n = 3$). The inset shows representative curves of the raw data.

For experiments varying the time of applied potential, the electric field remained constant and intensity changes for various times of electric field application were averaged (Fig. 4.5). The largest intensity change was observed for 10 s of applied potential, suggesting that at 10 s of applied potential, the most rhodamine 123 is excluded. Similar to increasing electric field strength, though, increased time of applied potential above 10 s could also mean that the excluded material was being more influenced by diffusional forces in the reservoir, resulting in less material being allowed to immediately flow down the channel once the electric field was released. At shorter times of applied potential, there was significantly less intensity change, indicating that less dye was being

excluded from the channel. Intensity changes for 20 and 30 s of applied potential were not significantly different from each other, indicating that the same amount of dye was excluded for both times.

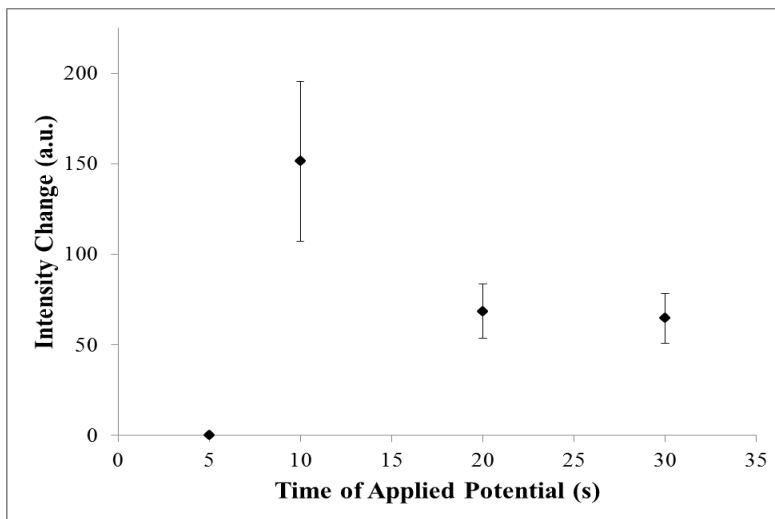


Figure 4.5. Average intensity changes for various times of applied potential. Times varied from 5 s – 30 s (-200 V/cm, n = 3, exception: t = 5 s, n = 2).

Large standard deviations were sometimes observed when averaging multiple trials (Figs. 4.4 & 4.5). As mentioned previously, the area where exclusion occurred is complex and nonlinear. The three dimensional nature of the concentration gradient about the interface was being collapsed as the collected material traveled through the channel, where one dimensional intensity measurements were performed. In addition, factors such as in-channel temperature changes and surface modifications between trials can contribute to somewhat different exclusion profiles, even when the general pattern of exclusion

is the same. The standard deviations are reflective of the nonlinear nature of the interface where exclusion occurs.

4.3.3 Separation of rhodamine 123 and polystyrene beads

Experiments were performed that demonstrated the ability of the technique to differentiate fluorescent dye from polystyrene microspheres. The beads were negatively-charged at the pH of the buffer (2.95). Based on the intensity measurements performed in-channel, rhodamine 123 was successfully separated from the polystyrene beads (Fig. 4.6). Before the application of potential, all species were flowing through the system, with only the presence of hydrodynamic flow (Fig. 4.6A). After a -300 V/cm electric field was applied to the system for 30 s, the polystyrene microspheres were still moving through the system, but the fluorescence intensity decreased, consistent with rhodamine 123 being prevented from entering the channel (Fig. 4.6B). The electrophoretic velocity of the positively-charged dye was greater than the opposing hydrodynamic flow. The microspheres, conversely, were not excluded—as a result of their negative charge. Instead they were carried down the channel with the hydrodynamic flow and electric field. Once the potential was released, the data suggests the excluded dye flowed through the channel along with the microspheres under hydrodynamic flow (Fig. 4.6C). This experiment successfully demonstrated the ability of the device to separate species with differing charges and of different sizes.

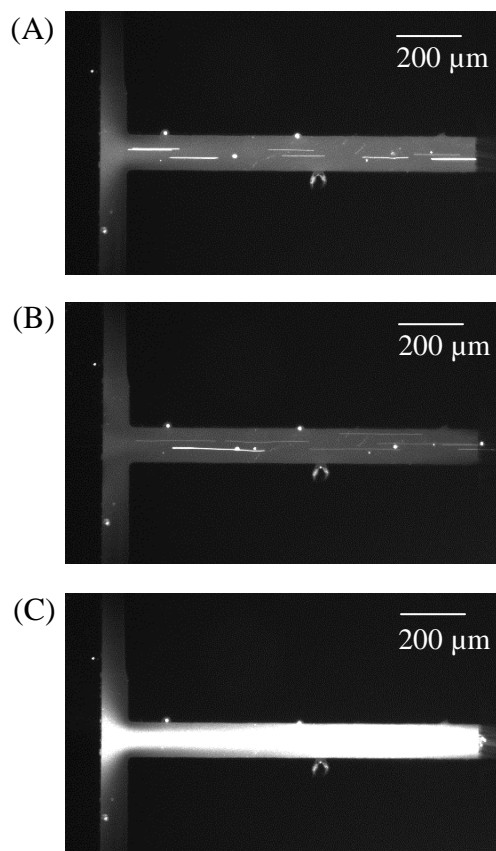


Figure 4.6. Still images taken from video demonstrating the separation of rhodamine 123 from carboxylated spheres. (A) The system before the initiation of the electric field. (B) The system after 30 s of applied potential. (C) The system after the electric field is removed.

4.3.4 The effects of variable channel and electrode geometry on electrophoretic exclusion

The same electrophoretic exclusion pattern of behavior was observed consistently between different experiments. In the presence of a large enough electric field, dye or small particles were excluded from a channel and when the potential was released, the excluded material flowed through the channel. This pattern was observed visually during experiments by watching the fluorescence

intensity change (rhodamine 123) or the number of particles change (polystyrene microspheres) throughout the course of an experiment.

Differences in intensity values occurred when the electrode alignment slightly changed (images not shown). For example, intensity differences were measured, given the same experimental conditions (-200 V/cm, 30 seconds) (Figs. 4.4 & 4.5). The average for 30 s of applied electric field (-200 V/cm) reported in Fig. 4.4 was 103 ± 24 a.u. while in Fig. 4.5, it was reported to be 51 ± 13 a.u. Even when intensity values were different between days, the same exclusion patterns were observed. Comparing the results of varying the electric field strength between days still yields -200 V/cm as the minimum field strength required for exclusion of rhodamine 123. On different days, and even with different devices used on the same day, the electrode alignment was slightly different, varying by as much as ~ 200 μm , in part due to the PDMS shrinkage. With slight differences in the placement of the PDMS on the glass slide, the shape of the electric field about the entrance was altered. One of the factors necessary for electrophoretic exclusion is an electric field, and because the exclusion took place at the electrode and channel entrance area, any small changes in the alignment of the electrode slide and the reservoir/channel interface altered the electric field geometry, and therefore, slightly changed the details of exclusion behavior.

A COMSOL model was used to demonstrate the importance of the electrode alignment (Fig. 4.7). Electrode placement at the channel entrance (Fig. 4.7A) and a shift of 250 μm (Fig. 4.7B) resulted in a difference in the electric

field strength and geometry at the channel entrance. When the electrode was shifted from the channel entrance, the electric field strength was less at the channel entrance/reservoir exit. Because exclusion occurred at this interface, small changes in alignment, and therefore electric field, influence the results. Studies that include characterization of the channel/electrode geometry and its effect on the electric field, and therefore exclusion, are being conducted to allow for better utilization of this separation technique on the microscale.

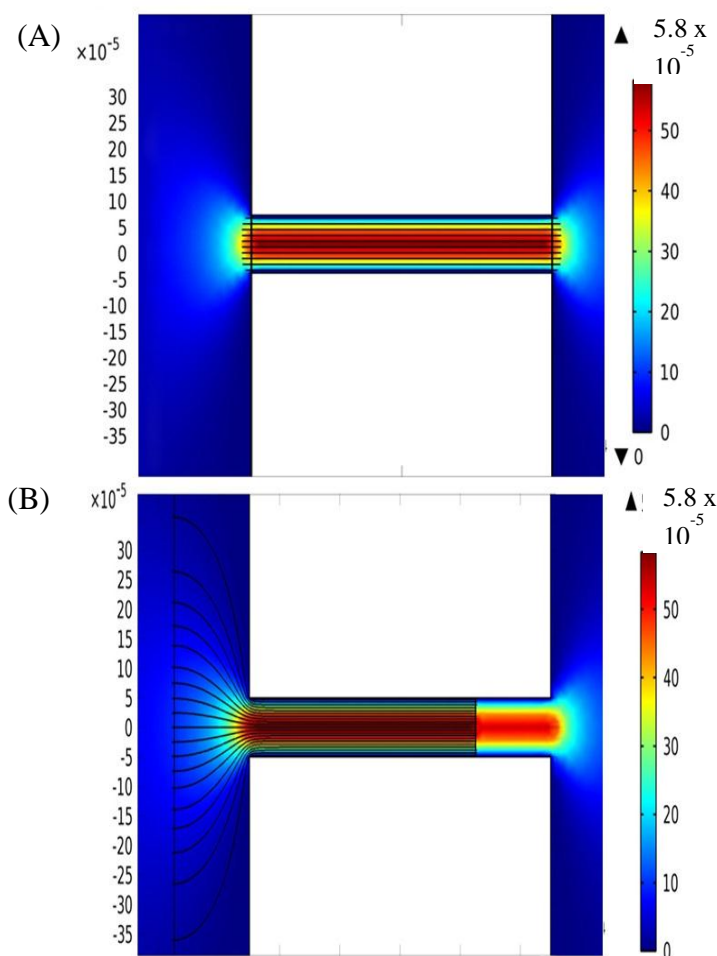


Figure 4.7. COMSOL figures demonstrating fluid velocity and electric fields. (A) Electrode placement at the channel entrance. (B) Electrode 250 μm away from channel entrance. Surface velocity magnitude is flow field, while streamlines represent the electric field.

4.3.5 Future design: Separation-based array format

This work was a continuation of the studies conducted on a macroscale device using absorbance detection for small molecules [5]. In the macroscale experiments, the electrode fully encircled the capillary entrance and was radially symmetric. In the microscale format, the electrode was plated on one surface of the device, the glass slide, which left three sides of the rectangular channel as insulating material. This resulted in different electric field and flow field shapes

between the two designs and this difference in field shapes affected the exclusion profile. This device is meant to bridge from the macroscale device [62, 63] to the first demonstration on a microfluidic format and, there are significant differences between the two designs.

The main advantages of exploiting microdevices are precise and varied control of the flow and electric fields about the entrance of the channel and the possibility to include several channels on one chip. Several designs can be envisioned where many channels and reservoirs with well-controlled flow and electric field interfaces are created to form separation-based arrays and even more complex systems.

4.4 Concluding remarks

This work provides a step towards creating complex highly efficient separations based on the exclusion principles. The direct visualization of the exclusion process on small molecules, the differentiation of particles and molecules and performance of exclusion on a microdevice format are all demonstrated for the first time here. The manipulation of particles and small molecule bracket the potential targets in terms of size, demonstrating a broad range of applicability. Combined with previous results using proteins, this suggests nearly all targets of typical electrophoretic separation can be addressed within a microchip format. This work sets the fundamental studies directly observing exclusion of materials at a flow-electric field interface on a microdevice that can lead to much more complex devices on small footprint formats.

4.5 References

- [1] Jorgenson, J. W., Lukacs, K. D., *Anal. Chem.* 1981, 53, 1298-1302.
- [2] Jorgenson, J. W., Lukacs, K. D., *Science* 1983, 222, 266-272.
- [3] Breadmore, M. C., Dawod, M., Quirino, J. P., *Electrophoresis* 2011, 32, 127-148.
- [4] Kenyon, S. M., Meighan, M. M., Hayes, M. A., *Electrophoresis* 2011, 32, 482-493.
- [5] Meighan, M. M., Staton, S. J. R., Hayes, M. A., *Electrophoresis* 2009, 30, 852-865.
- [6] Vyas, C. A., Flanigan, P. M., Shackman, J. G., *Bioanalysis* 2010, 2, 815-827.
- [7] Polson, N. A., Savin, D. P., Hayes, M. A., *J. Microcolumn Sep.* 2000, 12, 98-106.
- [8] Yu, H., Lu, Y., Zhou, Y. G., Wang, F. B., He, F. Y., Xia, X. H., *Lab Chip* 2008, 8, 1496-1501.
- [9] Reschke, B. R., Luo, H., Schiffbauer, J., Edwards, B. F., Timperman, A. T., *Lab Chip* 2009, 9, 2203-2211.
- [10] Reschke, B. R., Schiffbauer, J., Edwards, B. F., Timperman, A. T., *Analyst* 2010, 135, 1351-1359.
- [11] Kuo, C. H., Wang, J. H., Lee, G. B., *Electrophoresis* 2009, 30, 3228-3235.
- [12] Jacobson, S. C., Ramsey, J. M., *Electrophoresis* 1995, 16, 481-486.
- [13] Lichtenberg, J., Verpoorte, E., de Rooij, N. F., *Electrophoresis* 2001, 22, 258-271.
- [14] Xu, L., Hauser, P. C., Lee, H. K., *J. Chromatogr. A.* 2009, 1216, 5911-5916.
- [15] Walker, P. A., Morris, M. D., Burns, M. A., Johnson, B. N., *Anal. Chem.* 1998, 70, 3766-3769.
- [16] Bahga, S. S., Chambers, R. D., Santiago, J. G., *Anal. Chem.* 2011, 83, 6154-6162.
- [17] Grass, B., Neyer, A., Johnck, M., Siepe, D., Eisenbeiss, F., Weber, G., Hergenroder, R., *Sens. Actuators, B* 2001, 72, 249-258.

- [18] Jung, B., Bharadwaj, R., Santiago, J. G., *Anal. Chem.* 2006, 78, 2319-2327.
- [19] Persat, A., Santiago, J. G., *New J. Phys.* 2009, 11.
- [20] Pumera, M., Wang, J., Opekar, F., Jelinek, I., Feldman, J., Lowe, H., Hardt, S., *Anal. Chem.* 2002, 74, 1968-1971.
- [21] Hofmann, O., Che, D. P., Cruickshank, K. A., Muller, U. R., *Anal. Chem.* 1999, 71, 678-686.
- [22] Cong, Y. Z., Liang, Y., Zhang, L. H., Zhang, W. B., Zhang, Y. K., *J. Sep. Sci.* 2009, 32, 462-465.
- [23] Cui, H. C., Horiuchi, K., Dutta, P., Ivory, C. F., *Anal. Chem.* 2005, 77, 1303-1309.
- [24] Huang, X. Y., Ren, J. C., *Electrophoresis* 2005, 26, 3595-3601.
- [25] Ishibashi, R., Kitamori, T., Shimura, K., *Lab Chip* 2010, 10, 2628-2631.
- [26] Gebauer, P., Mala, Z., Bocek, P., *Electrophoresis* 2011, 32, 83-89.
- [27] Hori, A., Matsumoto, T., Nimura, Y., Ikedo, M., Okada, H., Tsuda, T., *Anal. Chem.* 1993, 65, 2882-2886.
- [28] Culbertson, C. T., Jorgenson, J. W., *Anal. Chem.* 1994, 66, 955-962.
- [29] Danger, G., Ross, D., *Electrophoresis* 2008, 29, 3107-3114.
- [30] Ge, Z. W., Yang, C., Tang, G. Y., *Int. J. Heat Mass Transfer* 2010, 53, 2722-2731.
- [31] Lin, H., Shackman, J. G., Ross, D., *Lab Chip* 2008, 8, 969-978.
- [32] Munson, M. S., Meacham, J. M., Locascio, L. E., Ross, D., *Anal. Chem.* 2008, 80, 172-178.
- [33] Munson, M. S., Meacham, J. M., Ross, D., Locascio, L. E., *Electrophoresis* 2008, 29, 3456-3465.
- [34] Ross, D., Gaitan, M., Locascio, L. E., *Anal. Chem.* 2001, 73, 4117-4123.
- [35] Tang, G. Y., Yang, C., *Electrophoresis* 2008, 29, 1006-1012.
- [36] Koegler, W. S., Ivory, C. F., *J. Chromatogr. A* 1996, 726, 229-236.

- [37] Humble, P. H., Kelly, R. T., Woolley, A. T., Tolley, H. D., Lee, M. L., *Anal. Chem.* 2004, 76, 5641-5648.
- [38] Kelly, R. T., Li, Y., Woolley, A. T., *Anal. Chem.* 2006, 78, 2565-2570.
- [39] Sun, X. F., Li, D., Woolley, A. T., Farnsworth, P. B., Tolley, H. D., Warnick, K. F., Lee, M. L., *J. Chromatogr. A* 2009, 1216, 6532-6538.
- [40] Lin, S.-L., Li, Y., Tolley, H. D., Humble, P. H., Lee, M. L., *J. Chromatogr. A* 2006, 1125, 254-262.
- [41] Liu, J. K., Sun, X. F., Farnsworth, P. B., Lee, M. L., *Anal. Chem.* 2006, 78, 4654-4662.
- [42] Huang, Z., Ivory, C. F., *Anal. Chem.* 1999, 71, 1628-1632.
- [43] Petsev, D. N., Lopez, G. P., Ivory, C. F., Sibbett, S. S., *Lab Chip* 2005, 5, 587-597.
- [44] Myers, P., Bartle, K. D., *J. Chromatogr. A* 2004, 1044, 253-258.
- [45] Burke, J. M., Smith, C. D., Ivory, C. F., *Electrophoresis* 2010, 31, 902-909.
- [46] Burke, J. M., Huang, Z., Ivory, C. F., *Anal. Chem.* 2009, 81, 8236-8243.
- [47] Ross, D., *Electrophoresis* 2010, 31, 3650-3657.
- [48] Ross, D., *Electrophoresis* 2010, 31, 3658-3664.
- [49] Ross, D., Kralj, J. G., *Anal. Chem.* 2008, 80, 9467-9474.
- [50] Ross, D., Romantseva, E. F., *Anal. Chem.* 2009, 81, 7326-7335.
- [51] Ross, D., Shackman, J. G., Kralj, J. G., Atencia, J., *Lab Chip* 2010, 10, 3139-3148.
- [52] Shackman, J. G., Munson, M. S., Ross, D., *Anal. Chem.* 2007, 79, 565-571.
- [53] Strychalski, E. A., Henry, A. C., Ross, D., *Anal. Chem.* 2009, 81, 10201-10207.
- [54] Strychalski, E. A., Henry, A. C., Ross, D., *Anal. Chem.* 2011, 83, 6316-6322.
- [55] Davis, N. I., Mamunooru, M., Vyas, C. A., Shackman, J. G., *Anal. Chem.* 2009, 81, 5452-5459.

- [56] Shackman, J. G., Ross, D., *Anal. Chem.* 2007, 79, 6641-6649.
- [57] Jellema, L. C., Mey, T., Koster, S., Verpoorte, E., *Lab Chip* 2009, 9, 1914-1925.
- [58] Jellema, L. J. C., Markesteijn, A. P., Westerweel, J., Verpoorte, E., *Anal. Chem.* 2010, 82, 4027-4035.
- [59] Liu, C., Luo, Y., Fang, N., Chen, D. D. Y., *Anal. Chem.* 2011, 83, 1189-1192.
- [60] Liu, C., Luo, Y., Maxwell, E. J., Fang, N., Chen, D. D. Y., *Anal. Chem.* 2010, 82, 2182-2185.
- [61] Vyas, C. A., Mamunooru, M., Shackman, J. G., *Chromatographia* 2009, 70, 151-156.
- [62] Meighan, M. M., Keebaugh, M. W., Quihuis, A. M., Kenyon, S. M., Hayes, M. A., *Electrophoresis* 2009, 30, 3786-3792.
- [63] Meighan, M. M., Vasquez, J., Dziubcynski, L., Hews, S., Hayes, M. A., *Anal. Chem.* 2011, 83, 368-373.
- [64] Pacheco, J. R., Chen, K. P., Hayes, M. A., *Electrophoresis* 2007, 28, 1027-1035.
- [65] Zilberstein, G. V., Baskin, E. M., Bukshpan, S., *Electrophoresis* 2003, 24, 3735-3744.
- [66] Zilberstein, G. V., Baskin, E. M., Bukshpan, S., Korol, L. E., *Electrophoresis* 2004, 25, 3643-3651.
- [67] Zilberstein, G., Korol, L., Bukshpan, S., Baskin, E., *Proteomics* 2004, 4, 2533-2540.
- [68] Ivory, C. F., *Electrophoresis* 2007, 28, 15-25.

Chapter 5

Development of the Resolution Theory for Electrophoretic Exclusion

5.1 Introduction

This dissertation has addressed the importance of separations science for analyzing complicated samples, particularly those which contain targets that are challenging to isolate from background species. Traditionally, these types of samples have been studied using techniques such as chromatography (size exclusion and affinity) [1, 2] and capillary electrophoresis [3]. Although these common techniques are extensively used for complex samples, they result in diffusion and dilution over the course of their separation. Equilibrium gradient methods, in contrast, utilize separating and focusing forces simultaneously to effectively counteract dispersion, including diffusion, resulting in better detection limits [4]. Isoelectric focusing (IEF), the best known example of an equilibrium gradient technique, employs a pH gradient with a constant electric field, to separate species based on differences in their pI 's [5-7]. Other more recent examples of equilibrium gradient techniques include counterflow electric field gradient focusing (EFGF) methods [8-14]. As with other equilibrium gradient methods, species in EFGF separations are isolated and concentrated simultaneously.

A successful separation is usually defined by generating adequate resolution, more so for analytical scale or complex samples, compared to some well characterized samples of preparative scale systems where this requirement can be relaxed. The resolving capabilities of the more common separations

techniques, including chromatography [15, 16], IEF [4], and CE [17], are well-established and experimentally confirmed. Capillary electrophoresis separations on a microchip in a spiral channel have proven to be very successful, with theoretical plates as high as 1,000,000 having been reported [18]. More recently, resolution equations for EFGF techniques have been developed. Tolley *et al.* described the resolution of electromobility focusing [19] and Kelly and Woolley described EFGF resolution by comparing the focusing effects near the zero-force point to a spring and invoked the mathematics of Hooke's Law to describe the forces [10]. Ultimately, these theories described the properties of EFGF as it successfully increases sample concentration and separates species with similar electrophoretic mobilities.

Reducing dimensions to the microscale has the potential to improve EFGF devices. Gradient elution moving boundary electrophoresis (GEMBE), another equilibrium gradient technique, has been used to perform electrophoretic separations in short channels [20-22]. Ross developed a theoretical framework to describe the resolving capability of GEMBE and compared it to CE, showing that GEMBE works on the same time-scale and provides similar resolution as CE separations [23].

Electrophoretic exclusion, somewhat related to EFGF techniques, is a separation method first introduced by Polson *et al.* as an enrichment scheme [24] and exploits the counteracting forces of hydrodynamic flow and electrophoretic velocity. However, unlike EFGF techniques, the electric field remains constant in the channel, and a sharp local gradient is initiated right at the channel entrance,

allowing for highly localized separation just outside of the channel entrance in bulk solution rather than in a channel. This difference, though it may seem subtle, allows for parallelization and is predicted (in this chapter) to positively affect the overall resolution capabilities.

The success of electrophoretic exclusion has been demonstrated experimentally using both mesoscale [24-27] and microscale [28] devices. The technique has proven to be applicable to a variety of analytes with various properties and sizes, including small molecules, polystyrene microspheres, and proteins. Additionally, studies have been conducted to model the physicality and actions of the electrode/solution/channel interface [29]. However, a thorough study of the resolution capabilities of the technique from a traditional separations science point-of-view has not yet been conducted. Resolution and dynamic range of electrophoretic exclusion will be defined using common dimensionalities, materials, and electric potential magnitudes of current devices, thereby developing a foundational framework to interrogate the resolving power of electrophoretic exclusion enabled by the localized microgradient. By extension, since the interface can be parallelized or placed in series, a variety of new capabilities can be envisioned.

5.2 Theory

For comparison to other electrophoretic techniques (traditional and gradient), resolution is described in terms of closest electrophoretic mobilities of two species that can be differentiated – one fully excluded and one fully entering the channel. Resolution, R , will be described as:

$$R = \frac{\Delta X}{4\sigma} \quad (1)$$

In this equation, ΔX is the distance between separated elements and σ is the standard deviation of the elements. Both of these variables are easily defined within traditional separations, with ΔX and σ described in terms of distance or time reflecting the distribution of the separated concentration profiles. The interface under study here does not produce traditional concentration profiles, or peaks, and the distance between two separated species cannot be defined in a traditional sense. However, this interface does provide for separation of species and properties of the interface and the physicality of the target species allow for direct quantitative comparison to be made to other techniques.

To provide a basis for discussion, the principles of exclusion and conventions of the model are briefly outlined. This discussion will focus on the centerline and other factors (laminar flow) will be considered. Flow is established inward, towards, and within a channel and an electric field is introduced within the channel itself only, introducing a gradient at the entry region. Electrophoretic exclusion occurs when the electrophoretic velocity (product of the electrophoretic mobility and the electric field) of a species is opposite and greater than or equal to the fluid velocity into the channel. Under these conditions, the species is excluded from entering the capillary. Species with electrophoretic velocities smaller than the opposing fluid flow will instead flow through the channel. This narrative will focus exploring the smallest difference in electrophoretic mobilities where this differentiation can be obtained.

For ease of discussion, visualizing the system, and adhering to existing experimental results that will be discussed later, a device description is included (Fig. 5.1A). The materials and details are not central to the theoretical approach, as it is a general model, but this is presented to aid in communication and establish physicality for later discussion. The device is composed of two reservoirs connected with a capillary. Bulk flow is from left to right through the system, driven by a pressure differential in the chambers. The end of the capillary (or channel) in chamber 1 contains an integral electrode that is constructed by removing approximately 3 mm of polyimide coating from a capillary tip and then sputtering with 30 nm of Ti and 50 nm of Pt. Silver conductive epoxy is then used to physically connect the tip of the sputter-coated capillary to a 1 cm piece of Pt wire. Power can be applied to the wire and when potential is applied, the tip of the capillary acts as an electrode. As a result of the capillary tip electrode and the Pt wire in the reservoir, no potential field exists in the bulk of reservoir 1. A ground electrode is placed in chamber 2. The area of interest, where exclusion occurs, is in chamber 1, at the entry region or interface of the capillary.

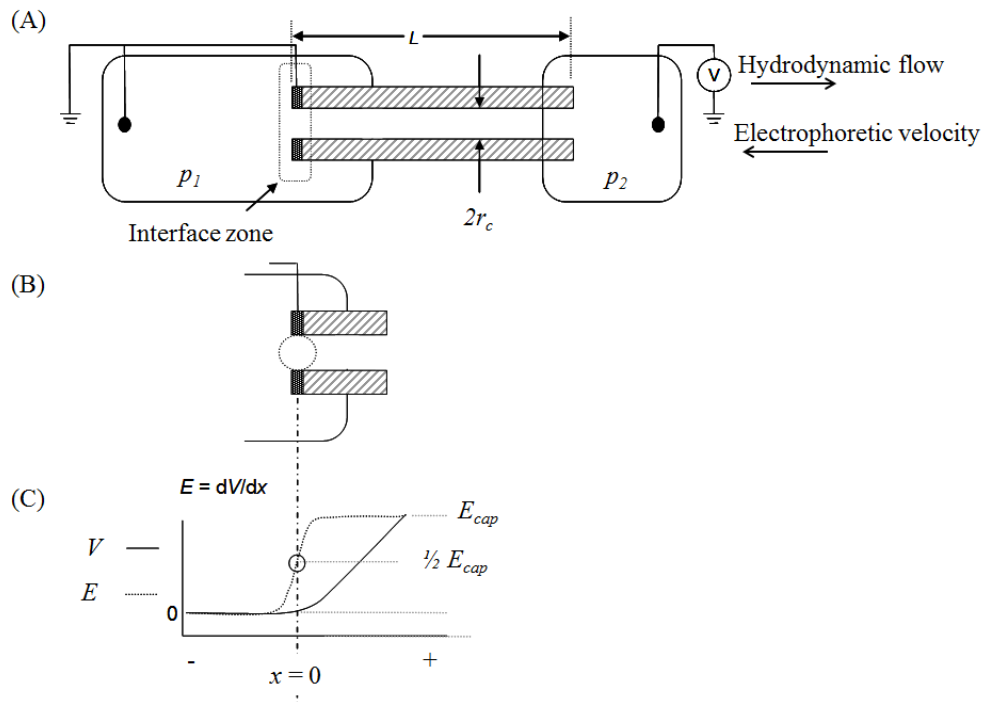


Figure 5.1. Device schematic and interface description. (A) Schematic of the device used to capture data. A 10 cm capillary with a sputtered electrode attached to two vials. The vial on the left is filled with sample and the vial on the right is filled with buffer. The capillary has a small window burned in it (~ 5 mm) where detection occurs. (B) The area of interest, immediately outside the capillary entrance, where exclusion occurs. (C) Voltage and electric field near the channel entrance, where exclusion occurs.

5.2.1. Defining the interface

Exclusion occurs when the electrophoretic velocity of a species (v) is greater than, or equal to, the opposing hydrodynamic flow velocity (u):

$$v \geq -u \quad (2)$$

The calculated fluid flow velocity (u) through the system is given by:

$$u = \frac{\Delta p r_c^2}{8L\eta} \quad (3)$$

where Δp is the pressure difference between the two chambers, r_c is the radius of the capillary, L is the length of the capillary, and η is the viscosity of the buffer. Electroosmosis is suppressed for the purposes of this model, but it can be added trivially without changing u , but could reduce Taylor dispersion.

Consider two arbitrarily closely related targets with electrophoretic mobilities μ_1 and μ_2 (ostensibly, one excluded, the other not), the average electrophoretic mobility (μ_{ave}) is:

$$\mu_{ave} = \frac{(\mu_1 + \mu_2)}{2}. \quad (4)$$

The electrophoretic velocity is the product of the electrophoretic mobility and the local electric field strength (E), so the average electrophoretic velocity (v_{ave}) of the target pair is:

$$v_{ave} = \mu_{ave} E \quad (5)$$

5.2.2 Structure of flow and electric fields near/within the interface

In electrophoretic exclusion, the electric field is initiated at the electrode-channel entrance interface; there is no field in the reservoir away from the capillary entrance. Within the body of the capillary, the electric field is constant and set at E_{cap} (Fig. 5.1B & C). Immediately outside the capillary entrance, in the middle of the linear electric field gradient, where $E = 1/2 E_{cap}$, v_{ave} is defined as the opposite of the bulk flow:

$$v_{ave} = -\frac{1}{2} E_{cap} \mu_{ave} \quad (6)$$

Assuming μ_1 is greater than μ_2 , the species with μ_1 is completely excluded (effects of dispersion addressed below), while the species with μ_2 is not excluded,

but allowed to travel past the interface and down the length of the capillary. Flow rate near the entrance is assumed to be constant over the length of the scale of the electric field gradient (penetrating $\sim 1/2$ the capillary diameter into the reservoir).

5.2.3 Steady state, fully developed concentration profile

The concentration profile for a fully excluded analyte is described (Fig. 5.2). The maximum concentration is in the reservoir, which decreases to zero at the channel entrance (Fig. 5.2B). The area of most interest is the slope across the interface. The steepness of the slope varies, depending on focusing and dispersive forces and defines a characteristic variance.

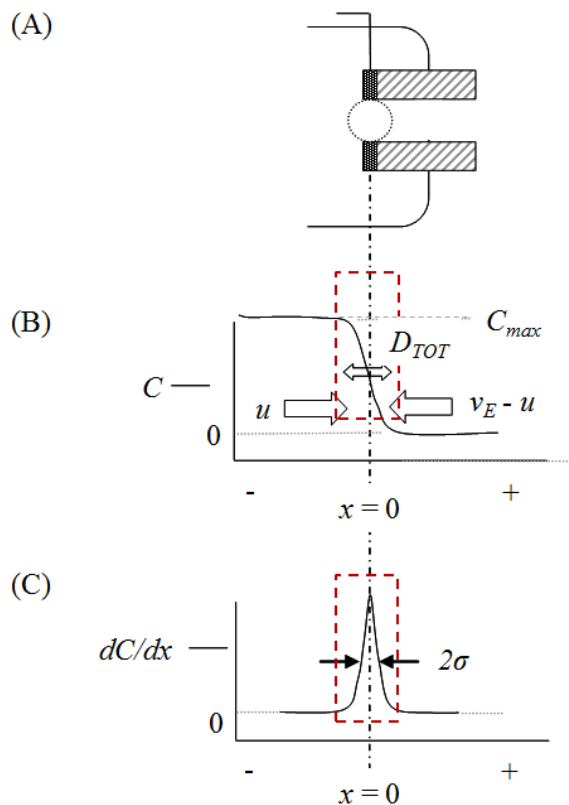


Figure 5.2 Development of the concentration profile at the interface. (A) The area of interest where exclusion occurs. (B) The concentration profile in the reservoir in the area of exclusion. Max concentration is in the reservoir, with concentration reaching zero in the channel. The shape of the concentration profile is modeled as an error function, as indicated with the red box. The focusing forces and dispersive forces affect the steepness of the gradient. (C) The first derivative of the concentration profile indicates that the largest change in concentration occurs at the channel entrance. The steeper the gradient, the narrower the peak of the first derivative.

Using the practice of Giddings, a steady state separation has a constant concentration profile with time ($dc/dt = 0$), where, in this case, the dispersion forces are equivalent and opposite to flow/electric field forces [30]. The structure of this concentration profile at steady state can be described by an error function which also lends itself to simple assessment of the variance of the concentration profile of this interfacial region [23]. The derivative of an error function is a

Gaussian profile with a characteristic variance. This variance provides a standard means of comparison for steady state methods and is defined by including all dispersive forces (D_{TOT}) competing with the restorative forces and is equal to [4]:

$$\sigma^2 = \frac{D_{TOT}}{\text{change in velocity with position}} \quad (7)$$

The total dispersive forces cause band broadening, while focusing forces counteract it. D_{TOT} includes diffusion (D_{diff}) and Taylor-Aris dispersion [31]:

$$D_{TOT} = D_{diff} + \frac{u^2 d^2}{192 D_{diff}} \quad (8)$$

To understand the local velocity of the target species across this interfacial zone, the approach (and notation) given by Giddings [30] that states the overall transport (W) in the system is:

$$W = U + v, \quad (9)$$

where W is the overall component velocity, U is the drift velocity due to external fields (field-induced velocity), and v is the flow velocity. For electrophoretic exclusion, substitute, $-u$ for v (eqn. 1) so that:

$$W = U - u \quad (10)$$

In this case, only U varies with x , so the equation can be rewritten as:

$$W = ax - u \quad (11)$$

where a is change in velocity (slope) with respect to x , describing the focusing effects (field gradient dE/dx at the entrance). Within the bulk reservoir, at negative values of x and outside the interface zone, the target species move at an average velocity of u or less. The electrophoretic velocity of the species is less than the flow velocity due to small or nonexistent E . At exactly $x = 0$ (the

capillary entrance/electrode solution interface, Fig. 5.2), the average velocity is zero because u is exactly offset by $1/2E_{cap}\mu_{ave}$. At x values above zero (within the capillary, past the interfacial zone) the velocity is $u + \mu E_{cap}$.

The change in the electrophoretic velocity near the entrance, a , is:

$$a = \mu_{aves} dE/dx, \quad (12)$$

and therefore

$$W = \mu_{aves} \frac{dE}{dx} x - \frac{1}{2} \mu_{aves} E_{cap} \quad (13)$$

The local slope of the electric field (dE/dx) can be approximated and linearized by the change in the field across the interface divided by the diameter of the entrance. Noting eqns. 7, 8 and 12, variance is:

$$\sigma^2 = \frac{D_{diff} + \frac{u^2 d^2}{192 D_{diff}}}{\mu_{aves} \frac{dE}{dx}}, \quad (14)$$

and standard deviation is equal to:

$$\sigma = \sqrt{\frac{D_{diff} + \frac{u^2 d^2}{192 D_{diff}}}{\mu_{aves} \frac{dE}{dx}}}, \quad (15)$$

resulting in a form very similar to other tradition gradient models, but with the local gradient at the entrance rather than the global gradient of standard techniques [10].

5.2.4 Determining the two closest resolvable species

A construct must be created to determine the closest two electrophoretic mobilities that can be resolved with these associated variances. In this system, the linearized local slope (dE/dx) at the entrance (approximated by E_{cap} divided by the diameter, d) controls what can and cannot enter the capillary. This must be varied

in time or space. It is easier to conceptualize slowly varying the capillary potential and monitor what can enter the capillary, but this strategy omits the inherent advantages of the local gradient by slowly releasing any collected materials at the interface and smearing out the narrow concentration gradients. Alternatively, we choose to model in space, where a construct is created that sets E_{cap} between adjacent capillary entrances as a direct function of the distance between the centerline of those capillaries (Fig. 5.3). This solves three problems: 1) it retains the advantages present in the local gradient at each capillary entrance, 2) sets a physically meaningful construct reflective of real experiment apparatus, and 3) provides a function definition of ΔX that is easily conceptualized and tested.

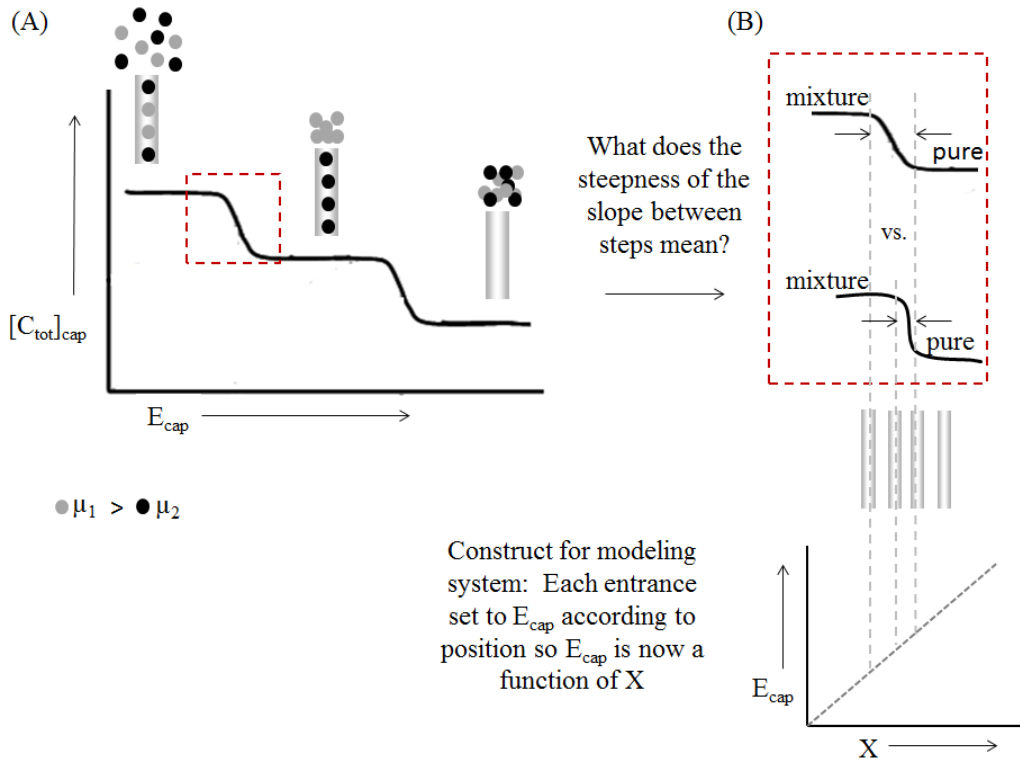


Figure 5.3. Using distance to determine the two closest resolvable species. A. Graph showing the total concentration inside the capillary for varying E_{cap} values. A large E_{cap} value corresponds to lower concentration inside the capillary due to exclusion. B. The transition between the channels entrances is related to the distance between the capillaries. The sharper the transition, the closer the capillaries can be.

A short description of the construct is presented as an example. Three channels are considered with three different E_{cap} values. One channel has a small enough E_{cap} that neither species will be excluded from the capillary entrance (Fig. 5.3A, left), allowing both species to flow through the capillary with the hydrodynamic flow (resulting in the highest total concentration in the channel). A second channel has an increased E_{cap} , such that the species with the larger mobility (represented with gray circles) are excluded (Fig. 5.3A, center), producing an increased concentration of that larger mobility species immediately

outside of the capillary and complete passage of the other through the channel. In a third channel, E_{cap} is such that the species with the smaller mobility will also be completely excluded (Fig. 5.3A, right), and both species are completely prevented from entering the channel. In this case, the applied field is too large to achieve separation of the specified analytes.

Conceptually, the sharper the transition between channel entrances, the closer the capillaries can be in (in terms of ΔX and E_{cap}) and still achieve successful differentiation (Fig. 5.3B). The change in E_{cap} between the entrances defines $\Delta dE/dx$, or the change in dE/dx , between to nearest neighbor channel entrances:

$$\Delta X = \frac{\Delta v}{\frac{d\mu}{dx}} = \frac{\Delta \mu E_{ave}}{\frac{1}{2} \mu_{ave} (\Delta \frac{dE}{dx})} \quad (16)$$

Note this differentiation is for only one of these ‘steps’ (Fig. 3) and resolution can be described by:

$$R = \frac{\Delta X}{4\sigma} = \frac{\frac{\Delta \mu E_{ave}}{\frac{1}{2} \mu_{ave} (\Delta \frac{dE}{dx})}}{4 \sqrt{\frac{D_{diff} + \frac{u^2 d^2}{192 D_{diff}}}{\mu_{ave} \frac{dE}{dx}}}} = \frac{\Delta \mu E_{ave} \sqrt{\frac{dE}{dx}}}{2 \sqrt{\mu_{ave} \Delta \frac{dE}{dx}} \sqrt{D_{diff} + \frac{u^2 d^2}{192 D_{diff}}}} \quad (17)$$

which suggests several things, including a steep gradient at the entrance and minimizing the difference between these local gradients in adjoining capillaries would maximize resolution.

The smallest change in electrophoretic mobilities is identified as the best resolution for the technique, so the resolution was solved for $\Delta \mu$:

$$\Delta\mu = \frac{R * 2 * \sqrt{\mu_{ave}} \Delta \frac{dE}{dx} \sqrt{D_{diff} + \frac{u^2 d^2}{192 D_{diff}}}}{E_{ave} \sqrt{\frac{dE}{dx}}} \quad (18)$$

If resolution is set to 1 (complete separation in traditional separations), $\Delta\mu$ becomes $\Delta\mu_{min}$ (the smallest change in mobilities that can be separated with adequate resolution) and is equal to:

$$\Delta\mu_{min} = \frac{2 * \sqrt{\mu_{ave}} \Delta \frac{dE}{dx} \sqrt{D_{diff} + \frac{u^2 d^2}{192 D_{diff}}}}{E_{ave} \sqrt{\frac{dE}{dx}}} \quad (19)$$

5.3 Results and discussion

According to this model and theoretical assessment, several factors can influence resolution including capillary diameter, flow rate, average electrophoretic mobility, and field strength – within the capillary or channel and the difference in field strength between adjoining entrances. All other factors can be derived from these parameters. A good example is the capillary diameter. It influences resolution through Taylor-Aris dispersion (eqn. 7) and the steepness of the gradient (dE/dx , approximated by E_{cap}/d) at the entrance of the channel.

5.3.1 Capillary diameter and flow rate

Because the relationship between resolution and capillary diameter and flow rate are not algebraically simple (they are not trivial linear, exponential, or logarithmic relationships), they are assessed graphically (Fig. 5.4). Most of the following discussion is centered on finding the minimum difference in electrophoretic mobilities which can be separated because this value is easily compared to other electrophoretic techniques. In this assessment, the smaller $\Delta\mu$

is, the better the resolution. Accordingly, resolution is best when the capillary diameter is smaller and flow rate is lower. The strongest effect is a reduction in Taylor-Aris dispersion at small diameters and low flow rates, and an additional effect is an increased gradient at the capillary entrance. Since the smaller diameters positively influence resolution through two mechanisms, increased gradient and reduced dispersion, it dominates the relationship relative to flow. Resolution can be significantly increased by reducing channel diameters – by orders of magnitude, but at the cost of reduced volume flow rate. This is directly offset by the opportunity to operate this strategy with massively parallel interfaces, all with small diameter, high resolution interfaces, while attaining the desired bulk fluid transfer.

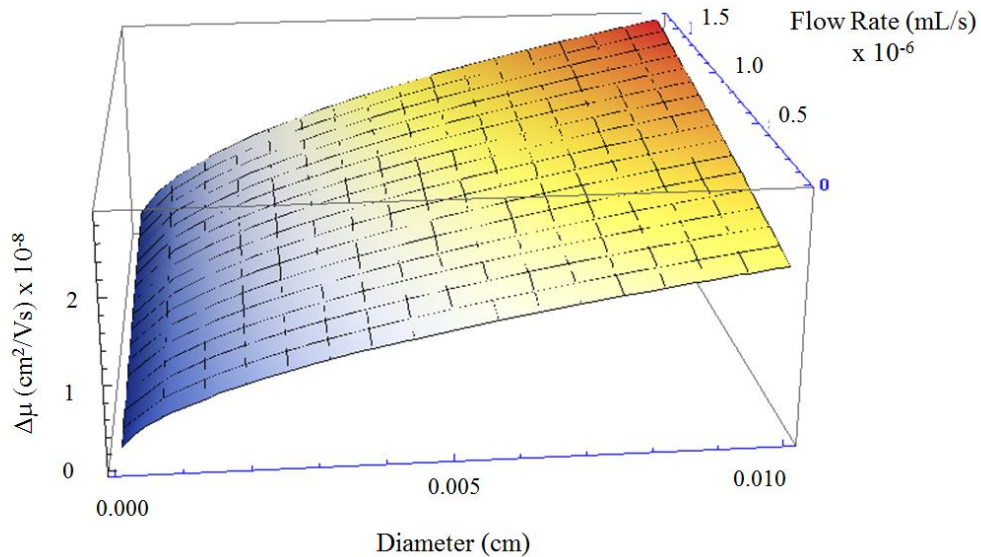


Figure 5.4. Resolution as a function of capillary diameter and flow rate. Resolution is described by $\Delta\mu_{\min}$ and increases most notably with smaller capillary diameters.

5.3.2 Smallest separable difference in electrophoretic mobilities

According to the calculations presented here, the smallest difference in mobilities of species ($\Delta\mu_{\min}$) that can be separated ($R = 1$) is $\sim 10^{-9}$ cm²/Vs. This occurs at the smallest common capillary diameter of 1 μm , a relatively low fluid velocity of 100 $\mu\text{m/s}$, and $\Delta dE/dx$ of 10 V/cm² (assuming a large diffusion coefficient of 6×10^{-4} cm²/s, and a μ_{ave} of 5.0×10^{-5} cm²/Vs). Driving these down to obvious limits where assumed physics breakdown (200 nm channel diameter, 3000 V/cm field, 50 $\mu\text{m/s}$ flow velocity) gives $\sim 10^{-11}$ cm²/Vs. As a comparison, results were noted from the Jorgenson group [32, 33]. According to the data presented in their impressive experimental studies, flow counterbalanced CE could separate species with electrokinetic mobilities as similar as 10^{-7} cm²/Vs in several hours [32], while an ultrahigh voltage CE study separated species with mobilities as close as 10^{-8} cm²/Vs in approximately 1 hour [33]. Additionally, Culbertson *et al.* performed a CE study using a spiral channel on a microchip to separate dichlorofluorescein from a contaminant that differed by as little as 10^{-6} cm²/Vs in tens of seconds [18]. According to these experimental results, the resolution theory developed here is on par with CE studies.

Aside from traditional CE studies, there are several examples in the literature where species have been differentiated at an interface similar to the one described by this theory, including GEMBE [23] and previous electrophoretic exclusion studies [26, 28]. To compare these studies, the variance of the concentration gradient at the entrance must be determined; however, it is difficult to quantitatively assess these data. GEMBE studies vary the flow rate and

introduce dispersion associated with the transport of the concentrated species to the detection element, and an increase in measured dispersion from the detection element itself. The calculation and subtraction of these additional dispersion elements to estimate the entrance dispersion are of little value since they are much larger. Nevertheless, GEMBE reports $\Delta\mu_{\min}$ values on the order of 10^{-5} cm²/Vs for short separation time (tens of seconds), and improved resolution with increased analysis time. In these GEMBE experiments, the detection window standard deviation is estimated to be 0.5 mm, which is noted to say that the initial width of the analyte boundary as it enters the capillary is negligible. According to the theory presented here, in fact, the standard deviation for the experimental conditions noted is approximately 15 μ m, or about 3%, supporting their assertion.

Meighan *et al.* reported several data which can be assessed [26]. The flow injection analysis mode, however, also added Taylor-Aris dispersion and resulted in standard deviations measured at the detector of 3 - 13 mm, whereas the entrance contribution was merely about 40 μ m according to the theory presented here. The calculated dispersion induced by the Taylor-Aris mechanism only accounted for a little over a millimeter of this distance and; therefore, some other mechanism is likely dispersing the concentration gradient. This is supported by the poor resolution (as report by $\Delta\mu_{\min}$) for two proteins differing in electrophoretic mobilities of 8×10^{-5} cm²/Vs at $R = 0.68$. The theoretical $\Delta\mu_{\min}$ ($R = 1$) is approximately 10^{-8} cm²/Vs for the conditions reported. These previous studies where indirect and dynamic strategies are used are not especially helpful in clarifying exactly what resolution is possible with this overall strategy.

Fortunately, direct observation of the local interface is available and indicates very sharp concentration gradients [28] and the flow and electric field forces of the interface have been experimentally quantified [27]. The concentration gradients are shown to be less than 100 μm wide for small molecules (fluorescent dye). This was produced at an asymmetric interface not optimized for resolution, but does indicate that steep concentration gradients consistent with these calculations are observed. The flow and electric field effects are consistent with the model presented here.

5.3.3 Peak capacity

Another measure of the quality of a separation process is peak capacity. Peak capacity is defined as the amount of distinguishable peaks, or elements, that can be separated in a given space or time. Peak capacity is a valuable separations metric because it accounts for the total amount of differentiable elements, as opposed to just comparing between two species as in resolution. In electrophoretic exclusion, peak capacity is the total number of species that can be differentiated in individual reservoirs, assuming $R = 1$.

The calculated peak width (2σ) varies across the experimental space. To account for this variation, $\Delta\mu$ was calculated at both the lowest reasonable electrophoretic mobility and the highest for an otherwise constant system. To calculate this theoretical peak capacity (n_c), several assumptions were made. First, it was determined that the range of electric fields that could successfully be used for separation were between 10 and 1000 V/cm (this could be extended to 3 kV/cm for a microdevice). A channel diameter of 1 μm was assumed and the

$\Delta dE/dx$ between entrances was 10 V/cm². Diffusion (D) was set at 6×10^{-4} cm²/s and hydrodynamic velocity ranged between 0.1 and 1 mm/s. Next, the smallest μ_{ave} (referred to as μ_{min}) was calculated using the lowest linear velocity and the largest electric field strength to be $\mu_{min} = 10^{-5}$ cm²/Vs. The largest μ_{ave} (referred to as μ_{max}) was determined by using the highest linear velocity divided by the lowest electric field $\mu_{max} = 10^{-2}$ cm²/Vs.

The smallest separable difference in mobilities between species at $R = 1$, $\Delta\mu_{min}$, was calculated at both the μ_{min} and μ_{max} that was defined above. For $\Delta\mu_{min}$ at μ_{min} , $\Delta\mu_{min}$ was calculated using eqn. 18, which resulted in:

$$\Delta\mu_{min\mu_{min}} = 10^{-10} \text{ cm}^5 / \text{Vs} \quad (21)$$

Similarly, $\Delta\mu_{min}$ at μ_{max} was calculated, except the smallest electric field (10 V/cm) was used for E_{ave} , the largest flow velocity (1 mm/s) was used, and dE/dx was calculated as 1.0×10^{-5} V/cm²:

$$\Delta\mu_{min\mu_{max}} = 10^{-5} \text{ cm}^2 / \text{Vs} \quad (22)$$

Finally, the total peak capacity was calculated by using the range of mobilities divided by the average $\Delta\mu_{min}$:

$$n_c = \frac{\mu_{max} - \mu_{min}}{\Delta\mu_{min\mu_{min}} + \Delta\mu_{min\mu_{max}} / (2)} = 1200 \quad (23)$$

These calculations indicate that electrophoretic exclusion can be used for the isolation of analytes in samples that contain a large number of species and whose species cover a large range of mobilities. A similar technique, electric field gradient focusing, suggested peak capacities of over 10,000 could be

achieved [19], while capillary isoelectric focusing reported an experimental peak capacity of over 4000 [34].

Although the peak capacity for electrophoretic exclusion is already comparable to some of the better one dimensional separation techniques, it can be further improved by stacking separation steps, while varying the buffer pH, ionic strength, etc. (moving the effluent from a single element, changing the buffer and separating on a new element), which changes the electrophoretic mobilities of the species and allows them to be isolated in different locations. Electrophoretic exclusion is a dynamic technique that allows for adjustments to further improve its separation efficiency.

5.4. Concluding remarks

To understand the applicability of a separations technique to various samples, the resolving capabilities of the technique must be understood. Here, the theoretical resolution of electrophoretic exclusion has been described, along with a brief analysis of previously published experimental data. Theoretically, results indicated that electrophoretic exclusion can separate species with very similar mobilities ($\Delta\mu_{\min} = 10^{-9} \text{ cm}^2/\text{Vs}$), better even than experimental results reported for CE. The assessment of the experimental data indicated that electrophoretic exclusion is less capable of resolving species than what was theoretically indicated, due to various dispersion forces, particularly on the meso-scale. However, when reducing the size scale to a microchip, the dispersive forces decreased, suggesting the possibility of better resolution. To further improve resolution, an optimized electrode design can be created, reducing the dispersive

forces even further. With better resolution, more similar species can be differentiated and; therefore, more complex samples can be analyzed and separated. The engineering of an interface with high resolving capabilities can be used in designs that include several of these interfaces in series and parallel that can be envisioned for the complex sample analysis.

5.5 References

- [1] Ricker, R. D., Sandoval, L. A., *J. Chromatogr. A* 1996, 743, 43-50.
- [2] Kanner, S. B., Reynolds, A. B., Parsons, J. T., *J. Immunol. Methods* 1989, 120, 115-124.
- [3] Geiger, M., Hogerton, A. L., Bowser, M. T., *Anal. Chem.* 2012, 84, 577-596.
- [4] Giddings, J. C., Dahlgren, K., *Sep. Sci.* 1971, 6, 345-356.
- [5] Cong, Y. Z., Liang, Y., Zhang, L. H., Zhang, W. B., Zhang, Y. K., *J. Sep. Sci.* 2009, 32, 462-465.
- [6] Cui, H. C., Horiuchi, K., Dutta, P., Ivory, C. F., *Anal. Chem.* 2005, 77, 7878-7886.
- [7] Hofmann, O., Che, D. P., Cruickshank, K. A., Muller, U. R., *Anal. Chem.* 1999, 71, 678-686.
- [8] Greenlee, R. D., Ivory, C. F., *Biotechnol. Prog.* 1998, 14, 300-309.
- [9] Ross, D., Locascio, L. E., *Anal. Chem.* 2002, 74, 2556-2564.
- [10] Kelly, R. T., Woolley, A. T., *J. Sep. Sci.* 2005, 28, 1985-1993.
- [11] Shackman, J. G., Ross, D., *Electrophoresis* 2007, 28, 556-571.
- [12] Danger, G., Ross, D., *Electrophoresis* 2008, 29, 3107-3114.
- [13] Burke, J. M., Ivory, C. F., *Electrophoresis* 2010, 31, 893-901.
- [14] Huang, Z., Ivory, C. F., *Anal. Chem.* 1999, 71, 1628-1632.
- [15] Giddings, J. C., *J. Chromatogr.* 1960, 3, 520-523.

- [16] Giddings, J. C., *Anal. Chem.* 1963, 35, 2215-2216.
- [17] Foret, F., Deml, M., Bocek, P., *J. Chromatogr.* 1988, 452, 601-613.
- [18] Culbertson, C. T., Jacobson, S. C., Ramsey, J. M., *Anal. Chem.* 2000, 72, 5814-5819.
- [19] Tolley, H. D., Wang, Q. G., LeFebre, D. A., Lee, M. L., *Anal. Chem.* 2002, 74, 4456-4463.
- [20] Shackman, J. G., Munson, M. S., Ross, D., *Anal. Chem.* 2007, 79, 565-571.
- [21] Ross, D., Kralj, J. G., *Anal. Chem.* 2008, 80, 9467-9474.
- [22] Ross, D., Romantseva, E. F., *Anal. Chem.* 2009, 81, 7326-7335.
- [23] Ross, D., *Electrophoresis* 2010, 31, 3650-3657.
- [24] Polson, N. A., Savin, D. P., Hayes, M. A., *J. Microcolumn Sep.* 2000, 12, 98-106.
- [25] Meighan, M. M., Keebaugh, M. W., Quihuis, A. M., Kenyon, S. M., Hayes, M. A., *Electrophoresis* 2009, 30, 3786-3792.
- [26] Meighan, M. M., Vasquez, J., Dziubcynski, L., Hews, S., Hayes, M. A., *Anal. Chem.* 2011, 83, 368-373.
- [27] Keebaugh, M. W., Mahanti, P., Hayes, M. A., *Electrophoresis* 2012, 33, 1924-1930.
- [28] Kenyon, S. M., Weiss, N. G., Hayes, M. A., *Electrophoresis* 2012, 33, 1227-1235.
- [29] Pacheco, J. R., Chen, K. P., Hayes, M. A., *Electrophoresis* 2007, 28, 1027-1035.
- [30] Giddings, J. C., *Sep. Sci. Technol.* 1979, 14, 871-882.
- [31] Taylor, G., *Proc. R. Soc. London A* 1953, 219, 186-203.
- [32] Culbertson, C. T., Jorgenson, J. W., *Anal. Chem.* 1994, 66, 955-962.
- [33] Hutterer, K. M., Jorgenson, J. W., *Anal. Chem.* 1999, 71, 1293-1297.
- [34] Shen, Y. F., Berger, S. J., Smith, R. D., *Anal. Chem.* 2000, 72, 4603-4607.

Chapter 6

The Development of a Microfluidic Array for Use in Electrophoretic

Exclusion Separations

6.1 Introduction

Previous chapters have discussed the role of separations in complex sample analysis and have established the potential advantages and applications for array-based separations. Electrophoretic exclusion, with its ability to separate native species in bulk solution based upon their electrophoretic mobilities, is especially appropriate for array separations. Because species are separated based upon their mobilities, the technique does not require molecular recognition elements and can be dynamically adjusted during the course of an experiment by simply altering the electric field strength. By separating species in bulk solution, as opposed to in a channel, channel length becomes essentially irrelevant, allowing for a smaller device footprint and for numerous capture zones in series and parallel for addressing complex samples.

In addition to being ideal for a multiplexed format, avoiding separation in-channel reduces dispersive forces. In traditional separations, species are injected onto a column in plug form, and during the course of the experiment, species move differentially along the channel. During this process, species migrate at different rates in the column based upon their specific properties. Although analytes are spatially separated, they also disperse and diffuse as the experiment continues. This dispersion limits the resolving capabilities of the technique. Electrophoretic exclusion exploits restoring forces, the electric field gradient at

the channel entrance, to help balance the diffusive and dispersive effects; therefore, increasing resolution of the technique. Theory indicates that electrophoretic exclusion has resolving capabilities comparable to those of CE, in a dramatically different format (Chapter 5). Additionally, peak capacities have been theoretically calculated to be on the order of 1,000 (Chapter 5). Having high resolving capabilities and high peak capacities is a necessity when studying complex samples so that similar species can be differentiated. High resolution is also essential for creating a separations-based array so that many species, some of which will be very similar, can be individually isolated and then later, studied. Electrophoretic exclusion is uniquely suited for array-based separations, particularly when designed for a microdevice.

For several decades, microfluidics has been used to manipulate and move fluids on the small scale. Microfabricated devices have been used for many applications such as DNA sequencing [1, 2], clinical studies [3, 4], and separations [5, 6], including array applications from Protein Forest [7-9]. Some of the most notable advantages of performing analyses on microdevices include decreased analysis time and reagent consumption. This is especially important when it is not feasible to obtain or use large amounts of sample, for example when studying samples from biological and environmental sources. Additionally, microdevices can often be made portable, making them ideal for environmental [10, 11] and, in some cases, biological testing [12]. These advantages have contributed to the increase in popularity of microfluidic devices over the last several decades.

The creation of features and channels in microfluidic devices was originally achieved with photolithography and etching techniques. Although the techniques were well understood, due to their origins in microelectronics, there were several disadvantages to using them [13]. Silicon is expensive and cannot be used for systems that require optical detection, and devices must be assembled in a clean room. Glass, though transparent and less expensive, still requires the use of a cleanroom for assembly. This increases the time investment to make every device in a clean room. More recently, polymers have been used for creating the features in a microdevice, with polydimethylsiloxane (PDMS) being the most popular choice [14]. There are several advantages to using PDMS, including optical transparency, low cost, low curing temperature, irreversible or reversible sealing, fast prototyping, and biocompatibility. When using PDMS for creating the features in a microdevice, a master template must first be fabricated for subsequent replica molding. After a replica is made, the resulting polymer layer must be sealed to a flat substrate. For irreversible sealing, oxygen plasma is required. The patterned PDMS layer can be sealed to another PDMS layer, glass, silicon, etc. for feature completion [15].

Glass is often used as the substrate in a microfluidic device with PDMS [15]. It is an attractive option because it is optically transparent; it can be used with fluorescence detection, with laser induced fluorescence being popular because of the small dimensions and sample sizes [16]. Fluorescence detection is attractive because it is sensitive and can be performed during the course of an experiment, in real-time. However, analytes must either be natively fluorescent,

or they must be labeled. Other common options for detection include electrochemistry [17-19], and mass spectrometry [20, 21]. Electrochemical detection is sensitive, but adds another level of complication for fabrication purposes, particularly if electrodes are already required for the experimental parameters. Mass spectrometry (MS) is incredibly sensitive as well, but it requires an additional interface for transfer to the MS.

When designing microfluidic devices, feature sizes, including channels, reservoirs, and electrodes, must be considered. As the name suggests, for channels and reservoirs, at least one dimension has to be on the micrometer scale. It is not uncommon, though, for channel widths and lengths to be on the centimeter scale. Such is the case with chips that are used for IEF [22-24] and free flow electrophoresis [25, 26]. When designing the fluid elements, factors such as detection method, fluid flow rates, and sample amounts must be considered. Additionally, when electrodes are used on the device, in cases such as electrophoresis, electrode dimensions, location, and material must be considered [27]. For electrophoretic separations, electrodes can be embedded in a channel [28, 29] or remain separate from the channel [30, 31].

Based upon the information above, the practicality of microfluidic devices has been well established, along with the major parameters that must be considered when creating a device. The rest of this chapter is devoted to development of a microfluidic array to be used for electrophoretic exclusion. Thus far, it has been well established that separations-based arrays have a potentially important place in complex sample analysis, and electrophoretic

exclusion is suited to this type of application. However, an array device has yet to be used, or even fabricated. Here, the initial array device for electrophoretic exclusion is constructed and tested.

6.2 Materials and methods

Device design and fabrication was very similar to that described in Chapter 4, where changes are noted below.

6.2.1 Design and fabrication of array device

A photograph of the device design (top-view) (Fig. 6.1). Hybrid glass/PDMS devices were used for all experiments and each device contained two separate arrays.

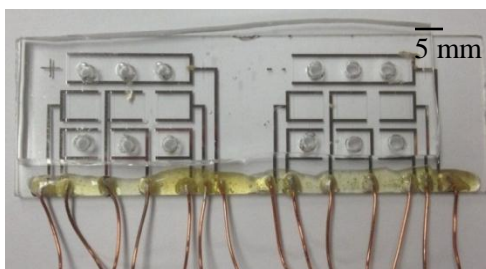


Figure 6.1. Experimental array device. Top-view photograph of the hybrid/glass array device. The standard glass microscope slide contained Ti/Pt electrodes, while the PDMS layer contained the channels and reservoirs. Each device contained two arrays.

A PDMS layer was made using standard photolithography techniques. Each array design contained an entrance reservoir, followed by three channels in parallel, each connected to a central reservoir, a second channel, and an exit reservoir. The entrance reservoir was 19 mm x 5 mm, the central and exit reservoirs were 5 mm x 5 mm, and each channel was 1 mm long and 100 μm

wide with a uniform depth throughout of 10 μm . A schematic representation is included (Fig. 6.2, left).

Electrodes were plated on standard microscope slides. Electrodes were 500 μm wide and bracketed each reservoir (entrance, central, and exit) on three sides, allowing for a flat potential field in the reservoir. The flat potential field ensured that exclusion only occurred at the electrode aligned at the channel entrance. A schematic of the electrode design is included (Fig. 6.2 right). Each electrode had an electrode pad that lead to the bottom of the slide for attachment of leads with silver conductive epoxy. Photolithography steps were the same as those reported in Chapter 4; however, after development, 30 nm layer of Ti, followed by a 50 nm layer of Pt were deposited using electron beam evaporation (PVD75, Kurt J. Lesker Company, Clairton, PA).

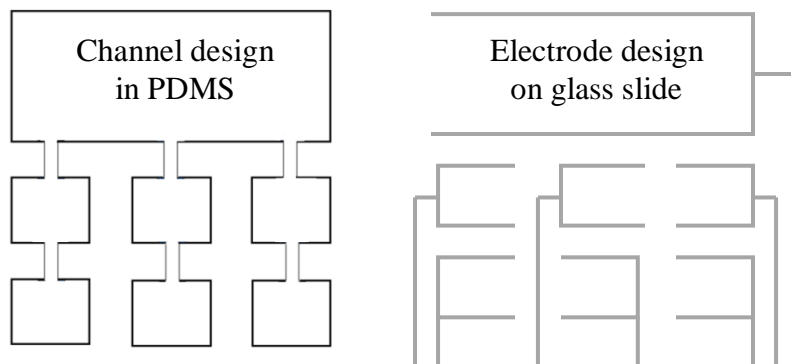


Figure 6.2. Schematic representations of PDMS and electrode patterns.

6.2.2 Materials

Aspartic acid (Sigma-Aldrich, St. Louis, MO), hydrochloric acid, rhodamine 123 (Invitrogen, Carlsbad, CA, USA), DMSO, rhodamine 6G

(Invitrogen), true blue chloride (Invitrogen), and 8-hydroxy-1,3,6-pyrenetrisulfonic acid trisodium salt (HPTS) (Acros Organics, Geel, Belgium) were all used as received. Aspartic acid buffer was prepared to 5 mM concentration at a pH of 2.95 using 18 M Ω Milli-Q water. Stock solutions of rhodamine 123 and rhodamine 6G were prepared to 2 mM in DMSO and then diluted to 10 μ M in aspartic acid buffer on the day of experiments. A stock solution of HPTS was prepared in 18 M Ω Milli-Q water, and diluted to 40 μ M for experiments. A stock solution of true blue chloride (~1 mM) was obtained and diluted with water (1:1). On the day of experiments, solutions were diluted using aspartic acid buffer.

6.2.3 Experimental design

The PDMS layer was bonded to the glass slide with the Ti/Pt electrodes using oxygen plasma operated at 50 W for 60 s. Each array design was filled with dye by pipetting 7 μ L of solution into each of the three holes in the entrance reservoir, for a total of 21 μ L in each array. For experiments that used two dyes, equal volumes of each dye were combined so that the final concentration of each was of that mentioned above. The combination of dyes was then pipetted into the device. Flow rates for all experiments were approximately 1 - 10 nL/min. Potential (0 – 1500 V) was applied using a HVS448-3000D LabSmith power supply (Livermore, CA). Seven individual potentials were applied; one to each electrode pad so that each reservoir was individually addressed and potentials were applied so that there was a flat potential field in each reservoir.

A voltage divider was constructed in-house from 100 k Ω , 120 k Ω , and 1 M Ω resistors (Fig. 6.3). Each voltage divider was connected to a thin wire that was coiled at the end. The coiled end was then slipped over the leads that were epoxied to the microscope slide. Output potentials were monitored using a digital multimeter throughout the course of the experiment. Output voltages from the voltage divider ranged between 0 V and 25 V, with the resulting electric fields varying between 0 and 250 V/cm.

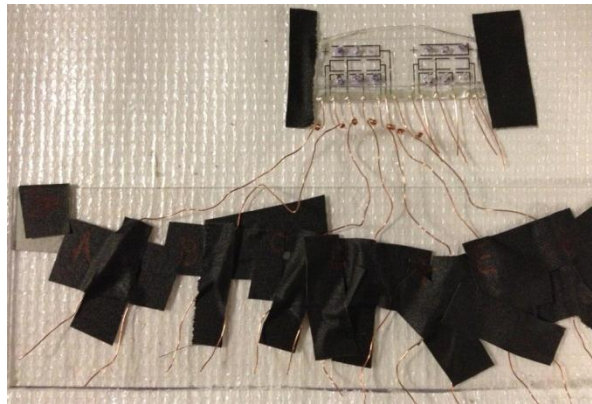


Figure 6.3. Voltage divider connected to an array device. One voltage divider was constructed for each lead.

Experiments were monitored using the same microscope setup reported in Chapter 4, with the exception of a 1.25X objective in addition to the 4X objective. Additionally, Streampix 5 was used in place of Streampix 3 (NorPix, Montreal, Quebec, Canada). ImageJ (NIH, Bethesda, Maryland) was used for intensity measurement analysis.

6.3 Results and Discussion

6.3.1 Device design

The array device was designed based upon the success of the initial microfluidic device used for electrophoretic exclusion at a single interface (Chapter 4). To allow for an array, additional interfaces were included.

6.3.1.1 Device parameters

A PDMS layer with reservoirs and channels was sealed to a glass microscope slide plated with electrodes. Because of the success of the original microfluidic electrophoretic exclusion experiments, the same size reservoirs and channels were used for the array design.

Electrode width remained the same as those used previously. Although the electrodes were wide (500 μm), this allowed for easier alignment with the PDMS layer containing the channels and reservoirs. This step was performed manually. More important than the width of the electrode, is its alignment at the channel entrance. The effect of electrode alignment has been discussed previously (Chapter 4). The width of the electrodes also did not negatively impact the electric field shape at the channel entrance, which is essential for exclusion and directly impacts the success of the separation process. Electric field lines converged at the edge of the electrode nearest the channel. Additionally, the width of the electrodes allowed for easier epoxying of the leads to the chip.

Although the electrodes used in this array were the same width as those used in the initial microchip designs, the electrodes for the array, were made from

Ti/Pt instead of Cr/Au (Chapter 4). The decision to switch to Ti/Pt was made based upon experimental evidence that suggested Ti/Pt electrode slides were more robust, meaning that they could be reused more often than the Cr/Au electrodes

6.3.1.2 Selection of analytes

Fluorescence detection was chosen to monitor the exclusion process because it allows for the direct visualization of exclusion and is ideal for the PDMS/glass hybrid device that was designed. Four dyes were chosen for testing the array device based upon their fluorescent emission (dyes had to fluoresce within red, blue, or green wavelengths to be suitable for use with the available triple bandpass filter cube) and their charges in the aspartic acid buffer that was used for all experiments. Experiments were performed at pH 3 to largely eliminate electroosmotic flow (EOF). By reducing the pH to 3, EOF could be greatly decreased [32-34], without the additional step of coating the PDMS channels. Because of this, dyes were used, as opposed to biological samples, due to their relative instability in an acidic pH. Biological samples typically must remain at physiological pH and are more complex analytes. At pH 3, true blue chloride, rhodamine 123, and rhodamine 6G were positively charged, while HPTS was negatively charged. All dyes were fluorescently green, aside from true blue chloride, which fluoresced blue in the buffer conditions.

6.3.2 Terminology used in the array device

Before continuing with the analysis of results, terminology must be established for addressing the various locations in the array device. The large reservoir used for sample introduction is referred to as the main or entrance

reservoir. The channels leading from the entrance reservoir to each of the central reservoirs will be referred to as entrance channels 1-3, with channel 1 being on the left. The central reservoirs, where isolation was designed to occur, will be referred to as central reservoirs 1-3, with reservoir 1 being on the left. Similarly, the channels leading from the central reservoirs to the exit reservoirs will be referred to as exit channels 1-3, corresponding to central reservoirs 1-3. End reservoirs will be addressed as exit reservoirs 1-3, with reservoir 1 on the left (Fig. 6.4).

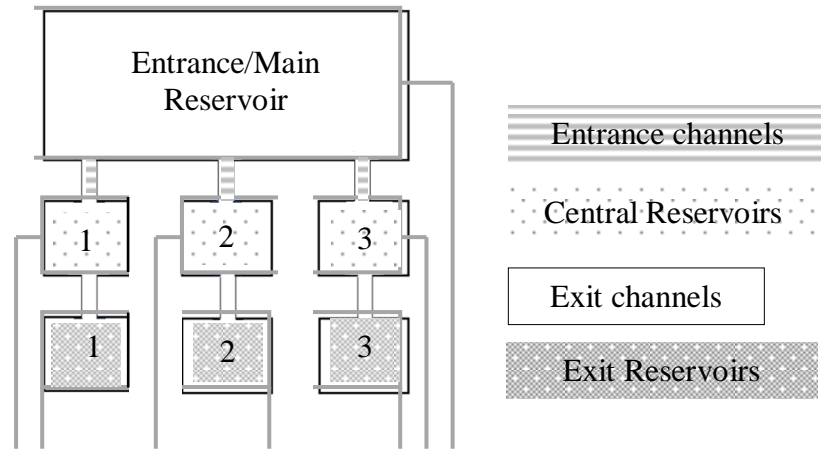


Figure 6.4. Schematic explaining the array device terminology. Numbers and shading indicate reservoirs and channels.

6.3.3 Basics of electrophoretic exclusion in an array device

Electrophoretic exclusion is achieved at an electrode/solution interface when the electrophoretic velocity of a species is greater than or equal to the opposing hydrodynamic fluid velocity through a channel. The array prototype was designed with a total of six interfaces, three in the entrance reservoir (one at each entrance channel) and three in the central reservoirs (one at each exit

channel). Although exclusion could occur at six different interfaces, experiments were designed so that species could be isolated individually in each of the three central reservoirs. The main reservoir was used for sample introduction and the electrodes at the entrance channels were designed to control what species were allowed to leave the entrance reservoir and travel to the central reservoirs. Similarly, the electrodes at the exit channels were programmed to prevent certain species from leaving the central reservoirs. Using this principle, species can be selectively isolated and concentrated in the central reservoirs. Because all experiments detailed in this chapter used the same buffer (aspartic acid buffer at pH 3) and flow rates were assumed to remain constant throughout the course of an experiment (1 – 10 nL/min.), the electric field was manipulated for the differentiation of species.

Experiments were designed so that HPTS would be captured in central reservoir 1, while positively charged dyes would be captured in central reservoirs 2 and 3. A representative potential sequence is shown (Fig. 6.5).

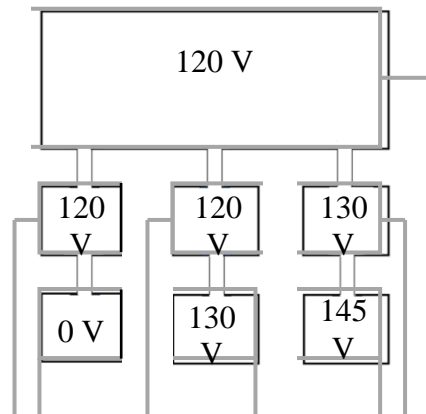


Figure 6.5. Representative potential sequence used for exclusion experiments.

Exclusion only occurred when there was a gradient in the electric field at the electrode-solution interface at a channel. In instances when there was no potential difference between reservoirs in series, exclusion was not intended to occur. For a hypothetical example, if the potential sequence above was applied to an array, all species would flow between the entrance reservoir and central reservoirs 1 and 2. However, based upon the positive potential difference between exit reservoir 1 and central reservoir 1, the negatively charged HPTS would be prevented from exiting central reservoir 1, resulting in its isolation in that location. Similarly, the negative potential difference applied between exit reservoir 2 and central reservoir 2, would result in certain positively charged species being excluded (based upon the species' mobilities) and isolated in the central reservoir. Assuming two positively charged dyes with differing mobilities, central reservoir 2 was designed to capture the positively charged species with the larger electrophoretic mobility since a lower potential difference was applied. The potential difference between the entrance reservoir and central

reservoir 3 was set equal to that of the difference between central reservoir 2 and exit reservoir 2. This was done to prevent the positively charged dye with the larger mobility from entering central reservoir 3. Finally, the largest negative potential difference was initiated between central reservoir 3 and exit reservoir 3. This was done to exclude the positively charged species with the smaller mobility. Based upon a potential sequence such as the one indicated, three species could be isolated individually in each central reservoir, and if experiments are run long enough, concentrated in their isolation locations.

6.3.4 Assessment of initial array design

As mentioned previously, the array device was designed based upon many of the parameters from the initial microchip studies outlined in Chapter 4. However, before complex samples, or even a somewhat simple sample (three analytes) can be separated with the device, its basic performance had to be assessed. The main variables tested were the power supply, electrode design, and reservoir integrity. The majority of this chapter is dedicated to testing the initial array design.

6.3.4.1 Electrode design

Electrodes were slightly modified after initial experiments were performed. During the course of experiments, unexpected exclusion behavior repeatedly occurred in the entrance reservoir at entrance channel 2 (data not shown). Because experiments were designed so that no electric field existed at this channel entrance, exclusion should not have occurred. Inspection of several electrode slides revealed an error in the electrode mask at the entrance reservoir.

There was a small break in the connection between the electrode pad and the entrance reservoir, which prevented the application of potential to that reservoir. Instead of being held at a constant potential, this electrode was always at 0 V. This allowed it to act as a capacitor, resulting in inconsistent exclusion behavior. To rectify this, silver conductive epoxy was used to bridge the gap. However, a new mask was also made to correct the error.

6.3.4.2 Voltage divider

A voltage divider was constructed in-house (Fig. 6.3) using 100 k Ω , 120 k Ω , and 1 M Ω resistors to divide voltages from the power supply by \sim 1:10 and 1:100. In previous experiments it was determined that the voltages coming from the power supply varied by \pm 5 V at any given moment, resulting in fluctuations of approximately \pm 5%. Due to these fluctuations, potential differences between reservoirs were sometimes eliminated when they were intended to exist, and other times, they were created. This resulted in some instances of exclusion when it was not predicted to, specifically when an experiment was designed to have no potential difference between reservoirs. And in other instances, exclusion did not occur, or was not maintained, when it was predicted, particularly when differences in applied potential were small (5 – 10 V).

For example, during a single dye experiment with rhodamine 123, an electric field of -100 V/cm (-10 V difference) was applied between central reservoir 2 and exit reservoir 2, and between the main reservoir and central reservoir 3. Because of this potential sequence, exclusion was expected to occur at entrance channel 3. A 20 min experiment was performed where still images

were taken at various intervals throughout the study and fluorescence intensity was then measured in ImageJ. For this study, intensity measurements were taken in central reservoirs 2 & 3 at the top of the reservoirs, just below the electrode. A successful exclusion process resulted in a decrease in the fluorescence at this location. Based upon the applied potentials, an exclusion process was expected only at entrance channel 3, resulting in a decrease in the fluorescence intensity at the observation location. The decrease in fluorescence was the result of the material being excluded at entrance channel, and, therefore, prevented from entering the central reservoir. Initially, successfully exclusion was observed (reservoir 3), as indicated by a decrease in fluorescence intensity (Fig. 6.6). However, after approximately 4 min, the fluorescence intensity began to increase again, indicating that the excluded material was released and allowed to flow down the channel and into the reservoir. This behavior was consistent with the reduction in electric field strength, which can result from fluctuating voltages from the power supply.

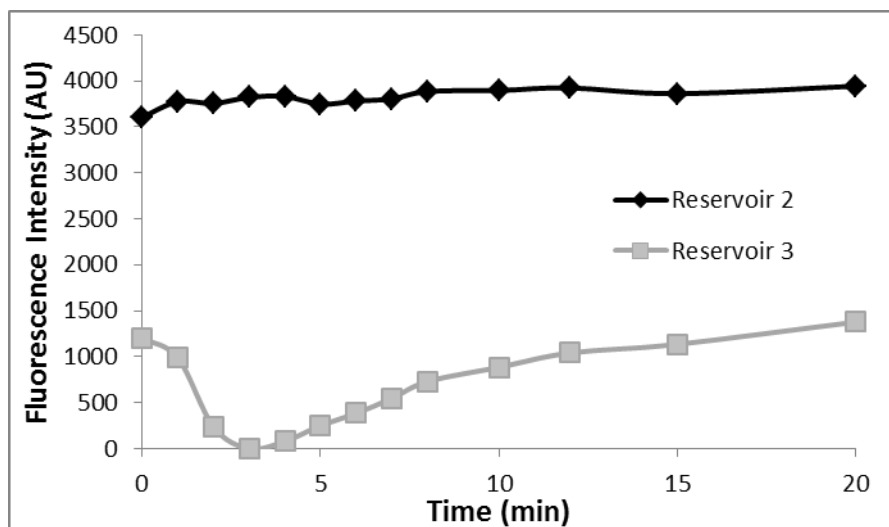


Figure 6.6. Fluorescence intensity graph. Measurements were made near the entrance electrode in central reservoirs 1 and 2. The decrease in intensity, followed by the increase in intensity in reservoir 3 indicates potential is fluctuating

To reduce these fluctuations in applied potentials, a voltage divider was added to the experimental design. An initial voltage divider experiment was performed using a single dye so that the functionality of the device could be tested. Output potentials were measured, and instead of the varying by \pm tens of percent when using the lower voltages, voltages only fluctuated by 0.05 depending on which voltage divider was used. This was the predicted outcome when the voltage divider was being employed and it was expected to improve the stability of the applied potentials and allow for anticipated exclusion behavior.

The tunability of the voltage divider was also tested. An experiment using HPTS as the analyte initially exhibited unexpected exclusion in the entrance reservoir at entrance channel 1 (Fig. 6.7), despite the potential sequence being designed not to elicit exclusion at this channel. Before potential was applied, no

exclusion was observed, as indicated by the consistent fluorescence intensity (Fig. 6.7A, red box). Once potential was applied, exclusion at the entrance reservoir became evident, as demonstrated by the fluorescence intensity decrease at the top of central reservoir 1 and within entrance channel 1 (Fig. 6.7B, red box). When exclusion was observed, the potential was measured with a voltage divider. It was determined that there was a small positive potential difference causing the exclusion of HPTS. The voltage was then adjusted at central reservoir 1 during the experiment to eliminate the potential difference. Exclusion immediately halted. This was shown by increased fluorescence intensity in the channel (Fig. 6.7C, red box) once the potential sequence was adjusted accordingly. The increase in fluorescence intensity resulted from the excluded material traveling down the channel again. This demonstrated the possibility for adjustment during the course of an experiment, and consequently, the potential for dynamic experiments where potentials could be changed to selectively isolate and move species through an array.

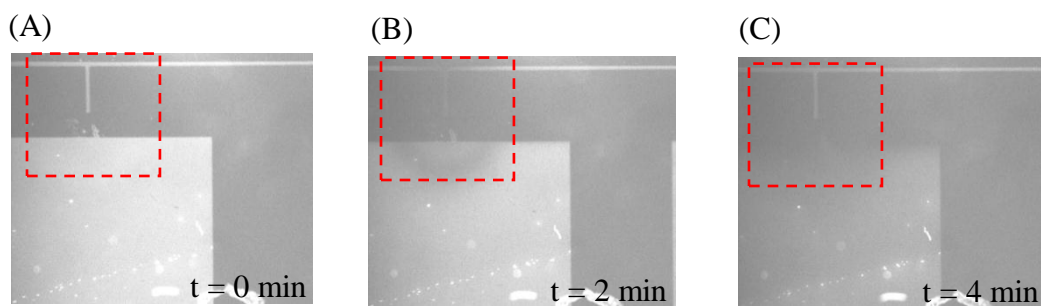


Figure 6.7. Voltage divider experiment. Still images taken in central reservoir 1 during the course of an exclusion experiment with HPTS while using the voltage divider. (A) Before the application of potential. (B) Exclusion. (C) Exclusion being halted when the voltage divider was being adjusted. Images were taken using a 1.25X objective.

6.3.4.3 Addition of posts to the central reservoirs

While the addition of a voltage divider allowed for the application of more stable potentials, another challenge arose during the course of the testing. The devices still occasionally suffered from collapsing reservoirs. A single collapsed reservoir rendered an entire array unusable. Most commonly, it was the central reservoirs that collapsed. On some occasions, the reservoirs would collapse before experiments began, preventing the device from ever being used. On other occasions the reservoirs collapsed during the course of experiments, preventing the completion of an experiment. Eliminating the reservoir failure is essential to allow for future experiments.

It was determined that the reservoirs were collapsing due to the small height to width ratio. Interestingly, this was not an evident problem with the initial microfluidic design (Chapter 4), likely due to the fact that single channels were filled and used immediately. To counteract the collapsing reservoirs, posts were added to the central reservoirs (Fig. 6.8). Four different post designs, in addition to the original design without posts (Fig. 6.8A), were included. One design included four posts, 500 μm in diameter, each 750 μm from the edge of the reservoir (Fig. 6.8B). The second design also contained four posts, each 1 mm in diameter and 500 μm away from the edge of the reservoir (Fig. 6.8C). The remaining two designs each contained 16 posts. One of these designs contained posts evenly spaced throughout the reservoir, 250 μm in diameter and 1 mm apart (Fig. 6.8D). The last design contained posts grouped together in four clusters,

which were 500 μm in diameter and 200 μm away from the edge of the reservoir (Fig. 6.8E).

All five designs were compared by filling two arrays with rhodamine 123 according to the experimental protocol. Once each array was filled, images of the central reservoir were captured. The design without posts (Fig. 6.8A) had the largest degree of central reservoir collapsed, as indicated by the dark area in the central reservoir. Each design with four posts also suffered from collapse (Fig. 6.8B & C), while the designs with 16 posts showed no signs of reservoir collapse (Fig. 6.8D & E). Because of these results, it was determined that either of the central reservoir designs with 16 posts is suitable for experimental use. Future experimental devices will incorporate posts.

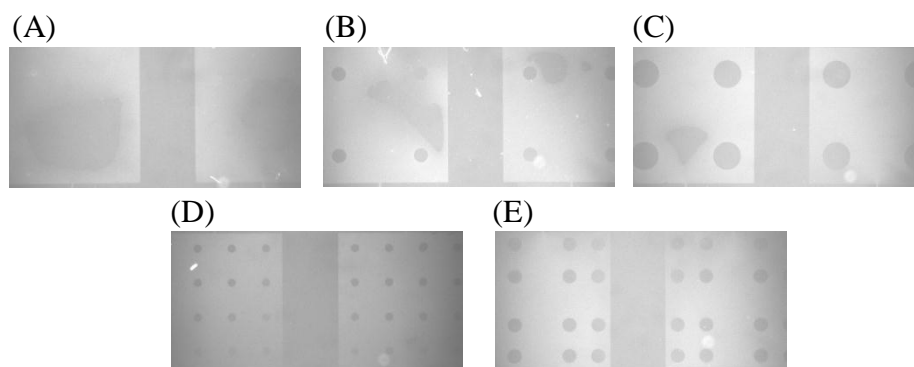


Figure 6.8. Images of central reservoirs with various post designs. (A) No posts. (B) Four posts per reservoir. (C) Four posts per reservoir. (D) Sixteen posts per reservoir. (E) Sixteen posts per reservoir. Designs other than those with 16 posts suffered from collapse. Images were taken using a 1.25X objective.

6.3.5 Interpretation of results

Although most of this chapter has been dedicated to describing the development process of the array, experimental data was obtained with two dyes

in the device simultaneously. For these experiments, either dilutions of true blue chloride and rhodamine 123 or true blue chloride and rhodamine 6G were used to fill the array. The first example used rhodamine 123 and true blue chloride (Fig. 6.9). Before potential was applied to the system (Fig. 6.9A), fluorescence intensity remained constant throughout the device. The fluorescent species traveled with the hydrodynamic flow through the channels (from top to bottom). The observation area was exit channel 2.

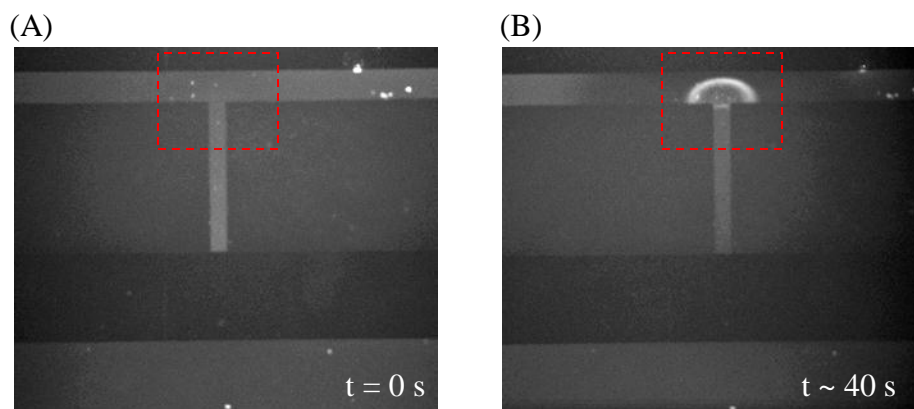


Figure 6.9. Observation of rhodamine 123 and true blue chloride in array device. (A) Before potential is applied, fluorescence intensity remains constant. (B) After the application of potential, a band of focused material is visible. Images were captured using a 4X objective.

After the application of potential, a band of material became visible in the central reservoir, just below the electrode (Fig. 6.9B). This band indicates that at least one of the species was focused while under the influence of the electric field and hydrodynamic flow. When potential was removed, the focused species flowed down the channel with the hydrodynamic flow. Since this behavior only

occurred during the application of potential, the focusing is presumed to be the result of electrophoretic exclusion.

Similarly, when rhodamine 6G and true blue chloride were put into the device, a focusing effect was evident (Fig. 6.10). Again, before the application of potential, the fluorescence intensity remained constant (Fig. 6.10A). During the application of potential bands of material were visible (Fig. 6.10B). In this instance, however, the bands of material were located in the channel, as opposed to in the reservoir. Although this was not ideal, it could be the result of uncontrolled variables. This data was obtained before the electrode error was identified and before the construction of the voltage divider. Both of these variables made it difficult to determine the exact potential that was applied to the system.

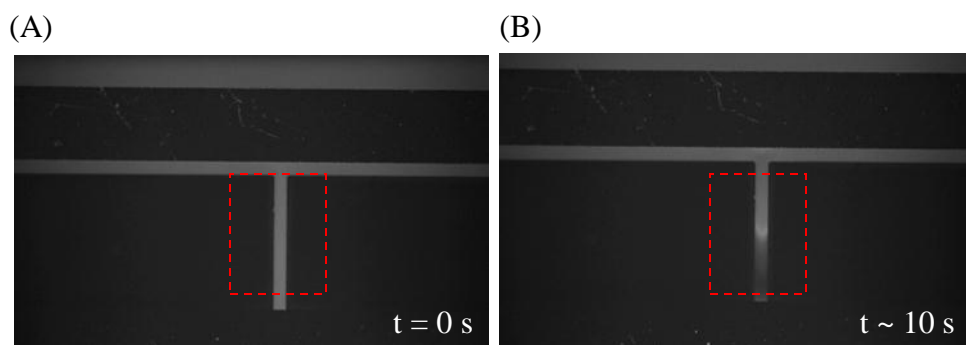


Figure 6.10. Observation of rhodamine 6G and true blue chloride in the array device. (A) Before the application of potential, fluorescent intensity is constant. (B) After the application of potential, band of focused material are present. Images were captured using a 4X objective.

The presence of focused bands of material during the application of potential indicates that with continued refinements, electrophoretic exclusion will

be successful for separation of multiple species on an array device. The movement of material in the channels indicates that the species are being influenced by the electric field, meaning that their electrophoretic velocities are countering the hydrodynamic velocity and resulting in exclusion behavior. Additionally, the estimated band widths for these experiments are on the order of tens of microns, which is comparable to the value reported for the previous array device (Chapter 5). Narrow band widths are necessary for better resolving capabilities, and therefore, better separation capabilities.

6.4 Concluding remarks

This chapter detailed the steps that have contributed to the design and fabrication of an array-based device. Although the array was intended for the isolation of species in complex samples, most of the chapter was devoted to identifying the problems associated with its design. Throughout the course of the study, it was determined that electrode design, power supply instability, and reservoir structure all contributed to irreproducible results. By systematically addressing each of these issues, future designs can further advance the technique towards a successful separations-based array.

6.5 References

- [1] Blazej, R. G., Kumaresan, P., Mathies, R. A., *Proc. Natl. Acad. Sci. U. S. A.* 2006, *103*, 7240-7245.
- [2] Paegel, B. M., Blazej, R. G., Mathies, R. A., *Curr. Opin. Biotechnol.* 2003, *14*, 42-50.
- [3] Ahn, C. H., Choi, J. W., Beaucage, G., Nevin, J. H., Lee, J. B., Puntambekar, A., Lee, J. Y., *Proc. IEEE* 2004, *92*, 154-173.

- [4] Fan, R., Vermesh, O., Srivastava, A., Yen, B. K. H., Qin, L. D., Ahmad, H., Kwong, G. A., Liu, C. C., Gould, J., Hood, L., Heath, J. R., *Nat. Biotechnol.* 2008, 26, 1373-1378.
- [5] Schasfoort, R. B. M., Schlautmann, S., Hendrikse, L., van den Berg, A., *Science* 1999, 286, 942-945.
- [6] Henley, W. H., Ramsey, J. M., *Electrophoresis* 2012, 33, 2718-2724.
- [7] Zilberstein, G., Korol, L., Bukshpan, S., Baskin, E., *Proteomics* 2004, 4, 2533-2540.
- [8] Zilberstein, G. V., Baskin, E. M., Bukshpan, S., *Electrophoresis* 2003, 24, 3735-3744.
- [9] Zilberstein, G. V., Baskin, E. M., Bukshpan, S., Korol, L. E., *Electrophoresis* 2004, 25, 3643-3651.
- [10] Date, A., Pasini, P., Daunert, S., *Anal. Bioanal. Chem.* 2010, 398, 349-356.
- [11] Strychalski, E. A., Henry, A. C., Ross, D., *Anal. Chem.* 2011, 83, 6316-6322.
- [12] Yeung, S. W., Lee, T. M. H., Cai, H., Hsing, I. M., *Nucleic Acids Res.* 2006, 34.
- [13] Xia, Y. N., Whitesides, G. M., *Annu. Rev. Mater. Sci.* 1998, 28, 153-184.
- [14] Duffy, D. C., McDonald, J. C., Schueller, O. J. A., Whitesides, G. M., *Anal. Chem.* 1998, 70, 4974-4984.
- [15] McDonald, J. C., Duffy, D. C., Anderson, J. R., Chiu, D. T., Wu, H. K., Schueller, O. J. A., Whitesides, G. M., *Electrophoresis* 2000, 21, 27-40.
- [16] Seia, M. A., Pereira, S. V., Fontan, C. A., De Vito, I. E., Messina, G. A., Raba, J., *Sens. Actuators, B* 2012, 168, 297-302.
- [17] Wongkaew, N., Kirschbaum, S. E. K., Surareungchai, W., Durst, R. A., Baeumner, A. J., *Electroanalysis* 2012, 24, 1903-1908.
- [18] Dong, H., Li, C. M., Zhang, Y. F., Cao, X. D., Gan, Y., *Lab Chip* 2007, 7, 1752-1758.
- [19] Dawoud, A. A., Kawaguchi, T., Markushin, Y., Porter, M. D., Jankowiak, R., *Sens. Actuators, B* 2006, 120, 42-50.

- [20] Moon, H., Wheeler, A. R., Garrell, R. L., Loo, J. A., Kim, C. J., *Lab Chip* 2006, 6, 1213-1219.
- [21] Baker, C. A., Roper, M. G., *Anal. Chem.* 2012, 84, 2955-2960.
- [22] Cong, Y. Z., Liang, Y., Zhang, L. H., Zhang, W. B., Zhang, Y. K., *J. Sep. Sci.* 2009, 32, 462-465.
- [23] Poitevin, M., Peltre, G., Descroix, S., *Electrophoresis* 2008, 29, 1687-1693.
- [24] Shimura, K., Takahashi, K., Koyama, Y., Sato, K., Kitamori, T., *Anal. Chem.* 2008, 80, 3818-3823.
- [25] Fonslow, B. R., Bowser, M. T., *Anal. Chem.* 2005, 77, 5706-5710.
- [26] Fonslow, B. R., Bowser, M. T., *Anal. Chem.* 2008, 80, 3182-3189.
- [27] Shang, T., Teng, E., Woolley, A. T., Mazzeo, B. A., Schultz, S. M., Hawkins, A. R., *Electrophoresis* 2010, 31, 2596-2601.
- [28] Polson, N. A., Hayes, M. A., *Anal. Chem.* 2000, 72, 1088-1092.
- [29] Lin, R. S., Burke, D. T., Burns, M. A., *Anal. Chem.* 2005, 77, 4338-4347.
- [30] Strychalski, E. A., Henry, A. C., Ross, D., *Anal. Chem.* 2009, 81, 10201-10207.
- [31] Ross, D., Shackman, J. G., Kralj, J. G., Atencia, J., *Lab Chip* 2010, 10, 3139-3148.
- [32] Jorgenson, J. W., Lukacs, K. D., *Anal. Chem.* 1981, 53, 1298-1302.
- [33] Jorgenson, J. W., Lukacs, K. D., *Clin. Chem.* 1981, 27, 1551-1553.
- [34] Jorgenson, J. W., Lukacs, K. D., *Science* 1983, 222, 266-272.

Chapter 7

Concluding Remarks

7.1 Electrophoretic exclusion at a single interface

Separation science has often been employed to study complex samples because of its ability to remove interferents and isolate species of interest. An ideal separations technique would be fast, sensitive, selective, and have the ability to address many types of analytes covering a large range of concentrations. Throughout this dissertation, arguments were made for applying electrophoretic exclusion to an array-based microfluidic device for the analysis of complex samples.

Although array-based separations were identified as the ultimate goal, the electrophoretic exclusion studies presented in this dissertation focused primarily on characterizing the differentiation of species in bulk solution at a single interface. Initial work described the exclusion of small molecules on a benchtop design (Chapter 3). Planar microchip experiments demonstrated the ability to exclude small dye molecules or particles at a single interface. These results indicated that the technique was useful for addressing analytes with varying properties. Additionally, the separation of small dye molecules from polystyrene spheres was demonstrated. This work demonstrated the first direct visualization of electrophoretic exclusion behavior (Chapter 4).

7.2 Resolution and the potential for array-based separations

In addition to single interface studies, resolution theory for electrophoretic exclusion was developed and it suggested that the technique is capable of

separating species with very similar electrophoretic mobilities (Chapter 5). An array prototype was designed and tested (Chapter 6) based on the parameters of the single interface microdevice. Studies indicated that with further refinements, electrophoretic exclusion can be successfully used as an array-based technique for complex sample analysis.

REFERENCES

CHAPTER 1

- [1] Pieper, R., Gatlin, C. L., Makusky, A. J., Russo, P. S., Schatz, C. R., Miller, S. S., Su, Q., McGrath, A. M., Estock, M. A., Parmar, P. P., Zhao, M., Huang, S. T., Zhou, J., Wang, F., Esquer-Blasco, R., Anderson, N. L., Taylor, J., Steiner, S., *Proteomics* 2003, 3, 1345-1364.
- [2] Anderson, N. L., Anderson, N. G., *Mol Cell Proteomics* 2002, 1, 845-867.
- [3] Ekins, R. P., *Clin. Chem.* 1998, 44, 2015-2030.
- [4] Hartmann, M., Roeraade, J., Stoll, D., Templin, M., Joos, T., *Anal. Bioanal. Chem.* 2009, 393, 1407-1416.
- [5] MacBeath, G., *Nat. Genet.* 2002, 32, 526-532.
- [6] Soper, S. A., Brown, K., Ellington, A., Frazier, B., Garcia-Manero, G., Gau, V., Gutman, S. I., Hayes, D. F., Korte, B., Landers, J. L., Larson, D., Ligler, F., Majumdar, A., Mascini, M., Nolte, D., Rosenzweig, Z., Wang, J., Wilson, D., *Biosens. Bioelectron.* 2006, 21, 1932-1942.
- [7] Wu, J., Fu, Z. F., Yan, F., Ju, H. X., *Trac-Trend Anal Chem* 2007, 26, 679-688.
- [8] Giddings, J. C., *Unified Separation Science*, Wiley-Interscience Publication, New York 1991.
- [9] Shen, Y. F., Kim, J., Strittmatter, E. F., Jacobs, J. M., Camp, D. G., Fang, R. H., Tolie, N., Moore, R. J., Smith, R. D., *Proteomics* 2005, 5, 4034-4045.
- [10] Bushey, M. M., Jorgenson, J. W., *J. Chromatogr.* 1989, 480, 301-310.
- [11] Capriotti, A. L., Cavaliere, C., Foglia, P., Samperi, R., Lagana, A., *J. Chromatogr. A.* 2011, 1218, 8760-8776.
- [12] Hjerten, S., Liao, J. L., Yao, K., *J. Chromatogr.* 1987, 387, 127-138.
- [13] Jacobs, J. M., Adkins, J. N., Qian, W. J., Liu, T., Shen, Y. F., Camp, D. G., Smith, R. D., *J. Proteome Res* 2005, 4, 1073-1085.
- [14] Jorgenson, J. W., Lukacs, K. D., *Anal. Chem.* 1981, 53, 1298-1302.
- [15] Jorgenson, J. W., Lukacs, K. D., *Clin. Chem.* 1981, 27, 1551-1553.
- [16] Jorgenson, J. W., Lukacs, K. D., *Science* 1983, 222, 266-272.

- [17] Cao, C. X., *J. Chromatogr. A* 1997, 771, 374-378.
- [18] Beard, N. R., Zhang, C. X., deMello, A. J., *Electrophoresis* 2003, 24, 732-739.
- [19] Mikkers, F. E. P., Everaerts, F. M., Verheggen, T., *J. Chromatogr.* 1979, 169, 11-20.
- [20] Culbertson, C. T., Jorgenson, J. W., *Anal. Chem.* 1994, 66, 955-962.
- [21] Giddings, J. C., Dahlgren, K., *Sep. Sci.* 1971, 6, 345-&.
- [22] O'Farrell, P. H., *Science* 1985, 227, 1586-1589.
- [23] Giddings, J. C., *Sep. Sci. Technol.* 1979, 14, 871-882.
- [24] Hjerten, S., Zhu, M. D., *J. Chromatogr.* 1985, 346, 265-270.
- [25] Danger, G., Ross, D., *Electrophoresis* 2008, 29, 3107-3114.
- [26] Huber, D. E., Santiago, J. G., *Proc. R. Soc. A* 2008, 464, 595-612.
- [27] Ross, D., Locascio, L. E., *Anal. Chem.* 2002, 74, 2556-2564.
- [28] Greenlee, R. D., Ivory, C. F., *Biotechnol. Prog.* 1998, 14, 300-309.
- [29] Kelly, R. T., Woolley, A. T., *J. Sep. Sci.* 2005, 28, 1985-1993.
- [30] Ansell, R. J., Tunon, P. G., Wang, Y. T., Myers, P., Ivory, C. F., Keen, J. N., Findlay, J. B. C., *Analyst* 2009, 134, 226-229.
- [31] Huang, Z., Ivory, C. F., *Anal. Chem.* 1999, 71, 1628-1632.
- [32] Shim, J., Dutta, P., Ivory, C. F., *Electrophoresis* 2007, 28, 572-586.
- [33] Ross, D., Kralj, J. G., *Anal. Chem.* 2008, 80, 9467-9474.
- [34] Strychalski, E. A., Henry, A. C., Ross, D., *Anal. Chem.* 2009, 81, 10201-10207.
- [35] Davis, N. I., Mamunooru, M., Vyas, C. A., Shackman, J. G., *Anal. Chem.* 2009, 81, 5452-5459.
- [36] Mamunooru, M., Jenkins, R. J., Davis, N. I., Shackman, J. G., *J. Chromatogr. A* 2008, 1202, 203-211.
- [37] Shackman, J. G., Ross, D., *Electrophoresis* 2007, 28, 556-571.

- [38] Polson, N. A., Savin, D. P., Hayes, M. A., *J. Microcolumn Sep.* 2000, 12, 98-106.
- [39] Giddings, J. C., *J. Chromatogr.* 1960, 3, 520-523.
- [40] Giddings, J. C., *Anal. Chem.* 1963, 35, 2215-&.
- [41] Foret, F., Deml, M., Bocek, P., *J. Chromatogr.* 1988, 452, 601-613.
- [42] Tolley, H. D., Wang, Q. G., LeFebre, D. A., Lee, M. L., *Anal. Chem.* 2002, 74, 4456-4463.
- [43] Ross, D., *Electrophoresis* 2010, 31, 3650-3657.
- [44] Pacheco, J. R., Chen, K. P., Hayes, M. A., *Electrophoresis* 2007, 28, 1027-1035.
- [45] Keebaugh, M. W., Mahanti, P., Hayes, M. A., *Electrophoresis* 2012, 33, 1924-1930.
- [46] Meighan, M. M., Keebaugh, M. W., Quihuis, A. M., Kenyon, S. M., Hayes, M. A., *Electrophoresis* 2009, 30, 3786-3792.
- [47] Meighan, M. M., Vasquez, J., Dziubcynski, L., Hews, S., Hayes, M. A., *Anal. Chem.* 2011, 83, 368-373.
- [48] Kenyon, S. M., Weiss, N. G., Hayes, M. A., *Electrophoresis* 2012, 33, 1227-1235.

CHAPTER 2

- [1] Hofmann, O., Che, D. P., Cruickshank, K. A., Muller, U. R., *Anal. Chem.* 1999, 71, 678-686.
- [2] Righetti, P. G., Drysdale, J. W., *Ann. NY Acad. Sci.* 1973, 209, 163-186.
- [3] Vesterbe, O., Svensson, H., *Acta Chem. Scand.* 1966, 20, 820-&.
- [4] Hannig, K. Z., *Anal. Chem.* 1961, 181, 244-254.
- [5] Hoffstetterkuhn, S., Kuhn, R., Wagner, H., *Electrophoresis* 1990, 11, 304-309.
- [6] Tang, G. Y., Yang, C., *Electrophoresis* 2008, 29, 1006-1012.
- [7] Ge, Z. W., Yang, C., Tang, G. Y., *Int. J. Heat Mass Transfer* 2010, 53, 2722-2731.

- [8] Jellema, L. C., Mey, T., Koster, S., Verpoorte, E., *Lab Chip* 2009, 9, 1914-1925.
- [9] Becker, M., Marggraf, U., Janasek, D. J., *Chromatogr. A* 2009, 1216, 8265-8269.
- [10] Fonslow, B. R., Bowser, M. T., *Anal. Chem.* 2008, 80, 3182-3189.
- [11] Kostal, V., Fonslow, B. R., Arriaga, E. A., Bowser, M. T., *Anal. Chem.* 2009, 81, 9267-9273.
- [12] Turgeon, R. T., Bowser, M. T., *Electrophoresis* 2009, 30, 1342-1348.
- [13] Zalewski, D. R., Kohlheyer, D., Schlautmann, S., Gardeniers, H., *Anal. Chem.* 2008, 80, 6228-6234.
- [14] Vollmer, S., Astorga-Wells, J., Alvelius, G., Bergman, T., Jornvall, H., *Anal. Biochem.* 2008, 374, 154-162.
- [15] Gebauer, P., Mala, Z., Bocek, P., *Electrophoresis* 2010, 31, 886-892.
- [16] Mala, Z., Gebauer, P., Bocek, P., *Electrophoresis* 2009, 30, 866-874.
- [17] Meighan, M. M., Keebaugh, M. W., Quihuis, A. M., Kenyon, S. M., Hayes, M. A., *Electrophoresis* 2009, 30, 3786-3792.
- [18] Weiss, N. G., Zwick, N. L., Hayes, M. A., *J. Chromatogr. A* 2010, 1217, 179-182.
- [19] Ansell, R. J., Tunon, P. G., Wang, Y. T., Myers, P., Ivory, C. F., Keen, J. N., Findlay, J. B. C., *Analyst* 2009, 134, 226-229.
- [20] Burke, J. M., Smith, C. D., Ivory, C. F., *Electrophoresis* 2010, 31, 902-909.
- [21] Raymond, D. E., Manz, A., Widmer, H. M., *Anal. Chem.* 1994, 66, 2858-2865.
- [22] Turgeon, R. T., Fonslow, B. R., Jing, M., Bowser, M. T., *Anal. Chem.* 2010, 82, 3636-3641.
- [23] Kohlheyer, D., Eijkel, J. C. T., Schlautmann, S., van den Berg, A., Schasfoort, R. B. M., *Anal. Chem.* 2008, 80, 4111-4118.
- [24] Ross, D., Gaitan, M., Locascio, L. E., *Anal. Chem.* 2001, 73, 4117-4123.
- [25] Lin, H., Shackman, J. G., Ross, D., *Lab Chip* 2008, 8, 969-978.

- [26] Danger, G., Ross, D., *Electrophoresis* 2008, 29, 3107-3114.
- [27] Munson, M. S., Meacham, J. M., Locascio, L. E., Ross, D., *Anal. Chem.* 2008, 80, 172-178.
- [28] Munson, M. S., Meacham, J. M., Ross, D., Locascio, L. E., *Electrophoresis* 2008, 29, 3456-3465.
- [29] Reschke, B. R., Luo, H., Schiffbauer, J., Edwards, B. F., Timperman, A. T., *Lab Chip* 2009, 9, 2203-2211.
- [30] Reschke, B. R., Schiffbauer, J., Edwards, B. F., Timperman, A. T., *Analyst* 2010, 135, 1351-1359.
- [31] Kawamata, T., Yamada, M., Yasuda, M., Seki, M., *Electrophoresis* 2008, 29, 1423-1430.
- [32] Baker, C. A., Roper, M. G., *J. Chromatogr. A* 2010, 1217, 4743-4748.
- [33] Yu, H., Lu, Y., Zhou, Y. G., Wang, F. B., He, F. Y., Xia, X. H., *Lab Chip* 2008, 8, 1496-1501.
- [34] Kuo, C. H., Wang, J. H., Lee, G. B., *Electrophoresis* 2009, 30, 3228-3235.
- [35] Lee, J. H., Song, Y. A., Han, J. Y., *Lab Chip* 2008, 8, 596-601.
- [36] Noblitt, S. D., Henry, C. S., *Anal. Chem.* 2008, 80, 7624-7630.
- [37] Perdue, R. K., Laws, D. R., Hlushkou, D., Tallarek, U., Crooks, R. M., *Anal. Chem.* 2009, 81, 10149-10155.
- [38] Daghighi, Y., Li, D. Q., *Electrophoresis* 2010, 31, 868-878.
- [39] Jiang, H., Daghighi, Y., Chon, C. H., Li, D. Q., *J. Colloid Interface Sci.* 2010, 347, 324-331.
- [40] Hjerten, S., Zhu, M. D., *J. Chromatogr.* 1985, 346, 265-270.
- [41] Horka, M., Ruzicka, F., Hola, V., Slais, K., *Electrophoresis* 2009, 30, 2134-2141.
- [42] Poitevin, M., Peltre, G., Descroix, S., *Electrophoresis* 2008, 29, 1687-1693.
- [43] Chou, Y., Yang, R. J., *Electrophoresis* 2009, 30, 819-830.
- [44] Cong, Y. Z., Liang, Y., Zhang, L. H., Zhang, W. B., Zhang, Y. K., *J. Sep. Sci.* 2009, 32, 462-465.

- [45] Dauriac, V., Descroix, S., Chen, Y., Peltre, G., Senechal, H., *Electrophoresis* 2008, 29, 2945-2952.
- [46] Ou, J. J., Glawdel, T., Ren, C. L., Pawliszyn, J., *Lab Chip* 2009, 9, 1926-1932.
- [47] Poitevin, M., Shakalisava, Y., Miserere, S., Peltre, G., Viovy, J. L., Descroix, S., *Electrophoresis* 2009, 30, 4256-4263.
- [48] Shimura, K., Takahashi, K., Koyama, Y., Sato, K., Kitamori, T., *Anal. Chem.* 2008, 80, 3818-3823.
- [49] Shim, J., Dutta, P., Ivory, C. F., *Electrophoresis* 2007, 28, 572-586.
- [50] Everaerts, F. M., Verheggen, T., Mikkers, F. E. P., *J. Chromatogr.* 1979, 169, 21-38.
- [51] Nagata, H., Ishikawa, M., Yoshida, Y., Tanaka, Y., Hirano, K., *Electrophoresis* 2008, 29, 3744-3751.
- [52] Goet, G., Baier, T., Hardt, S., *Lab Chip* 2009, 9, 3586-3593.
- [53] Hirokawa, T., Takayama, Y., Arai, A., Xu, Z. Q., *Electrophoresis* 2008, 29, 1829-1835.
- [54] Xu, Z. Q., Murata, K., Arai, A., Hirokawa, T., *Biomicrofluidics* 2010, 4.
- [55] Baldock, S. J., Fielden, P. R., Goddard, N. J., Kretschmer, H. R., Prest, J. E., Brown, B. J., T. *Microelectron. Eng.* 2008, 85, 1440-1442.
- [56] Prest, J. E., Baldock, S. J., Fielden, P. R., Goddard, N. J., Brown, B. J. T., *Anal Bioanal Chem* 2009, 394, 1299-1305.
- [57] Prest, J. E., Beardah, M. S., Baldock, S. J., Doyle, S. P., Fielden, P. R., Goddard, N. J., Brown, B. J. T., *J. Chromatogr. A* 2008, 1195, 157-163.
- [58] Prest, J. E., Fielden, P. R., Goddard, N. J., Brown, B. J. T., *Meas. Sci. Technol.* 2008, 19.
- [59] Mani, A., Zangle, T. A., Santiago, J. G., *Langmuir* 2009, 25, 3898-3908.
- [60] Persat, A., Marshall, L. A., Santiago, J. G., *Anal. Chem.* 2009, 81, 9507-9511.
- [61] Persat, A., Santiago, J. G., *New J. Phys.* 2009, 11.
- [62] Persat, A., Suss, M. E., Santiago, J. G., *Lab Chip* 2009, 9, 2454-2469.

- [63] Schoch, R. B., Ronaghi, M., Santiago, J. G., *Lab Chip* 2009, 9, 2145-2152.
- [64] Zangle, T. A., Mani, A., Santiago, J. G., *Langmuir* 2009, 25, 3909-3916.
- [65] Zangle, T. A., Mani, A., Santiago, J. G., *Chem. Soc. Rev.* 2010, 39, 1014-1035.
- [66] Khurana, T. K., Santiago, J. G., *Anal. Chem.* 2008, 80, 279-286.
- [67] Khurana, T. K., Santiago, J. G., *Anal. Chem.* 2008, 80, 6300-6307.
- [68] Khurana, T. K., Santiago, J. G., *Lab Chip* 2009, 9, 1377-1384.
- [69] Lin, H., Storey, B. D., Santiago, J. G., *J. Fluid Mech.* 2008, 608, 43-70.
- [70] Bahga, S. S., Bercovici, M., Santiago, J. G., *Electrophoresis* 2010, 31, 910-919.
- [71] Baldessari, F., Santiago, J. G., *J. Colloid Interface Sci.* 2009, 325, 526-538.
- [72] Baldessari, F., Santiago, J. G., *J. Colloid Interface Sci.* 2009, 325, 539-546.
- [73] Bercovici, M., Kaigala, G. V., Backhouse, C. J., Santiago, J. G., *Anal. Chem.* 2010, 82, 1858-1866.
- [74] Bercovici, M., Kaigala, G. V., Santiago, J. G., *Anal. Chem.* 2010, 82, 2134-2138.
- [75] Bercovici, M., Lele, S. K., Santiago, J. G., *J. Chromatogr. A* 2009, 1216, 1008-1018.
- [76] Bercovici, M., Lele, S. K., Santiago, J. G., *J. Chromatogr. A* 2010, 1217, 588-599.
- [77] Chambers, R. D., Santiago, J. G., *Anal. Chem.* 2009, 81, 3022-3028.
- [78] Huber, D. E., Santiago, J. G., *Proc. R. Soc. A* 2008, 464, 595-612.
- [79] Masar, M., Sydes, D., Luc, M., Kaniansky, D., Kuss, H. M., *J. Chromatogr. A* 2009, 1216, 6252-6255.
- [80] Wang, J., Zhang, Y., Mohamadi, M. R., Kaji, N., Tokeshi, M., Baba, Y., *Electrophoresis* 2009, 30, 3250-3256.

- [81] Wang, L. H., Liu, D. Y., Chen, H., Zhou, X. M., *Electrophoresis* 2008, 29, 4976-4983.
- [82] Qi, L. Y., Yin, X. F., Liu, J. H., *J. Chromatogr. A* 2009, 1216, 4510-4516.
- [83] Chou, Y., Yang, R. J., *J. Chromatogr. A* 2010, 1217, 394-404.
- [84] Danger, G., Ross, D., *Electrophoresis* 2008, 29, 4036-4044.
- [85] Mamunooru, M., Jenkins, R. J., Davis, N. I., Shackman, J. G., *J. Chromatogr. A* 2008, 1202, 203-211.
- [86] Vyas, C. A., Mamunooru, M., Shackman, J. G., *Chromatographia* 2009, 70, 151-156.
- [87] Ross, D., Kralj, J. G., *Anal. Chem.* 2008, 80, 9467-9474.
- [88] Ross, D., Romantseva, E. F., *Anal. Chem.* 2009, 81, 7326-7335.

CHAPTER 3

- [1] Schmidt, T. C., Zwank, L., Elsner, M., Berg, M., Meckenstock, R. U., Haderlein, S. B., *Anal. Bioanal. Chem.* 2004, 378, 283-300.
- [2] Lee, W. C., Lee, K. H., *Anal. Biochem.* 2004, 324, 1-10.
- [3] Maurer, H. H., *Journal of Chromatography B* 1998, 713, 3-25.
- [4] Segura, J., Ventura, R., Jurado, C., *J. Chromatogr. B* 1998, 713, 61-90.
- [5] Jorgenson, J. W., Lukacs, K. D., *Anal. Chem.* 1981, 53, 1298-1302.
- [6] Bushey, M. M., Jorgenson, J. W., *J. Chromatogr.* 1989, 480, 301-310.
- [7] Giddings, J. C., Dahlgren, K., *Sep. Sci.* 1971, 6, 345-356.
- [8] Rodriguez-Diaz, R., Wehr, T., Zhu, M. D., *Electrophoresis* 1997, 18, 2134-2144.
- [9] Culbertson, C. T., Jorgenson, J. W., *Anal. Chem.* 1994, 66, 955-962.
- [10] Kelly, R. T., Li, Y., Woolley, A. T., *Anal. Chem.* 2006, 78, 2565-2570.
- [11] Lin, S.-L., Li, Y., Tolley, H. D., Humble, P. H., Lee, M. L., *J. Chromatogr. A* 2006, 1125, 254-262.
- [12] Petsev, D. N., Lopez, G. P., Ivory, C. F., Sibbett, S. S., *Lab Chip* 2005, 5, 587-597.

- [13] Sun, X. F., Li, D., Woolley, A. T., Farnsworth, P. B., Tolley, H. D., Warnick, K. F., Lee, M. L., *J. Chromatogr. A* 2009, *1216*, 6532-6538.
- [14] Koegler, W. S., Ivory, C. F., *J. Chromatogr. A* 1996, *726*, 229-236.
- [15] Danger, G., Ross, D., *Electrophoresis* 2008, *29*, 3107-3114.
- [16] Ge, Z. W., Yang, C., Tang, G. Y., *Int. J. Heat Mass Transfer* 2010, *53*, 2722-2731.
- [17] Lin, H., Shackman, J. G., Ross, D., *Lab Chip* 2008, *8*, 969-978.
- [18] Tang, G. Y., Yang, C., *Electrophoresis* 2008, *29*, 1006-1012.
- [19] Greenlee, R. D., Ivory, C. F., *Biotechnol. Prog.* 1998, *14*, 300-309.
- [20] Ross, D., Kralj, J. G., *Anal. Chem.* 2008, *80*, 9467-9474.
- [21] Ross, D., Romantseva, E. F., *Anal. Chem.* 2009, *81*, 7326-7335.
- [22] Ross, D., Shackman, J. G., Kralj, J. G., Atencia, J., *Lab Chip* 2010, *10*, 3139-3148.
- [23] Strychalski, E. A., Henry, A. C., Ross, D., *Anal. Chem.* 2011, *83*, 6316-6322.
- [24] Danger, G., Ross, D., *Electrophoresis* 2008, *29*, 4036-4044.
- [25] Davis, N. I., Mamunooru, M., Vyas, C. A., Shackman, J. G., *Anal. Chem.* 2009, *81*, 5452-5459.
- [26] Vyas, C. A., Mamunooru, M., Shackman, J. G., *Chromatographia* 2009, *70*, 151-156.
- [27] Hori, A., Matsumoto, T., Nimura, Y., Ikedo, M., Okada, H., Tsuda, T., *Anal. Chem.* 1993, *65*, 2882-2886.
- [28] Polson, N. A., Savin, D. P., Hayes, M. A., *J. Microcolumn Sep.* 2000, *12*, 98-106.
- [29] Meighan, M. M., Keebaugh, M. W., Quihuis, A. M., Kenyon, S. M., Hayes, M. A., *Electrophoresis* 2009, *30*, 3786-3792.
- [30] Meighan, M. M., Vasquez, J., Dziubcynski, L., Hews, S., Hayes, M. A., *Anal. Chem.* 2011, *83*, 368-373.
- [31] Humble, P. H., Kelly, R. T., Woolley, A. T., Tolley, H. D., Lee, M. L., *Anal. Chem.* 2004, *76*, 5641-5648.

CHAPTER 4

- [1] Jorgenson, J. W., Lukacs, K. D., *Anal. Chem.* 1981, 53, 1298-1302.
- [2] Jorgenson, J. W., Lukacs, K. D., *Science* 1983, 222, 266-272.
- [3] Breadmore, M. C., Dawod, M., Quirino, J. P., *Electrophoresis* 2011, 32, 127-148.
- [4] Kenyon, S. M., Meighan, M. M., Hayes, M. A., *Electrophoresis* 2011, 32, 482-493.
- [5] Meighan, M. M., Staton, S. J. R., Hayes, M. A., *Electrophoresis* 2009, 30, 852-865.
- [6] Vyas, C. A., Flanigan, P. M., Shackman, J. G., *Bioanalysis* 2010, 2, 815-827.
- [7] Polson, N. A., Savin, D. P., Hayes, M. A., *J. Microcolumn Sep.* 2000, 12, 98-106.
- [8] Yu, H., Lu, Y., Zhou, Y. G., Wang, F. B., He, F. Y., Xia, X. H., *Lab Chip* 2008, 8, 1496-1501.
- [9] Reschke, B. R., Luo, H., Schiffbauer, J., Edwards, B. F., Timperman, A. T., *Lab Chip* 2009, 9, 2203-2211.
- [10] Reschke, B. R., Schiffbauer, J., Edwards, B. F., Timperman, A. T., *Analyst* 2010, 135, 1351-1359.
- [11] Kuo, C. H., Wang, J. H., Lee, G. B., *Electrophoresis* 2009, 30, 3228-3235.
- [12] Jacobson, S. C., Ramsey, J. M., *Electrophoresis* 1995, 16, 481-486.
- [13] Lichtenberg, J., Verpoorte, E., de Rooij, N. F., *Electrophoresis* 2001, 22, 258-271.
- [14] Xu, L., Hauser, P. C., Lee, H. K., *J. Chromatogr. A.* 2009, 1216, 5911-5916.
- [15] Walker, P. A., Morris, M. D., Burns, M. A., Johnson, B. N., *Anal. Chem.* 1998, 70, 3766-3769.
- [16] Bahga, S. S., Chambers, R. D., Santiago, J. G., *Anal. Chem.* 2011, 83, 6154-6162.

- [17] Grass, B., Neyer, A., Johnck, M., Siepe, D., Eisenbeiss, F., Weber, G., Hergenroder, R., *Sens. Actuators, B* 2001, 72, 249-258.
- [18] Jung, B., Bharadwaj, R., Santiago, J. G., *Anal. Chem.* 2006, 78, 2319-2327.
- [19] Persat, A., Santiago, J. G., *New J. Phys.* 2009, 11.
- [20] Pumera, M., Wang, J., Opekar, F., Jelinek, I., Feldman, J., Lowe, H., Hardt, S., *Anal. Chem.* 2002, 74, 1968-1971.
- [21] Hofmann, O., Che, D. P., Cruickshank, K. A., Muller, U. R., *Anal. Chem.* 1999, 71, 678-686.
- [22] Cong, Y. Z., Liang, Y., Zhang, L. H., Zhang, W. B., Zhang, Y. K., *J. Sep. Sci.* 2009, 32, 462-465.
- [23] Cui, H. C., Horiuchi, K., Dutta, P., Ivory, C. F., *Anal. Chem.* 2005, 77, 1303-1309.
- [24] Huang, X. Y., Ren, J. C., *Electrophoresis* 2005, 26, 3595-3601.
- [25] Ishibashi, R., Kitamori, T., Shimura, K., *Lab Chip* 2010, 10, 2628-2631.
- [26] Gebauer, P., Mala, Z., Bocek, P., *Electrophoresis* 2011, 32, 83-89.
- [27] Hori, A., Matsumoto, T., Nimura, Y., Ikedo, M., Okada, H., Tsuda, T., *Anal. Chem.* 1993, 65, 2882-2886.
- [28] Culbertson, C. T., Jorgenson, J. W., *Anal. Chem.* 1994, 66, 955-962.
- [29] Danger, G., Ross, D., *Electrophoresis* 2008, 29, 3107-3114.
- [30] Ge, Z. W., Yang, C., Tang, G. Y., *Int. J. Heat Mass Transfer* 2010, 53, 2722-2731.
- [31] Lin, H., Shackman, J. G., Ross, D., *Lab Chip* 2008, 8, 969-978.
- [32] Munson, M. S., Meacham, J. M., Locascio, L. E., Ross, D., *Anal. Chem.* 2008, 80, 172-178.
- [33] Munson, M. S., Meacham, J. M., Ross, D., Locascio, L. E., *Electrophoresis* 2008, 29, 3456-3465.
- [34] Ross, D., Gaitan, M., Locascio, L. E., *Anal. Chem.* 2001, 73, 4117-4123.
- [35] Tang, G. Y., Yang, C., *Electrophoresis* 2008, 29, 1006-1012.

- [36] Koegler, W. S., Ivory, C. F., *J. Chromatogr. A* 1996, 726, 229-236.
- [37] Humble, P. H., Kelly, R. T., Woolley, A. T., Tolley, H. D., Lee, M. L., *Anal. Chem.* 2004, 76, 5641-5648.
- [38] Kelly, R. T., Li, Y., Woolley, A. T., *Anal. Chem.* 2006, 78, 2565-2570.
- [39] Sun, X. F., Li, D., Woolley, A. T., Farnsworth, P. B., Tolley, H. D., Warnick, K. F., Lee, M. L., *J. Chromatogr. A* 2009, 1216, 6532-6538.
- [40] Lin, S.-L., Li, Y., Tolley, H. D., Humble, P. H., Lee, M. L., *J. Chromatogr. A* 2006, 1125, 254-262.
- [41] Liu, J. K., Sun, X. F., Farnsworth, P. B., Lee, M. L., *Anal. Chem.* 2006, 78, 4654-4662.
- [42] Huang, Z., Ivory, C. F., *Anal. Chem.* 1999, 71, 1628-1632.
- [43] Petsev, D. N., Lopez, G. P., Ivory, C. F., Sibbett, S. S., *Lab Chip* 2005, 5, 587-597.
- [44] Myers, P., Bartle, K. D., *J. Chromatogr. A* 2004, 1044, 253-258.
- [45] Burke, J. M., Smith, C. D., Ivory, C. F., *Electrophoresis* 2010, 31, 902-909.
- [46] Burke, J. M., Huang, Z., Ivory, C. F., *Anal. Chem.* 2009, 81, 8236-8243.
- [47] Ross, D., *Electrophoresis* 2010, 31, 3650-3657.
- [48] Ross, D., *Electrophoresis* 2010, 31, 3658-3664.
- [49] Ross, D., Kralj, J. G., *Anal. Chem.* 2008, 80, 9467-9474.
- [50] Ross, D., Romantseva, E. F., *Anal. Chem.* 2009, 81, 7326-7335.
- [51] Ross, D., Shackman, J. G., Kralj, J. G., Atencia, J., *Lab Chip* 2010, 10, 3139-3148.
- [52] Shackman, J. G., Munson, M. S., Ross, D., *Anal. Chem.* 2007, 79, 565-571.
- [53] Strychalski, E. A., Henry, A. C., Ross, D., *Anal. Chem.* 2009, 81, 10201-10207.
- [54] Strychalski, E. A., Henry, A. C., Ross, D., *Anal. Chem.* 2011, 83, 6316-6322.

- [55] Davis, N. I., Mamunooru, M., Vyas, C. A., Shackman, J. G., *Anal. Chem.* 2009, *81*, 5452-5459.
- [56] Shackman, J. G., Ross, D., *Anal. Chem.* 2007, *79*, 6641-6649.
- [57] Jellema, L. C., Mey, T., Koster, S., Verpoorte, E., *Lab Chip* 2009, *9*, 1914-1925.
- [58] Jellema, L. J. C., Markesteijn, A. P., Westerweel, J., Verpoorte, E., *Anal. Chem.* 2010, *82*, 4027-4035.
- [59] Liu, C., Luo, Y., Fang, N., Chen, D. D. Y., *Anal. Chem.* 2011, *83*, 1189-1192.
- [60] Liu, C., Luo, Y., Maxwell, E. J., Fang, N., Chen, D. D. Y., *Anal. Chem.* 2010, *82*, 2182-2185.
- [61] Vyas, C. A., Mamunooru, M., Shackman, J. G., *Chromatographia* 2009, *70*, 151-156.
- [62] Meighan, M. M., Keebaugh, M. W., Quihuis, A. M., Kenyon, S. M., Hayes, M. A., *Electrophoresis* 2009, *30*, 3786-3792.
- [63] Meighan, M. M., Vasquez, J., Dziubcynski, L., Hews, S., Hayes, M. A., *Anal. Chem.* 2011, *83*, 368-373.
- [64] Pacheco, J. R., Chen, K. P., Hayes, M. A., *Electrophoresis* 2007, *28*, 1027-1035.
- [65] Zilberstein, G. V., Baskin, E. M., Bukshpan, S., *Electrophoresis* 2003, *24*, 3735-3744.
- [66] Zilberstein, G. V., Baskin, E. M., Bukshpan, S., Korol, L. E., *Electrophoresis* 2004, *25*, 3643-3651.
- [67] Zilberstein, G., Korol, L., Bukshpan, S., Baskin, E., *Proteomics* 2004, *4*, 2533-2540.
- [68] Ivory, C. F., *Electrophoresis* 2007, *28*, 15-25.

CHAPTER 5

- [1] Ricker, R. D., Sandoval, L. A., *J. Chromatogr. A* 1996, *743*, 43-50.
- [2] Kanner, S. B., Reynolds, A. B., Parsons, J. T., *J. Immunol. Methods* 1989, *120*, 115-124.

- [3] Geiger, M., Hogerton, A. L., Bowser, M. T., *Anal. Chem.* 2012, 84, 577-596.
- [4] Giddings, J. C., Dahlgren, K., *Sep. Sci.* 1971, 6, 345-356.
- [5] Cong, Y. Z., Liang, Y., Zhang, L. H., Zhang, W. B., Zhang, Y. K., *J. Sep. Sci.* 2009, 32, 462-465.
- [6] Cui, H. C., Horiuchi, K., Dutta, P., Ivory, C. F., *Anal. Chem.* 2005, 77, 7878-7886.
- [7] Hofmann, O., Che, D. P., Cruickshank, K. A., Muller, U. R., *Anal. Chem.* 1999, 71, 678-686.
- [8] Greenlee, R. D., Ivory, C. F., *Biotechnol. Prog.* 1998, 14, 300-309.
- [9] Ross, D., Locascio, L. E., *Anal. Chem.* 2002, 74, 2556-2564.
- [10] Kelly, R. T., Woolley, A. T., *J. Sep. Sci.* 2005, 28, 1985-1993.
- [11] Shackman, J. G., Ross, D., *Electrophoresis* 2007, 28, 556-571.
- [12] Danger, G., Ross, D., *Electrophoresis* 2008, 29, 3107-3114.
- [13] Burke, J. M., Ivory, C. F., *Electrophoresis* 2010, 31, 893-901.
- [14] Huang, Z., Ivory, C. F., *Anal. Chem.* 1999, 71, 1628-1632.
- [15] Giddings, J. C., *J. Chromatogr.* 1960, 3, 520-523.
- [16] Giddings, J. C., *Anal. Chem.* 1963, 35, 2215-2216.
- [17] Foret, F., Deml, M., Bocek, P., *J. Chromatogr.* 1988, 452, 601-613.
- [18] Culbertson, C. T., Jacobson, S. C., Ramsey, J. M., *Anal. Chem.* 2000, 72, 5814-5819.
- [19] Tolley, H. D., Wang, Q. G., LeFebre, D. A., Lee, M. L., *Anal. Chem.* 2002, 74, 4456-4463.
- [20] Shackman, J. G., Munson, M. S., Ross, D., *Anal. Chem.* 2007, 79, 565-571.
- [21] Ross, D., Kralj, J. G., *Anal. Chem.* 2008, 80, 9467-9474.
- [22] Ross, D., Romantseva, E. F., *Anal. Chem.* 2009, 81, 7326-7335.
- [23] Ross, D., *Electrophoresis* 2010, 31, 3650-3657.

- [24] Polson, N. A., Savin, D. P., Hayes, M. A., *J. Microcolumn Sep.* 2000, *12*, 98-106.
- [25] Meighan, M. M., Keebaugh, M. W., Quihuis, A. M., Kenyon, S. M., Hayes, M. A., *Electrophoresis* 2009, *30*, 3786-3792.
- [26] Meighan, M. M., Vasquez, J., Dziubcynski, L., Hews, S., Hayes, M. A., *Anal. Chem.* 2011, *83*, 368-373.
- [27] Keebaugh, M. W., Mahanti, P., Hayes, M. A., *Electrophoresis* 2012, *33*, 1924-1930.
- [28] Kenyon, S. M., Weiss, N. G., Hayes, M. A., *Electrophoresis* 2012, *33*, 1227-1235.
- [29] Pacheco, J. R., Chen, K. P., Hayes, M. A., *Electrophoresis* 2007, *28*, 1027-1035.
- [30] Giddings, J. C., *Sep. Sci. Technol.* 1979, *14*, 871-882.
- [31] Taylor, G., *Proc. R. Soc. London A* 1953, *219*, 186-203.
- [32] Culbertson, C. T., Jorgenson, J. W., *Anal. Chem.* 1994, *66*, 955-962.
- [33] Hutterer, K. M., Jorgenson, J. W., *Anal. Chem.* 1999, *71*, 1293-1297.
- [34] Shen, Y. F., Berger, S. J., Smith, R. D., *Anal. Chem.* 2000, *72*, 4603-4607.

CHAPTER 6

- [1] Blazej, R. G., Kumaresan, P., Mathies, R. A., *Proc. Natl. Acad. Sci. U. S. A.* 2006, *103*, 7240-7245.
- [2] Paegel, B. M., Blazej, R. G., Mathies, R. A., *Curr. Opin. Biotechnol.* 2003, *14*, 42-50.
- [3] Ahn, C. H., Choi, J. W., Beaucage, G., Nevin, J. H., Lee, J. B., Puntambekar, A., Lee, J. Y., *Proc. IEEE* 2004, *92*, 154-173.
- [4] Fan, R., Vermesh, O., Srivastava, A., Yen, B. K. H., Qin, L. D., Ahmad, H., Kwong, G. A., Liu, C. C., Gould, J., Hood, L., Heath, J. R., *Nat. Biotechnol.* 2008, *26*, 1373-1378.
- [5] Schasfoort, R. B. M., Schlautmann, S., Hendrikse, L., van den Berg, A., *Science* 1999, *286*, 942-945.
- [6] Henley, W. H., Ramsey, J. M., *Electrophoresis* 2012, *33*, 2718-2724.

- [7] Zilberstein, G., Korol, L., Bukshpan, S., Baskin, E., *Proteomics* 2004, 4, 2533-2540.
- [8] Zilberstein, G. V., Baskin, E. M., Bukshpan, S., *Electrophoresis* 2003, 24, 3735-3744.
- [9] Zilberstein, G. V., Baskin, E. M., Bukshpan, S., Korol, L. E., *Electrophoresis* 2004, 25, 3643-3651.
- [10] Date, A., Pasini, P., Daunert, S., *Anal. Bioanal. Chem.* 2010, 398, 349-356.
- [11] Strychalski, E. A., Henry, A. C., Ross, D., *Anal. Chem.* 2011, 83, 6316-6322.
- [12] Yeung, S. W., Lee, T. M. H., Cai, H., Hsing, I. M., *Nucleic Acids Res.* 2006, 34.
- [13] Xia, Y. N., Whitesides, G. M., *Annu. Rev. Mater. Sci.* 1998, 28, 153-184.
- [14] Duffy, D. C., McDonald, J. C., Schueller, O. J. A., Whitesides, G. M., *Anal. Chem.* 1998, 70, 4974-4984.
- [15] McDonald, J. C., Duffy, D. C., Anderson, J. R., Chiu, D. T., Wu, H. K., Schueller, O. J. A., Whitesides, G. M., *Electrophoresis* 2000, 21, 27-40.
- [16] Seia, M. A., Pereira, S. V., Fontan, C. A., De Vito, I. E., Messina, G. A., Raba, J., *Sens. Actuators, B* 2012, 168, 297-302.
- [17] Wongkaew, N., Kirschbaum, S. E. K., Surareungchai, W., Durst, R. A., Bäumner, A. J., *Electroanalysis* 2012, 24, 1903-1908.
- [18] Dong, H., Li, C. M., Zhang, Y. F., Cao, X. D., Gan, Y., *Lab Chip* 2007, 7, 1752-1758.
- [19] Dawoud, A. A., Kawaguchi, T., Markushin, Y., Porter, M. D., Jankowiak, R., *Sens. Actuators, B* 2006, 120, 42-50.
- [20] Moon, H., Wheeler, A. R., Garrell, R. L., Loo, J. A., Kim, C. J., *Lab Chip* 2006, 6, 1213-1219.
- [21] Baker, C. A., Roper, M. G., *Anal. Chem.* 2012, 84, 2955-2960.
- [22] Cong, Y. Z., Liang, Y., Zhang, L. H., Zhang, W. B., Zhang, Y. K., *J. Sep. Sci.* 2009, 32, 462-465.
- [23] Poitevin, M., Peltre, G., Descroix, S., *Electrophoresis* 2008, 29, 1687-1693.

- [24] Shimura, K., Takahashi, K., Koyama, Y., Sato, K., Kitamori, T., *Anal. Chem.* 2008, *80*, 3818-3823.
- [25] Fonslow, B. R., Bowser, M. T., *Anal. Chem.* 2005, *77*, 5706-5710.
- [26] Fonslow, B. R., Bowser, M. T., *Anal. Chem.* 2008, *80*, 3182-3189.
- [27] Shang, T., Teng, E., Woolley, A. T., Mazzeo, B. A., Schultz, S. M., Hawkins, A. R., *Electrophoresis* 2010, *31*, 2596-2601.
- [28] Polson, N. A., Hayes, M. A., *Anal. Chem.* 2000, *72*, 1088-1092.
- [29] Lin, R. S., Burke, D. T., Burns, M. A., *Anal. Chem.* 2005, *77*, 4338-4347.
- [30] Strychalski, E. A., Henry, A. C., Ross, D., *Anal. Chem.* 2009, *81*, 10201-10207.
- [31] Ross, D., Shackman, J. G., Kralj, J. G., Atencia, J., *Lab Chip* 2010, *10*, 3139-3148.
- [32] Jorgenson, J. W., Lukacs, K. D., *Anal. Chem.* 1981, *53*, 1298-1302.
- [33] Jorgenson, J. W., Lukacs, K. D., *Clin. Chem.* 1981, *27*, 1551-1553.
- [34] Jorgenson, J. W., Lukacs, K. D., *Science* 1983, *222*, 266-272.

APPENDIX A
PUBLISHED PORTIONS

Chapters 2 and 4 were published previously in the journals referenced below.

Kenyon, S. M., Meighan, M. M., Hayes, M. A., *Electrophoresis* 2011, 32, 482-493.

Kenyon, S. M., Weiss, N. G., Hayes, M. A., *Electrophoresis* 2012, 33, 1227-1235.

Chapter 5 was submitted to the journal as referenced below.

Kenyon, S. M., Keebaugh, M. W., Hayes, M. A., *Anal. Chem.*, submitted.

Published portions or portions in preparation for publication were included with the permission of all coauthors.